2015

International Journal of Computational Engineering Research

Volume 5 Issue 1, January 2015

International Journal of Computational Engineering Research (IJCER) is dedicated to protecting personal information and will make every reasonable effort to handle collected information appropriately. All information collected, as well as related requests, will be handled as carefully and efficiently as possible in accordance with IJCER standards for integrity and objectivity..]

IJCER Open access Journal

Editorial Board

Editor-In-Chief

Editorial Committees

Contents:

ISSN (e): 2250 – 3005 || Vol, 05 || Issue,01 || January – 2015 ||
International Journal of Computational Engineering Research (IJCER)

Constraint Aware Dynamic Web Service Composition for A Specific Business Requirement

Raghu Rajalingam[1], Shanthi[2]
[1] PG Scholar, Dept of Computer Science and Engineering, Prist University, Tanjore, Tamilnadu, India
[2] Asst Professor, Dept of Computer Science and Engineering, Prist University, Tanjore, Tamilnadu, India

ABSTRACT:
In today's fast moving technology world everyone wants a better and quality of IT services they consume. Here the IT services are referred to web services. In recent time development IT solutions is reduced and most of the time spent on integrating the existing IT solutions. In this space web services has dominating the software industry. Every one focusing converting the existing solution to some form web services and offering the services to customer. The existing technology of web services are extended to completely customize the way services are composed as per the customer requirement so that it will add or provide value as well as the maximum benefit to the customer. Dynamically composing the web services based on the user constraint and providing services to customer always challenging. The proposed paper focus on to addressing how to compose web services based on the user constraint dynamically. The proposal is win-win for both service provider as well as the service consumer.

KEYWORDS: *Service oriented computing; composition of services; dynamic composition; UDDI registry; web services.*

I. INTRODUCTION

In today's fast moving technology world everyone wants to have better quality of service whatever they want to use with their constraints addressed. Here user constraints wary from user to user and it cannot be same for everyone. User wants to use a better reliable service or user wants to use less expensive services or with multiple constraints such as less expensive with more reliable service constraints. Currently lots of research is focused on in this area how to compose web services dynamically to address user constraints.

Composition of web services plays a critical role in case of B2B and integration of enterprise application. Here some time composition of web service may be a single service or it could be more than one dependent different web service to complete the user request. Most of the time service composition consumes lots of development time as well as to create new application. Now there is another parameter is added called user constraint and this will add more time to the existing problem.

The problem with current scenario is Service Consumer (SC) and Service Provider (SP) get in to legal agreement for consuming and providing service for a pre-determined duration such as 1 years or 2 year time frame. SC has to use the services offered by the SP with whom he has a legal agreement for that duration whether the services offered by him is good or bad. Imagine if services offered by the SP are really bad or not meeting the expectation of the SC, then he has to terminate the agreement to find better SP or give feed back to the SP that he is not happy with his service. Here SC's are forced to use the available services and SP dominate with their services without any improvement. SC doesn't have a much choice as there are few SP's and there is no much competition to improve the quality of the services.

How about provide a multiple option's to SC's so that the overall service delivery quality will improve. SC's will choose the service only meet their explicitly expressed constraints. Here SC's are not tied to any SP's and they can choose any service as per their requirement as well as their constraints. This will create a healthy competition among the SP's to provide better quality of service. Following are some of issues need to be taken care.

- Web services are dynamically created and updated so the decision should be taken at execution time and based on recent information.
- How to access easily the different web services provided by the different service provider with different conceptual data model without any technical difficulties.
- How to ensure the access of the web services allowed only for the authorized user. It should not be the case where everyone accesses all web services.

Web services can be categorizedin two ways on the basis of their functionality.

- Semanticannotation describes the functionality of web service and
- Functional annotation describes how it performs itsfunctionality.

WSDL (Web Services Description Language) isused for specification of messages that are used forcommunication between service providers and consumer.Web services can be composed in two ways.One is static web service composition and other is automated/dynamic web service composition. In static web service composition, webservices are manually composed, i.e. each web service is executed sequentially order one by one to fulfill the service consumer request.

Static web service composition is time consuming and tedious task. This requires lots of developer effort to ensure services are properly composed.In case of automated web service composition, a generic framework with intelligence are used compose web services which may internally have many web services to fulfill the service consumer request. From the service consumer point of view it is consider as single service.

Web serviced are composed either centralized data flow or decentralized data flow approach. In case of dynamic web services composition, both have advantages and some limitations. The limitation of centralized dataflow is thatall component services must pass through a composite service.

Preliminaries

Below section provide some insight about the web services composition, automated web services composition and actors involved in dynamic web services composition.

1. Web Services Composition

Web services are distributed applications. The main advantage of web services over other techniques is that web services can be dynamically discovered and invoked on demand, unlike other applications in which static binding is required before execution and discovery.

Semantic and ontological concepts have been introduced to dynamically compose web services in which clients invoke web services by dynamically composing it without any prior knowledge of web services. Semantic and ontological techniques are used to dynamically discover andcompose at the same time (run time).

2. Automated Web services composition

The automated web service composition methods generate the request/response automatically. Most of these methods are based on AI planning. First request goes to Translator which performs translation from external form to a form used by system, and then the services are selected from repositories that meet user criteria.

Now the Process Generator composes these services. If there is more than one composite service that meetsuser criteria then Evaluator evaluates them and returns the best selected service to Execution Engine. The results are returned to clients (Requester). There should be well defined methods and interfaces through which clients interact with the system and get the response.

Proposed Solution

Here we are proposing a framework to address composing the web service dynamically based on the user context as well as with user constraints.

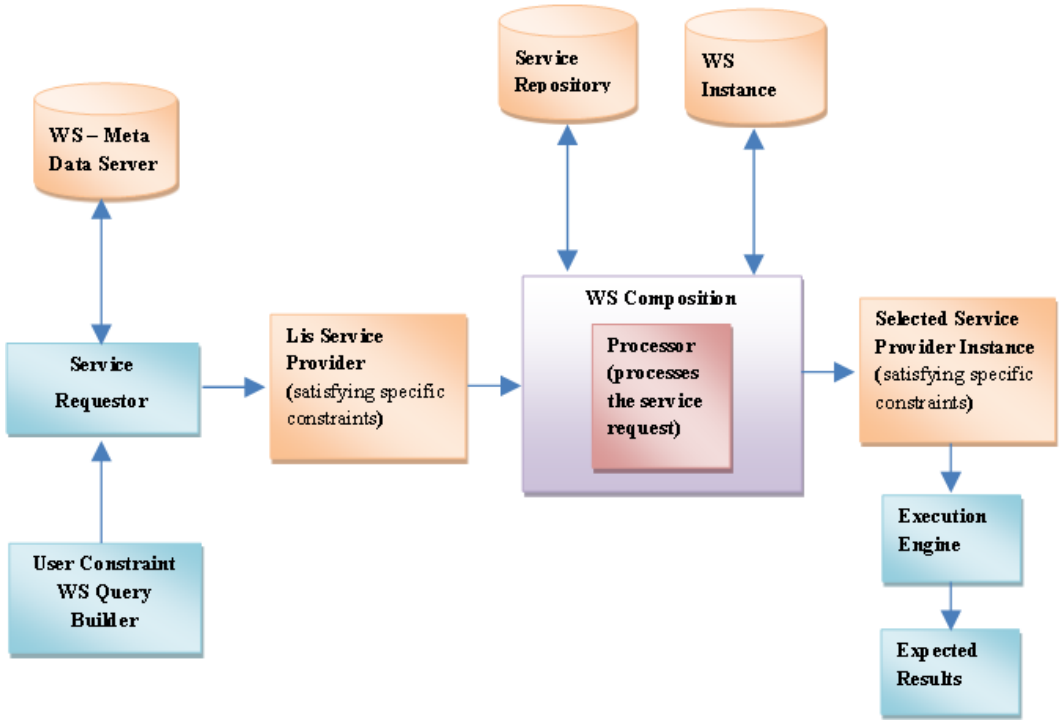

1. **User Constraint Query Builder** – User constraint query builder will construct the user query based on the user specific constraint for searching the web services from WS Meta Data server.
2. **Service Requester** – Constructs the user request object and submits the request to WS Meta data server.
3. **WS Meta data server** – All the Meta data related information is indexed for the faster retrieval of the search data.
4. **WS – Composition** – Constructs the WS – Client dynamically based on the user chosen web service.
5. **WS- Instance cache** – Is an in memory db to persist the instance of the frequently accessed WS instance.
6. **Service Repository** – Master DB of all the WS registered by the service provider.
7. **Execution engine** – A common framework to execute the WS calls.
8. **Response** – A common response object for the WS execution request.

Proposed Technique

A. Methodology

The methodology of proposed model is given as:

1. Web services Meta data are indexed for the faster retrieval during the search operation.
2. The web services are registered in registries.
2. Service requester send request for service.
3. Translator converts the query into a form used by internal system.
4. The request arrives at composition module. Matching Engine checks for the requested service from WSDBs. If it finds the desired interface base service composition then it sends results to Evaluator.
5. Evaluator evaluates these selected web services in two steps. In first step it evaluates the web services on the basis of interface based search, whereas in second step it performs the evaluation on basis of functionality based rule. After evaluation it sends selected services to composer. The purpose of composer is to compose these component web services. Multiple WSDBs are introduced, so that if one goes down then we can make use of other databases. A timestamp (aging) is maintained with each URI in WSDB. If the request arrives before the expiration of that time then it looks for the service in WSDB.
6. If Matching Engine does not find requested service composition from web services database then it start searching from web.
7. The web services are searched from multiple registries and results are returned to Evaluator. Matching Engine alsosaves their references in WSDB with aging factor. The purpose of aging is that it maintains the updated information about web services as the contents are refreshed each time when aging time expires.
8. Evaluator evaluates these web services based on interface based and functionality based rules.
9. Composer composes these evaluated resultant services and sends result to Execution Engine. Execution Engine executes these web services and through translator results are sent back to requester.

Pseudo Code
Algorithm: Dynamic Web services composition based on user constraints.
Input: Request for web service
Output: Composed service

Web services with their constraints data are ingested in WS-Meta data server;

User enters request for web service along with their constraints;

WS-Query builder translates the web service request;

Web Service request will be submitted to the WS-Meta data server;

WS-Meta data serversearch services for the submitted user query;
WS-Meta data serverreturns the matching services as per the user ws query;

User selects and submits web service matching his requirement to WS-Composition Engine.
WS-Composition search for the submitted web service from WS-Instance cache;
If selected ws instance is available from WS-Instance cache then
Return instance to Execution engine.
If selected ws instance is not available from WS-Instance cache then
    Create a new instance and add to the WS-Instance cache.
Return instance to Execution engine.
Execution engine will execute the selected web service and return the result;

Here we have query builder using which user can specify user constraints is. Based on the query a search request will be submitted to WS-Meta data server. WS-Meta data server will return the search result based on the user constraint. If any record match with the user query result will be returned to the user. User with the returned list of web service matching his constraint can choose one and complete his operation. When user chooses a specific service matches the constraint then a search is done in WS-Instance cache is there already an instance is available. If no instance is available then a query will be sent to service repository to ensure that service still registered and available. Sometime services are registered for a short time and later removed from the service register. To avoid such problem it is always good to make check before composing or executing the web service. Core component of this framework is WS-Meta data server. The Meta data server contains only the Meta data of the web services along with use full information such as pricing, availability, reliability, user rating, is partner etc. As these information may not available in service registry. Service registry may contain service name, service provider and name space etc. We are creating an index server which very fast in retrieving the required data based on the user query and it contains the Meta data of the services. The web services information along with the constraints are ingested in the Meta data and frequently kept updated as a when data changes. Sometime the data contained in Meta data server will obsolete as this is not the master database for the web services. This is a secondary server for fast searching data. Service registry will be the master copy of web services.WS-Instance cache is another important component as it contains the frequently used web services to speed up the web service composition and execution. There will be few services which will be used frequently by the user. We cache such service instances in WS-Instance cache so that in future if the same web service requested then it will retrieve from the cache instead of creating new one. If referred web service instance is already available in WS-Instance cache then retrieve the instance and execute the web service call. If it is not available then create the instance and add to the WS-Instance cache. This approach used to increase the speed of web service execution.

II. CONCLUSION

With dynamic composition of the web services based on the user constraints always ensures better quality of the services rendered to the service consumer. By this approach it will create a healthy eco system among the service provider to provide better quality service.

REFERENCES

[1]. A Constraint-Based Approach to Horizontal WebService Composition,Ahlem Ben Hassine, Shigeo Matsubara and Toru Ishida,3 Cruz et al. (Eds.): ISWC 2006, LNCS 4273, pp. 130–143, 2006,Springer-Verlag Berlin Heidelberg 2006.
[2]. An approach to dynamic web service composition, Dmytro Pukhkaiev, Tetiana Kot, Larysa Globa, UDC 621.93, National Technical University of Ukraine “Kyiv Polytechnic Institute”, Kyiv, Ukraine.

[3]. G. Alonso, F. Casati, H. Kunoand V. Machiraju. Web Services. Concepts, Architectures and Applications. - Springer, 2004. - 354 p.
[4]. M. P. Papazoglou, P. Traverso, S. Dustdar, F. Leymann: "Service-Oriented Computing: State of the Art and Research Challenges"; IEEE Computer, 40 (November 2007 (2007), 11; P. 38 - 45.
[5]. M.Papazoglou and D. Georgeakopoulos. "Service-OrientedComputing," Communications of the ACM, vol. 46, 2003. - P. 25-28.
[6]. W.M.P. van der Aalst, Benatallah B., Casati F. , Curbera F. , and Verbeek H.M.W.. Business Process Management: Where Business Processes and Web Services Meet. // Data and Knowledge Engineering. -2007. - 61(1). – P. 1-5.
[7]. Y. Jadeja, K. Modi, and A. Goswami. Context Based DynamicWeb Services Composition Approaches: a Comparative Study //International Journal of Information and Education Technology, vol. 2, Apr. 2012. - P.164-166.
[8]. S. Dustdar, and W. Schreiner, "A survey on web services com-position," in Int. J. Web and Grid Services, vol. 1, No. 1, 2005. - P.1–30.
[9]. S.Bansal, A. Bansal, and M.B. Blake, "Trust based Dynamic Web Service Composition using Social Network Analysis," IEEE International Workshop on Business Applications for Social Network Analysis (BASNA 2010), August 2010. - P. 1-8.
[10]. C. Molina-Jimenez, J. Pruyne, and A. van Moorsel. The Role of Agreements in ITManagement Software. Architecting Depend-able Systems III, LNCS 3549. Springer Verlag, Volume3549, 2005. – P. 36-58.
[11]. OMG Business Process Model and Notation (BPMN) [Online]. - 2011. - Available: http://www.omg.org/spec/BPMN/2.0/PDF
[12]. N. Russell, W.M.P. Van der Aalst, A.H.M. ter Hofstede, P. Wohed "On the suitability of UML 2.0 activity diagrams for business process modeling," Proceedings of the 3rd Asia-Pacific conference on Conceptual modeling APCCM '06, vol. 53, 2006. - P. 95-104.
[13]. Oberle, D., Bhatti, N., Brockmans, S., Niemann, M., Janiesch, C., "Countering Service Information Challenges in the Internet of Services," Journal of Business & Information System Engineering, vol.1, 2009. - P. 370-390.
[14]. H. Foster, S. Uchitel, J. Magee, J. Kramer, M. Hu "Using a Rigorous approach for engineering Web service compositions: a case study," in Proceedings of the 2005 IEEE International Conference on Services Computing (SCC '05), 2005. - P.217-224.
[15]. OASIS (2007) Web Services Business Process ExecutionLanguage (WSBPEL) [Online]. Available: http://docs.oasis-open.org/wsbpel/2.0/OS/wsbpel-v2.0-OS.pdf.
[16]. E.M. Maximilien and M.P. Singh., "A framework and ontology for dynamic web services selection," IEEE Internet Computing, vol. 8, Sep./Oct. 2004. - P. 84-93.
[17]. M. B. Blake, and D. J. Cummings, "Workflow Composition of Service-Level Agreements," in Proceedings of IEEE International Conference on Services Computing (SCC), July 2007,. - P.138-145.
[18]. A. Andrieux, K. Czajkowski, A. Dan, K. Keahey, H. Ludwig, T. Nakata, J. Pruyne, J. Rofrano, S. Tuecke, and M. Xu. (2007) Web Services Agreement Specification (WS-Agreement) Online]. Available: http://www.ogf.org/documents/GFD.107.pdf.
[19]. A graph-based approach to Web services compositionHashemian, S.V.; Mavaddat, F. Applications and the Internet, 2005. Proceedings. The 2005 Symposium on DOI: 10.1109/SAINT.2005.4 Publication Year: 2005, Page(s): 183- 189.
[20]. Van der Aalst, W.: Don't Go with the Flow: Web Services Composition Standards Exposed.IEEE Intelligent Systems (Jan/Feb 2003).
[21]. Tony Andrews and Francisco Curbera and Hitesh Dholakia and Yaron Goland and JohannesKlein and Frank Leymann and Kevin Liu and Dieter Roller and Doug Smith and SatishThatte and Ivana Trickovic and Sanjiva Weerawarana: Business Process Execution Languagefor Web Services (2003)

Author Profile

Raghu Rajalingam is a R & D specialist with deep understanding and hands on experience in the area of Java enterprise architecture, Service oriented Architecture and Cloud computing.

Shanthi is an academician with interest in the area of data mining and service oriented architecture. She has good teaching and research experience.

ISSN (e): 2250 – 3005 || Vol, 05 || Issue, 01 || January – 2015 ||
International Journal of Computational Engineering Research (IJCER)

C^0 Mixed Layerwise Quadrilateral Plate Element with Variable in and Out-Of-Plane Kinematics and Fixed D.O.F.

Icardi U.[1,] Sola F.[2]

[1]*Associate Professor - Dipartimento di Ingegneria Meccanica e Aerospaziale*
Politecnico di Torino - Corso Duca degli Abruzzi 24, 10129 Torino, Italy
Corresponding author. Tel: +39 (0)115646872; fax: +39 (0)115646899
[2]*PhD Student - Dipartimento di Ingegneria Meccanica e Aerospaziale*
Politecnico di Torino - Corso Duca degli Abruzzi 24, 10129 Torino, Italy

ABSTRACT:
A quadrilateral, eight-node, mixed plate element based upon a recent 3D, variable kinematics zig-zag plate model by the authors is developed. Representation can be refined across the thickness though the number of unknown does not depend on the number of constituent layers, the nodal variables being fixed. The out-of-plane stress continuity is a priori satisfied at the interfaces and the material properties are allowed to step-vary moving over the plane of the structure. In order to obtain a C0 model, all derivatives of unknowns are converted with a technique that does not introduce additional d.o.f. Equilibrium equations are satisfied just in approximate integral form, mid-plane displacements and interlaminar stresses, the nodal d.o.f., being interpolated using the same standard serendipity shape functions. As shown by numerical results, this does not result in any precision loss. Accuracy, solvability and convergence are assessed considering multi-layered monolithic and sandwich-like structures with different boundary conditions and abruptly changing material properties across the thickness, for which exact solutions are available. Also a bonded joint is studied, which is treated as a laminate with spatially variable properties. In all these cases, the element is shown to be fast convergent and free from spurious, oscillating results.

KEYWORDS: *partial hybrid formulation; intra-element equilibrium in an approximate integral form; fixed d.o.f.; hierarchic representation; C0 plate element;*

I. INTRODUCTION

Laminated and sandwich composites increasingly find use, as they enable design and construction of structures that achieve the target requirements with a lower mass than their metallic monolithic counterparts and they also offer the possibility to optimize the structural performances by properly choosing the fibre orientation and the stacking lay-up (see, e.g. Sliseris and Rocens [1]).

Manufacturing technologies such as automated fibre-placement (Barth [2]) pave the way to the spread of variable-stiffness composites in which the fibres follow curvilinear paths. Variable strength, stiffness and dissipation properties offer many advantages, as shown e.g. in Refs. [3] and [4], since the constituent materials can be designed using advanced optimization techniques for keeping maximal the overall performance parameters. At the same time, it is possible to relax the critical local stress concentrations inherent to the inhomogeneous microstructure of composites that give rise to damage. A recent, comprehensive discussion of the mechanisms of damage formation and evolution of composites and of their modelling is given by Càrdenas et al. [5].

Since the local damage can have very harmful effects, the simulations should accurately account for the stress fields responsible of the damage rise and growth, their strong concentrations at the interfaces, their effects on strength, stiffness and durability and the warping, shearing and straining deformations of the normal produced by the material discontinuities and the much bigger elastic moduli and strengths in the in-plane direction compared to those in the thickness. These so called zig-zag and layerwise effects should be described into details but with an affordable computational effort, as discussed by Chakrabarti et al. [6], Qatu et al. [7] and Zhang and Yang [8].

Displacement-based models and related finite elements should feature appropriate discontinuous derivatives of displacements in the thickness direction at the interfaces, while mixed models should assume appropriate continuous, self-equilibrated stresses. Composite plate and shell theories and elements satisfying

these requirements have been developed either in displacement-based or mixed form using different approaches. Displacement-based finite elements require fine meshes and a large computational effort to accurately determine stresses, since they are obtained from displacements (constitutive equations) or from in-plane stresses (integration of local equilibrium equations), thus accuracy deteriorates. Mixed/hybrid models and elements offer the advantage of a more easily enforcement of interfacial and boundary constraints, the stresses being treated as primary variables separately from displacements. Moreover, they provide more accurate results than displacement-based models with the same meshing and with a comparable processing time, as shown in the literature. On the other hand stability, convergence and solvability are more complex than those of their displacement-based counterparts.

An extensive discussion of the various techniques used to account for the layerwise effects and extensive assessments of their structural performances are presented by Chakrabarti et al. [6], Matsunaga [9]**Error! Reference source not found.**, Chen and Wu [10], Kreja [11], Tahani [12] and Gherlone [13]. Accuracy of finite element models for layered and sandwich composites is assessed by Carrera et al. [14]. Finite element models are also discussed in the papers by Chakrabarti et al. [6], Zhang and Yang [8], Shimpi and Ainapure [15], Elmalich and Rabinovitch [16], Dau et al. [17] and for what concerns mixed/hybrid methods in the book by Hoa and Feng [18], and in the papers by Feng and Hoa [19], Desai et al. [20], Ramtekkar et al. [21] and To and Liu [22]. Recent examples of finite elements for analysis of composites are those by Zhen et al [23], Cao et al. [24] (hybrid formulation) and Dey at al. [25].

Accuracy and computational costs of layerwise models and elements can considerably vary, depending on their number of unknowns. A separate representation in any computational layer results in a high accuracy (see, e.g. Reddy [26]), but since the number of variables increases with the number of physical/computational layers, computational costs can become unaffordable when analysing structures of industrial complexity. Models based on a combination of global higher-order terms and local layerwise functions are often used for analysis of composites, as they have been proven to be equally accurate with a much lower computational effort (see, e.g. Elmalich and Rabinovitch [16] and the references therein cited). The zig-zag models inspired by Di Sciuva [27] have also found many applications and related finite elements are widespread, being low cost partial layerwise models with just the three mid-plane displacements and the two transverse shear rotations as functional d.o.f., like equivalent single-layer models. Physically-based continuity functions are incorporated in the displacement field in order to a priori satisfy the continuity of out-of-plane stresses at the layer interfaces, whose expressions are determined once for all. Initially, just the piecewise variation of in-plane displacements across the thickness was considered, the transverse displacement being assumed constant. Refinements have been brought over years in order to incorporate a variable transverse displacement, since it has a significant bearing for keeping equilibrium in certain cases. A great amount of research work was also done to successfully treat panels with low length-to thickness ratio and abruptly changing material properties, like sandwiches, which can be described as multi-layered structures whenever a detailed description of local phenomena in the cellular structure is unnecessary [28]. Sublaminate models having top and bottom face d.o.f. were developed in order to stack computational layers [29]. The displacement field was recast in a global-local form to accurately predict stresses from constitutive equations (see, Li and Liu [30], Zhen and Wanji [31]), though at the expense of a larger number of functional d.o.f., because post-processing operations are unwise for finite elements and cannot always be precise [32].

As a result of these refinement studies, to date zig-zag models and elements offer a good accuracy with the lowest computational burden. Regrettably, derivatives of the functional d.o.f. are involved by such physically-based zig-zag models, and consequently they should appear as nodal d.o.f. in the finite elements, implying to use C1 or high-order interpolation functions with a lower computational efficiency than C0ones. Techniques such those proposed by Zhen and Wanji [31] and Sahoo and Singh [33] could be employed for converting derivatives, but they result in an increase of the nodal d.o.f and thus of the memory storage dimension. The Murakami's zig-zag function just based upon kinematic assumptions is often used as local layerwise function since it overcomes the problem and it is much easier to implement than the physically consistent zig-zag functions, though it is not always equally accurate. The assessments carried out by Gherlone [13] proven that Murakami's zig-zag is accurate for periodical stack-ups, but not for laminates with arbitrary stacking sequences, or for asymmetrical sandwiches with high face-to-core stiffness ratios, like when a weak layer is placed on the top or bottom to simulate a damaged face.

Aimed at carrying out the analysis of multi-layered and sandwich composites having abruptly changing material properties with the minimal computational burden, the recently developed physically-based zig-zag model of Ref. [34] was developed assuming a through-the-thickness variable representation of displacements that can be locally refined like for discrete layer models, though its functional d.o.f. are fixed (the classical displacements and shear rotations of the normal at the mid-plane). A high-order piecewise zig-zag variation of all the displacements was assumed in order to account for the core's crushing behaviour of sandwiches, for keeping equilibrium at cut-outs, free edges, nearby material/geometric discontinuities and to

predict stresses caused by temperature gradients, because in these cases the piecewise variation of the transverse displacement is as important as that of its in-plane counterparts (see, e.g. [23] and [35]). The physical constraints, i.e. the interfacial stress contact conditions, stress boundary conditions at the bounding faces and the indefinite equilibrium equations at selected points across the thickness were satisfied without increasing the number of unknown variables because symbolic calculus was used to obtain automatically and once for all relations in closed-form as functions of the assumed five d.o.f. Accurate results were obtained in numerical applications with a computational effort considerably lower than for other layerwise models, thus model [34] is of practical interest toward development of finite elements.

In the present paper, the energy updating technique of Refs. [36] – [38], here referred as SEUPT, is used to convert derivatives without resulting in an increased number of nodal variables. SEUPT was originally developed as an iterative post-processing technique for improving the predictive capability of shear deformable commercial finite plate elements. The present revised version of SEUPT consists of a technique that allows obtainment of an equivalent C0 version (EM model) of the zig-zag model [34] by the energy standpoint, which is used to develop an efficient plate element in mixed form having the displacements and the interlaminar stresses at the reference mid-plane as nodal d.o.f. A priori corrections of displacements are obtained in closed-form through SEUPT using symbolic calculus by making the energy of the model [34] free from derivatives equal to that of its counterpart containing all the derivatives. Hermite's polynomials are assumed in the energy balance equations for the consistent zig-zag model, while Lagrange's polynomials are used for the equivalent counterpart model free from d.o.f. derivatives. The equivalent C0 displacement fields and the out-of-plane stresses derived in this way are used to develop the present mixed element. It is a partial hybrid one, because, according to Ref. [19], it only includes out-of-plane stresses as nodal d.o.f., just these stresses having to be continuous across the material interfaces and being essential for analysis of composites. The stresses by the EM model are modified adding new continuity functions that restore the equilibria at the interfaces, because stress continuity could be lost in the equivalent model.

Displacement and stress interpolating functions all of the same order are considered, the same C0 interpolation by standard serendipity polynomials being used for all the nodal d.o.f. , so the intra element equilibrium equations are satisfied just in an approximate integral form. This option was chosen because it reduces the effort for developing the element without losing accuracy, as shown in the pioneering paper by Loubignac et al. [39] and in the book by Nakazawa [40].

Accuracy, solvability and convergence behaviour of the present mixed element will be assessed comparing its results for laminates and sandwiches with different boundary conditions and abruptly changing material properties with the exact solutions computed with the technique by Pagano [41]. The sample cases by Zhen et al. [23], Vel and Batra [42], Icardi [43], Brischetto et al. [44], Tessler et al. [45] and Robbins and Reddy [46] are considered. As an application to a practical case, the stress field of a double lap joint computed by the present mixed element is compared to the exact solution by Nemes and Lachaud [47].

The paper is structured as follows. First, the basic features of the zig-zag plate model are overviewed. Then, SEUPT is recast in a form suited for the present element. Finally, the element is developed and applied to the analysis of sample cases.

II. STRUCTURAL MODEL

A rectangular Cartesian reference frame (x, y, z) with (x, y) on the middle surface of the plate (Ω) and z normal to it is assumed as reference system. The displacement field is assumed as the as the sum of four separated contributions:

$$\begin{aligned} u(x,y,z) &= U^{0}(x,y,z) + U^{i}(x,y,z) + U^{c}(x,y,z) + U^{c-ip}(x,y,z) \\ v(x,y,z) &= V^{0}(x,y,z) + V^{i}(x,y,z) + V^{c}(x,y,z) + V^{c-ip}(x,y,z) \\ w(x,y,z) &= W^{0}(x,y,z) + W^{i}(x,y,z) + W^{c}(x,y,z) + W^{c-ip}(x,y,z) \end{aligned} \tag{1}$$

Here the symbols u, v and w respectively define the elastic displacements in the directions x, y and z.

The first three contributions are the same of the model developed in Ref. [34], the latter one was added in Ref. [38] to treat properties and/or lay-up suddenly varying in x, y directions, like across adherends and overlap of bonded joints.

2.1 Basic contribution $\square^0$

The basic contributions, indicated with superscript ^{0} or in compact form as Δ^0, repeat the kinematics of the FSDPT model, thus they contain just a linear expansion in z:

$$\begin{aligned} U^{0}(x,y,z) &= u^{0}(x,y) + z\left[\gamma_x^{0}(x,y) - w^{0}{}_{,x}(x,y)\right] \\ V^{0}(x,y,z) &= v^{0}(x,y) + z\left[\gamma_y^{0}(x,y) - w^{0}{}_{,y}(x,y)\right] \end{aligned} \tag{2}$$

$$W^{0}(x,y,z) = w^{0}(x,y)$$

Eq. (2) is well known and it has been used in many applications, therefore it does not need further explanations. Here it is only reminded that the displacements $u^0(x, y)$, $v^0(x, y)$, $w^0(x, y)$ and the transverse shear rotations at the middle plane $\gamma_x{}^0(x, y)$ and $\gamma_y{}^0(x, y)$ represent the five functional d.o.f.

2.2 Variable kinematics contribution Δ^i

The contributions with superscript ^{i}, indicated in compact form with the symbol Δ^i, allow the model adapting to local variation of solutions, enabling a refinement across the thickness. Therefore these contributions have a representation that can vary from point to point across the thickness:

$$\begin{aligned} U^{i}(x,y,z) &= A_{x1}z + A_{x2}z^{2} + A_{x3}z^{3} + A_{x4}z^{4} + \ldots + A_{xn}z^{n} \\ V^{i}(x,y,z) &= A_{y1}z + A_{y2}z^{2} + A_{y3}z^{3} + A_{y4}z^{4} + \ldots + A_{yn}z^{n} \\ W^{i}(x,y,z) &= A_{z1}z + A_{z2}z^{2} + A_{z3}z^{3} + A_{z4}z^{4} + \ldots + A_{zn}z^{n} \end{aligned} \tag{3}$$

The unknown coefficients $A_{x1}\ldots A_{zn}$ are computed by enforcing the conditions:

$$\sigma_{xz}|^{u} = 0 \quad \sigma_{xz}|_{l} = 0 \tag{4}$$

$$\sigma_{yz}|^{u} = 0 \quad \sigma_{yz}|_{l} = 0 \tag{5}$$

$$\sigma_{zz}|^{u} = p^{0}|^{u} \quad \sigma_{zz}|_{l} = p^{0}|_{l} \tag{6}$$

$$\sigma_{zz,z}|^{u} = 0 \quad \sigma_{zz,z}|_{l} = 0 \tag{7}$$

and the equilibrium at discrete points across the thickness:

$$\begin{aligned} &\sigma_{xx,x} + \sigma_{xy,y} + \sigma_{xz,z} = 0 \\ &\sigma_{xy,x} + \sigma_{yy,y} + \sigma_{yz,z} = 0 \\ &\sigma_{xz,x} + \sigma_{yz,y} + \sigma_{zz,z} = 0 \end{aligned} \tag{8}$$

The symbols $^{(k)}z^+$ and $^{(k)}z^-$ indicate the position of the upper$^+$ and lower $^-$ surfaces of the kth layer, while the superscript(k) designates the quantities that belong to a generic layer k. As customarily, a comma is used to indicate differentiation. Please notice that the expressions of the unknowns $A_{x1}\ \ldots\ A_{zn}$ are computed through automatic, symbolic calculus (MATLAB® symbolic software package) without any increase in the number of unknowns, being obtained in closed-form as functions of the d.o.f. and of their derivatives. Contributions (3) neither results into a considerably larger computational effort, nor into a larger memory storage dimension, because irrespectively of the number of points chosen, the number of d.o.f. is fixed because the constraint relations are obtained in closed-form once for all just in terms of the variables $u^0(x, y)$, $v^0(x, y)$, $w^0(x, y)$, $\gamma_x{}^0(x, y)$, $\gamma_y{}^0(x, y)$ and of their derivatives. Because derivatives are unwise for the development of finite elements, they will be converted with the technique described forward.

2.3 Zig-zag piecewise contribution Δ^c

The piecewise terms Δc, which constitutes the zig-zag contributions, are assumed as follows:

$$\begin{aligned} U^{c}(x,y) &= \sum_{k=1}^{n_i} \Phi_x^{k}(x,y)(z - z_k)H_k + \sum_{k=1}^{n_i} C_u^{k}(x,y)H_k \\ V^{c}(x,y) &= \sum_{k=1}^{n_i} \Phi_y^{k}(x,y)(z - z_k)H_k + \sum_{k=1}^{n_i} C_v^{k}(x,y)H_k \\ W^{c}(x,y) &= \sum_{k=1}^{n_i} \Psi^{k}(x,y)(z - z_k)H_k + \sum_{k=1}^{n_i} \Omega^{k}(x,y)(z - z_k)^2 H_k + \sum_{k=1}^{n_i} C_w^{k}(x,y)H_k \end{aligned} \tag{9}$$

The terms of Eq. (9) make the displacements continuous and with appropriate discontinuous derivatives in the thickness direction at the interfaces of physical/computational layers, thus allowing to a priori fulfil the continuity of interlaminar stresses at the material interfaces. In details, terms Φ_x^k, Φ_y^k are incorporated in order to satisfy:

$$\begin{aligned} \sigma_{xz}|_{(k)_{z^+}} &= \sigma_{xz}|_{(k)_{z^-}} \\ \sigma_{yz}|_{(k)_{z^+}} &= \sigma_{yz}|_{(k)_{z^-}} \end{aligned} \tag{10}$$

while Ψ_k, Ω_k are computed by enforcing the following continuity conditions:

$$\sigma_z|_{(k)_{z^+}} = \sigma_z|_{(k)_{z^-}}$$
$$\sigma_{z,z}|_{(k)_{z^+}} = \sigma_{z,z}|_{(k)_{z^-}} \quad (11)$$

which directly derive from the local equilibrium equations as a consequence of the continuity of transverse shear stresses.

The continuity of displacements at the points across the thickness where the representation is varied is restored by the functions C_u^k, C_v^k and C_w^k, whose expressions are computed imposing:

$$u\Big|_{(k)_{z^+}} = u\Big|_{(k)_{z^-}}$$
$$v\Big|_{(k)_{z^+}} = v\Big|_{(k)_{z^-}} \quad (12)$$
$$w\Big|_{(k)_{z^+}} = w\Big|_{(k)_{z^-}}$$

2.4 Variable in-plane representation Δ^{c_ip}

Differently to [34]**Error! Reference source not found.**, it is supposed that the in-plane representation of displacements can vary, consequently to a sudden change of the material properties moving along the x or y direction. To this purpose, contributions Δc_ip are incorporated in a form similar to that used in [38]:

$$U^{c\_ip} = \sum_{j=1}^{S}\sum_{k=1}^{T} {}_u^j\theta_x^k(x,y)(x-x_k)H_k + \sum_{j=1}^{S}\sum_{k=1}^{T} {}_u^j\theta_y^k(x,y)(y-y_k)H_k + \sum_{j=1}^{S}\sum_{k=1}^{T} {}_u^j\lambda_x^k(x,y)(x-x_k)^2H_k + \sum_{j=1}^{S}\sum_{k=1}^{T} {}_u^j\lambda_y^k(x,y)(y-y_k)^2H_k + \ldots \quad (13)$$

$$V^{c\_ip} = \sum_{j=1}^{S}\sum_{k=1}^{T} {}_v^j\theta_x^k(x,y)(x-x_k)H_k + \sum_{j=1}^{S}\sum_{k=1}^{T} {}_v^j\theta_y^k(x,y)(y-y_k)H_k + \sum_{j=1}^{S}\sum_{k=1}^{T} {}_v^j\lambda_x^k(x,y)(x-x_k)^2H_k + \sum_{j=1}^{S}\sum_{k=1}^{T} {}_v^j\lambda_y^k(x,y)(y-y_k)^2H_k + \ldots \quad (13)'$$

In Eqs. (13) and (13)' the exponent of $(x - x_k)^n$, $(y - y_k)^n$ is chosen in order to make continuous the stress gradient of order *n*. For instance, the continuity conditions $\sigma_{xx}|_{(k)x+} = \sigma_{xx}|_{(k)x-}$, $\sigma_{yy}|_{(k)x+} = \sigma_{yy}|_{(k)x-}$ and $\sigma_{zz}|_{(k)x+} = \sigma_{zz}|_{(k)x-}$ require just first order terms of $(x - x_k)$, while the continuity of gradients $\sigma_{xx,x}|_{(k)x+} = \sigma_{xx,x}|_{(k)x-}$, $\sigma_{yy,x}|_{(k)x+} = \sigma_{yy,x}|_{(k)x-}$ and $\sigma_{zz,x}|_{(k)x+} = \sigma_{zz,x}|_{(k)x-}$ requires second order terms $(x - x_k)^2$, while higher-order gradients require the higher order contributions omitted in previous equations. The continuity functions appearing in (13), (13)' are computed in a straightforward way by enforcing previous conditions.

III. ENERGY UPDATING TECHNIQUE

Equivalent forms of models by the energy standpoint can be constructed using energy-based weak form versions of governing equations. As shown in [36] and [37], an iterative post-processing technique working on a spline interpolation of FEA result can be used to construct an updated solution that locally improves the accuracy of a finite element analysis carried out using standard shear-deformable plate elements. As shown in [38], a modified expression of the displacements field by a structural model that is free from derivatives of the functional d.o.f. can be constructed in order to obtain a C0 equivalent model without any additional d.o.f. using symbolic calculus to obtain once for all the relations in closed-form. The comparison with exact solutions of sample test cases demonstrated that the equivalent model (EM) can provide equally accurate results than the original model (OM), even when the through-the-thickness stress distributions are rather intricate. This opens the possibility of developing an efficient finite element free from nodal derivatives of the d.o.f.

Hereafter, the technique developed in [38] is retaken and revised with the aim of constructing a version of SEUPT that produces an equivalent zig-zag model suited to develop an efficient and accurate mixed plate element for analysis of laminated and sandwich composites.

3.1 Equivalent zig-zag model

The basic assumption of SEUPT is that each displacement of the OM model appearing in Eq. (1), hereon indicated as $u(x, y, z)^{OM}$, $v(x, y, z)^{OM}$, $w(x, y, z)^{OM}$ (superscript ^{OM} will define all the quantities that refer to this model) can be reconstructed using energy equivalence concepts, so that all the derivatives of the functional d.o.f. can be replaced. The objective is to derive modified expressions of the displacements, i.e. u(x,

$u(x, y, z)^{EM}$, $v(x, y, z)^{EM}$, $w(x, y, z)^{EM}$ (superscript ^{EM} will refer to the equivalent model) that will be used within each energy integral, so to have the energy functional free from derivatives.

It is assumed that the displacements of the OM model (in compact form $\forall^{OM}$) can be recast as the sum of a part $\forall^{\varnothing}$ free from derivatives of the d.o.f. and terms $\forall^{\cup}$ containing the derivatives

$$\forall^{OM}(x, y, z) = \forall^{\varnothing}(x, y, z) + \forall^{\cup}(x, y, z) \tag{14}$$

The basic assumption of SEUPT is that each term $\forall^{\cup}$ can be replaced incorporating corrective terms that are free from derivatives Δu^0, Δv^0, Δw^0, $\Delta \gamma_x{}^0$, $\Delta \gamma_y{}^0$ (in compact form $\Delta \forall^{\varnothing}$)

$$\forall^{EM}(x, y, z) = \forall^{\varnothing}(x, y, z) + \Delta \forall^{\varnothing}(x, y, z) \tag{14'}$$

whose expressions are derived from the energy balance

$$\delta \int (.)|_E = \delta \int (.)|_{Ai} - \delta \int (.)|_{Af} + \delta \int (.)|_{Am} = 0 \tag{15}$$

in order to be equivalent by the energy standpoint. The principle of virtual works accounting for inertial forces is here used as the energy balance, but any other equivalent canonical functional could be successfully employed. As customarily, the symbols $\{\sigma_{ij}\}$ and $\{\varepsilon_{ij}\}$ represent the strain and stress vectors, respectively, b_i and t_i are the body and surface forces, ρ is the density and u_i are the displacements. The expressions of corrective terms $\Delta \forall^{\varnothing}$ are specific for any sub-integral constituting the virtual variations of the strain energy $\int (.)|_{Ai} = \frac{1}{2}\int_V \{\sigma_{ij}\}^T \{\varepsilon_{ij}\} dV$, work of external forces $\int (.)|_{Af} = \int_V b_i u_i dV + \int_S t_i u_i dS$ and work of inertial forces $\int (.)|_{Am} = \int_V -\rho \ddot{u}_i u_i \, dV$ Therefore, each corrective term is computed by splitting the energy balance into five independent balance equations, here indicated in compact form as

$$\left[\delta \int (.)|_E\right]^{u^0} = 0 ; \left[\delta \int (.)|_E\right]^{v^0} = 0 ; \left[\delta \int (.)|_E\right]^{w^0} = 0 ; \left[\delta \int (.)|_E\right]^{\gamma_x{}^0} = 0 ; \left[\delta \int (.)|_E\right]^{\gamma_y{}^0} = 0 ; \tag{16}$$

i.e. one for each primary variable δu^0, δv^0, δw^0, $\delta \gamma_x{}^0$, $\delta \gamma_y{}^0$, and then further splitting into all sub-integrals $\delta \int (.)|_{E\longrightarrow}$ that added together form the five separate contributions (16) (i.e. $\Sigma \delta \int (.)|_{E\longrightarrow} = \delta \int (.)|_E$)

Different corrective terms Δu^0, Δv^0, Δw^0, $\Delta \gamma_x{}^0$, $\Delta \gamma_y{}^0$ are computed for each sub-integral $\delta \int (.)|_{E\longrightarrow}$ by imposing the result by the OM model to be equal by the energy standpoint to its counterpart by the EM model, in symbols:

$$\begin{aligned}
&\left[\delta \int (.)|_{E\longrightarrow}\right]^{u^0 OM} = \left[\delta \int (.)|_{E\longrightarrow}\right]^{u^0 EM} = 0 ;\\
&\left[\delta \int (.)|_{E\longrightarrow}\right]^{v^0 OM} = \left[\delta \int (.)|_{E\longrightarrow}\right]^{v^0 EM} = 0 ;\\
&\left[\delta \int (.)|_{E\longrightarrow}\right]^{w^0 OM} = \left[\delta \int (.)|_{E\longrightarrow}\right]^{w^0 EM} = 0 ;\\
&\left[\delta \int (.)|_{\longrightarrow E}\right]^{\gamma_x{}^0 OM} = \left[\delta \int (.)|_{E\longrightarrow}\right]^{\gamma_x{}^0 EM} = 0 ;\\
&\left[\delta \int (.)|_{E\longrightarrow}\right]^{\gamma_y{}^0 OM} = \left[\delta \int (.)|_{E\longrightarrow}\right]^{\gamma_y{}^0 EM} = 0 ;
\end{aligned} \tag{17}$$

The displacement fields are described as Hermite polynomials within the sub-integrals with the superscript ^{OM}, while Lagrange polynomials are used within sub- integrals with the superscript ^{EM}, because the functional d.o.f. and their derivatives should be assumed as nodal d.o.f. whether a conforming element is derived by the OM model, while no derivatives are required for an element derived by the EM model, as in the current case. At least third order derivatives are involved by the OM model as a consequence of the enforcement of the interfacial stress continuity and of the stress boundary conditions, but higher order derivatives could be involved enforcing additional conditions.

Representing each functional d.o.f. (i.e. $u^0(x,y)$, $v^0(x,y)$, $w^0(x,y)$, $\gamma_x^0(x,y)$, $\gamma_y^0(x,y)$) in compact form with the symbol $\wp$, the inner representation of variables of the OM model is expressed as the sum of tensor products of Hermite's polynomials ${}^{\rho}\mathrm{H}_i$ in *x* and *y* of the following form (index i represents the nodes numbering):

$$\wp = \sum_{i=1}^{4} {}^{\wp}\mathrm{H}_i \, \wp_i + \sum_{i=1}^{4} {}^{\wp,x}\mathrm{H}_i \, \wp_{i,x} + \sum_{i=1}^{4} {}^{\wp,y}\mathrm{H}_i \, \wp_{i,y} + \sum_{i=1}^{4} {}^{\wp,xx}\mathrm{H}_i \, \wp_{i,xx} + \sum_{i=1}^{4} {}^{\wp,xy}\mathrm{H}_i \, \wp_{i,xy} + \sum_{i=1}^{4} {}^{\wp,yy}\mathrm{H}_i \, \wp_{i,yy} + \ldots\ldots \tag{18}$$

Explicit terms have been reported in Eq. (18) only up to the second order of derivation, but higher-order terms could be included since the order of the interpolating functions is a direct consequence of the order of derivation, which in turns depends on the type of physical constraints enforced.

No derivatives are involved within sub-integrals $\left[\delta \int (.)\,|_{E \longrightarrow}\right]^{EM}$, because the EM model is a C^0 model. Hence, a computationally efficient Lagrangian representation can be used for the EM model, the same discussed forward to develop the present finite element.

The corrective displacements are obtained from Eq. (17) as functions of the nodal unknowns using symbolic calculus. Their expressions hold irrespectively of the loading and boundary conditions, lay-up and geometry. Being obtained once for all in closed-form, they consistently speed up computations.

Former balance equations (17) state that since the consistent displacement field by the OM model satisfies the energy balance, the modified displacements by the EM model satisfy it too, thus they represent an admissible solution by the energy standpoint. Because the EM model is just equivalent form the energy standpoint to the OM model, not in a point form, it just provides a correct solution in terms of displacements, but it could be unable to satisfy all the boundary constraints in a point-wise sense. In particular, the continuity of displacement derivatives and stresses at nodes and sides could not be identically satisfied by the Lagrangian representation used within the EM model. On the contrary, it can be satisfied by the Hermitian representation used for the OM model and by a suited definition of contributions Δ^c, Δ^{c_ip} to displacements. Hence, the EM model just provides the solution in terms of displacement d.o.f. at any point, while all the quantities that contain derivatives, like the stresses, should be determined by the OM model using the analytic expressions obtained through symbolic calculus. These operations are indicated in compact form as:

$$\begin{aligned}
&\left[\delta \int (.)\,|_E\right]^{u^0 EM} \rightarrow \left[\delta \int (.)\,|_E\right]^{u^0 OM};\\
&\left[\delta \int (.)\,|_E\right]^{v^0 EM} \rightarrow \left[\delta \int (.)\,|_E\right]^{v^0 OM};\\
&\left[\delta \int (.)\,|_E\right]^{w^0 EM} \rightarrow \left[\delta \int (.)\,|_E\right]^{w^0 OM};\\
&\left[\delta \int (.)\,|_E\right]^{\gamma_x{}^0 EM} \rightarrow \left[\delta \int (.)\,|_E\right]^{\gamma_x{}^0 OM};\\
&\left[\delta \int (.)\,|_E\right]^{\gamma_y{}^0 EM} \rightarrow \left[\delta \int (.)\,|_E\right]^{\gamma_y{}^0 OM};
\end{aligned} \tag{19}$$

These energy balance equations could be used as a post-processing technique for obtaining a progressively refined solution from the results of a preliminary finite element analysis:

$$\begin{aligned}
&\left[\delta \int (.)\,|_E\right]^{u^0 EM} \Leftrightarrow \left[\delta \int (.)\,|_E\right]^{u^0 OM};\\
&\left[\delta \int (.)\,|_E\right]^{v^0 EM} \Leftrightarrow \left[\delta \int (.)\,|_E\right]^{v^0 OM};\\
&\left[\delta \int (.)\,|_E\right]^{w^0 EM} \Leftrightarrow \left[\delta \int (.)\,|_E\right]^{w^0 OM};\\
&\left[\delta \int (.)\,|_E\right]^{\gamma_x{}^0 EM} \Leftrightarrow \left[\delta \int (.)\,|_E\right]^{\gamma_x{}^0 OM};\\
&\left[\delta \int (.)\,|_E\right]^{\gamma_y{}^0 EM} \Leftrightarrow \left[\delta \int (.)\,|_E\right]^{\gamma_y{}^0 OM};
\end{aligned} \tag{20}$$

like in the former applications of SEUPT, but this is not of interest in this paper. Instead, the objective is the obtainment of accurate results without any post-processing operation. Indeed, Eqs. (19) and (20) are fast carried out using expressions obtained through symbolic calculus, but they however result in an increased

computational burden. A mixed element is developed to overcome the use of Eqs. (19), (20) as the stresses, which are interpolated separately from displacements, are predicted very accurately. The interlaminar stresses that are the ones critical by the viewpoint of strength, stiffness and durability are assumed as nodal d.o.f.

In order to enable the development of such a mixed element, the interlaminar stresses computed by the equivalent displacements of the EM model, here indicated as $\hat{\sigma}^{J}_{xz}$, $\hat{\sigma}^{J}_{yz}$ $\hat{\sigma}^{J}_{yz,}$ are modified incorporating unknown continuity functions $\Lambda^{(k)}$

$$\sigma^{J}_{xz} = \hat{\sigma}^{J}_{xz} + \sum_{k=1}^{S} \Lambda^{(k)} H_k \tag{21}$$

$$\sigma^{J}_{yz} = \hat{\sigma}^{J}_{yz} + \sum_{k=1}^{S} \Theta^{(k)} H_k \tag{22}$$

$$\sigma^{J}_{zz} = \hat{\sigma}^{J}_{zz} + \sum_{k=1}^{S} \Gamma^{(k)} H_k \tag{23}$$

That make continuous the stresses σ^{J}_{xz} , σ^{J}_{yz} , σ^{J}_{zz} at the layer interfaces

$$\sigma^{J(+)}_{xz} = \hat{\sigma}^{J(-)}_{xz} \qquad \sigma^{J(+)}_{yz} = \hat{\sigma}^{J(-)}_{yz} \qquad \sigma^{J(+)}_{zz} = \hat{\sigma}^{J(-)}_{zz} \tag{24}$$

The new continuity functions appearing in (21)-(23) are computed in a straightforward way since now they are not expressed in terms of displacements as before (9), thus no derivatives are involved, differently from [38] where the stresses were obtained from the displacements. Accordingly, their in-plane variation can be assumed in Lagrangian form like for the displacement d.o.f. In the present element, the mid-plane stresses are assumed as stress d.o.f. Once the finite element solution has been found, their variation across the thickness is computed by the constitutive equations (21)-(23) at any z.

It could be noticed that for keeping the model in C^0 form, the continuity of the transverse normal stress $\sigma^{J(+)}_{zz,z} = \sigma^{J(-)}_{zz,z}$ appearing in Eq. (11) has been disregarded in Eq. (24). In order to indirectly fulfil this necessary condition, the interlaminar stresses of the EM model are made consistent with those of the OM model that fulfil (11) by further enforcing the equivalence conditions

$$\begin{aligned}
\left[\int (\sigma_{xz}\,\delta\varepsilon_{xz})\,|_{E\longrightarrow}\right]^{OM} &= \left[\delta\int ((\sigma_{xz} + \Delta\sigma_{xz})\delta\varepsilon_{xz})\,|_{E\longrightarrow}\right]^{EM};\\
\left[\int (\sigma_{yz}\,\delta\varepsilon_{yz})\,|_{E\longrightarrow}\right]^{OM} &= \left[\delta\int ((\sigma_{yz} + \Delta\sigma_{yz})\delta\varepsilon_{yz})\,|_{E\longrightarrow}\right]^{EM};\\
\left[\int (\sigma_{zz}\,\delta\varepsilon_{zz})\,|_{E\longrightarrow}\right]^{OM} &= \left[\delta\int ((\sigma_{zz} + \Delta\sigma_{zz})\delta\varepsilon_{zz})\,|_{E\longrightarrow}\right]^{EM}
\end{aligned} \tag{25}$$

from which the corrective stresses $\Delta\sigma_{xz}$, $\Delta\sigma_{yz}$, $\Delta\sigma_{zz}$ are computed in closed-form once for all again using symbolic calculus. The Hermitian representation for the OM model and a Lagrangian one for the EM model are still used.

3.2 Finite element

Based on the updated version of SEUPT discussed above, an eight-node mixed plate element with standard Lagrangian interpolating functions is developed. The terms mixed is used to indicate that the master fields are internal fields. As nodal d.o.f. the nodal components of displacements $u(x,y,z)^{EM}$, $v(x,y,z)^{EM}$, $w(x,y,z)^{EM}$ and the stresses σ^{J}_{xz} , σ^{J}_{yz} , σ^{J}_{zz} at the reference middle plane are assumed (see Figure 1a), as mentioned above. In this way, only the continuity of interlaminar stresses is considered. It should be noticed that the continuity of stress components parallel to an interface should not be forced, being physically incorrect for multi-layered structures.

Since stresses and displacements can be varied separately, the Hellinger-Reissner multi-field principle:

$$\delta\Pi_{HR} = \delta\int_V \sigma_{ij}\varepsilon^{u}_{ij} - \frac{1}{2}\sigma_{ij}S_{ijkl}\sigma_{kl}\,dV - \delta\left(\int_V b_i u_i\,dV + \int_S t_i u_i\,dS\right) = \delta U_{HR} - \delta W_{HR} \tag{26}$$

is the governing functional. The symbol S_{ijkl} represent the components of the elastic compliance tensor, the inverse of the elastic stiffness tensor C_{ijkl}, so that $S_{ijkl}\,\sigma_{kl} = \varepsilon^{\sigma}_{ij}$ represents the strains obtained from the stress-strain relations

Accordingly, ½ $\sigma_{ij}\,S_{ijkl}\,\sigma_{kl}$ represents the complementary energy density in term of the master stress field. The slave fields are the strains $\varepsilon^{\sigma}_{ij}$ and ε^{u}_{ij} :

$$\varepsilon^{\sigma}{}_{ij} = C_{ijkl}\sigma_{kl}; \quad \varepsilon^{u}{}_{ij} = \frac{1}{2}\left(u_{i,j} + u_{j,i}\right) \tag{27}$$

The vector of the nodal d.o.f. for the generic element (e) in its natural reference system ^{J} is thus represented by:

$$\{q_e\}^T = \left\{ \{u_i{}^{EM}\}_{(e)}, \{v_i{}^{EM}\}_{(e)}, \{w_i{}^{EM}\}_{(e)}, \{\sigma_{xzi}{}^{J}\}_{(e)}, \{\sigma_{yzi}{}^{J}\}_{(e)}, \{\sigma_{zzi}{}^{J}\}_{(e)} \right\}^T \tag{28}$$

where $_i$ is the node number (i=1, 8).

Nevertheless the transverse normal stress gradient is not assumed as a functional d.o.f., in order to preserve from stress derivatives as nodal d.o.f., the numerical results will show that the boundary conditions (7) will be spontaneously satisfied since many physical constraints can be point-wise enforced, thus it is sufficient to enforce remaining ones in a weak form to obtain results in a very good agreement with exact solutions, as shown by Icardi and Atzori [48] and Icardi [49] using solid and a layerwise plate elements, respectively. Accurate solutions were obtained either for regular problem involving laminates and sandwiches (even when they are thick and the properties of their constituent layers are distinctly different), or singular problems like the case of a two material wedge with certain side angles and materials with dissimilar properties. Even no case was found where the lack of the enforcement of the continuity of the transverse normal stress gradient gave incorrect results, it could be noticed that this continuity can be accounted for by a suited definition of contributions (13), (13)'.

Hereon the basic steps towards derivation of the present element will be summarized. Details concerning standard aspects will be omitted, being explained in common textbooks. The displacements, represented in synthetic form as D and the interlaminar stresses as S, are interpolated separately as:

$$D = \sum_{1}^{8} D^{e} N^{e}_{disp}; \quad S = \sum_{1}^{8} S^{e} N^{e}_{stress} \tag{29}$$

since the basic assumption is that the intra-element equilibrium conditions are met in an approximate integral form, thus differently to customary mixed elements the nodal stresses are not required to be represented in a point-wise self-equilibrating form. Accordingly, the same inner representation in x, y can be assumed both for displacements and stresses, i.e. $N^{e}_{disp} = N^{e}_{stress} = N$. In the present case, computationally efficient parabolic Lagrange's polynomials are employed. This directly follows form the Hellinger-Reissner governing functional (26), since no second or higher-order derivatives of the primary variables (28) are involved, thus no derivatives of the d.o.f should be chosen as nodal quantities, consequently C^1 or higher-order interpolating functions are unnecessary.

The option of using the same representation was chosen because it makes easier the development of mixed elements without compromising accuracy, as shown since the pioneering papers by Loubignac et al. [39] and Nakazawa [40] and since an identical interpolation for displacements and stresses is acceptable by the viewpoint of numerical stability of mixed elements, as discussed forward.

The present element is not intended for use with nearly incompressible materials, because the mean stresses, i.e. the pressure, are not treated as independent from the total stresses. However, numerical tests demonstrated that accurate results can be obtained in these cases, as shown for a two-material wedge with one half incompressible [48].

The following standard interpolating functions are used for corner nodes (1, 2, 3, 4)

$$N_i = \frac{1}{4}(1 - \xi_{0i})(1 + (-1)^{i-1}\eta_{oi})(\xi_{oi} \cdot (-1)^{i-1}\eta_{oi} - 1) \tag{30}$$

and at mid-side nodes (5, 6, 7, 8)

$$\begin{aligned} N_5 &= \frac{1}{2}(1 - \eta_{o5})(1 - \xi_{05}{}^2) \\ N_6 &= \frac{1}{2}(1 - \eta_{o6}{}^2)(1 + \xi_{06}) \\ N_7 &= \frac{1}{2}(1 + \eta_{o7})(1 - \xi_{07}{}^2) \\ N_8 &= \frac{1}{2}(1 - \eta_{o8}{}^2)(1 - \xi_{08}) \end{aligned} \tag{31}$$

This parabolic representation is chosen just in order to obtain accurate results with a relatively coarse meshing.

Representations (30) and (31) meets the compatibility condition, as the displacements and the interlaminar stresses are continuous inside and at the edges of the elements. Consistency is also ensured at the interfaces. However, since the membrane stresses are not assumed as nodal d.o.f., they are not continuous across the interfaces, as mentioned above. But this incompatibility should not be removed since the theory of elasticity prescribes that in-plane stresses are discontinuous across the material interfaces. Of course, *z* should be the coordinate in the direction across the layer stack-up, while *x*, *y* lie in a plane parallel to the plane of layers. With this assumption, the stresses within the finite element are represented as:

$$\{\sigma\} = \begin{bmatrix} & [\hat{D}] & \\ \{0\} \{0\} \{0\} & \{N_{stress}\} & \{0\} \{0\} \\ \{0\} \{0\} \{0\} & \{0\} \{N_{stress}\} & \{0\} \\ \{0\} \{0\} \{0\} & \{0\} \{0\} & \{N_{stress}\} \end{bmatrix} \{q_{(e)}\} \tag{32}$$

$[\hat{D}]$ being the matrix that defines the in-plane stress components

$$\{\sigma_{xx} \ \sigma_{yy} \ \sigma_{xy}\}^T = [S^*][B]\{q_{(e)}\} = [\hat{D}]\{q_{(e)}\} \tag{33}$$

$[S^*]$ being the related elastic coefficients and $[B]$ the derivatives of the shape functions.

The "stiffness" matrix is derived in a straightforward, standard way from the internal energy functional U_{HR} substituting the discretized displacements and stresses:

$$\{q_{(e)}\}^T [\hat{K}]^e \{q_{(e)}\} = \{q_{(e)}\}^T \int_V [\hat{C}]^T [B] - \frac{1}{2}[\hat{C}]^T [S][\hat{C}] dV \{q_{(e)}\} \tag{34}$$

while the vector of generalized nodal forces is obtained from the work of forces W_{HR} substituting the finite element discretization of displacements. Assembly of the stiffness matrix and of the vector of nodal forces is carried out with the standard techniques.

The integrals defining the stiffness matrix and the nodal force vector are computed either in exact form using symbolic calculus, so to avoid numerical instabilities, or through Gaussian integration, because a reduced integration scheme could be used (even if it was never applied for obtaining the numerical results given next).

To standardize the computation of integrals, as customarily a topological transformation is carried out from the physical plane (*x, y*) to the natural plane (η, θ) that transforms any quadrilateral element into a square element with unit sides

$$x = \sum_{i=1}^{8} x_i N_i \quad \text{and} \quad y = \sum_{i=1}^{8} y_i N_i \tag{35}$$

In this way, the Jacobian matrix

$$[J] = \begin{bmatrix} \frac{\partial x}{\partial \xi} & \frac{\partial y}{\partial \xi} \\ \frac{\partial x}{\partial \eta} & \frac{\partial y}{\partial \eta} \end{bmatrix} \tag{36}$$

necessary for obtaining the physical derivatives $\frac{\partial}{\partial x}$, $\frac{\partial}{\partial y}$ from the derivatives $\frac{\partial}{\partial \xi}$, $\frac{\partial}{\partial \eta}$ over the natural plane

$$\begin{Bmatrix} \frac{\partial}{\partial x} \\ \frac{\partial}{\partial y} \end{Bmatrix} = [J]^{-1} \begin{Bmatrix} \frac{\partial}{\partial \xi} \\ \frac{\partial}{\partial \eta} \end{Bmatrix} \tag{37}$$

can be computed in an efficient way. As well known, stability, solvability and locking phenomena of mixed elements are governed by rather complex mathematical relations (see, Babuska [50] and Brezzi [51]). In particular, certain choices of the shape functions could not yield meaningful results. A necessary condition for solvability, which in most cases suffices for acceptability of mixed elements, is that the number of displacement d.o.f. n_u must be equal (like in the present element), or larger than the number of stress d.o.f. n_σ. A sufficient condition for solvability (see, Olson [52]) is that for a single element that is free of boundary conditions the

number of zero eigenvalues of $[\hat{K}]^e$ is equal to the number of rigid body modes, the total number of positive eigenvalues is equal to the number of stress d.o.f., while the total number of zero and negative eigenvalues is equal to the number of displacement d.o.f. However, even when these admissibility tests are passed, erroneous, highly oscillating results could be obtained. For homogeneous, isotropic materials this problem is usually overcome by relaxing the stress continuity impositions, but in laminated and sandwich composites the interfacial stress continuity conditions cannot be skipped, otherwise the physical meaning of solution is lost. The opposite possibility is that nevertheless these tests are failed, mixed elements could be effective for solving regular problems. Accordingly, mixed elements should be tested considering sample cases with the same features of the practical cases to be solved, whose solution in exact or approximate numerical form is available for comparisons.

In the forthcoming section, solvability, convergence and accuracy tests of the element will be presented, considering laminates and sandwiches with simply-supported and clamped edges, test cases with geometric/material discontinuities and intricate stress variation across the thickness, for which either exact solution in closed-form or in numerical form are available in the literature for comparison.

IV. NUMERICAL APPLICATIONS AND DISCUSSION

Accuracy, convergence and solvability of the present finite element will be assessed comparing its results with exact/numerical solutions of sample test cases available in the literature. Aiming at enhancing the intricacies of stress and displacement fields, cases with strongly asymmetrical lay-ups, clamped edges, distinctly different properties of layers and high face-to-core stiffness ratios will be analysed.

For what concerns the through-the-thickness discretization, please notice that all results presented throughout this section are obtained considering a number of computation layers equal to the number of physical layers, as well as a third order representation of the in-plane displacement and a fourth order representation of the transverse displacement for the contributions of Eq. (3).

4.1 Solvability and convergence

First of all, an eigenvalue solvability test is presented. In accordance with Olson [52], this test is carried out over a single finite element in the shape of a square plate with sides of unit length and free of boundary conditions (thickness should be sufficiently small to have a plane-stress, plane-strain problem). The same isotropic material analysed by Mijuca [53] in a similar test is here considered with the following mechanical properties E_1 (= E_2 = E_3) =1 and υ=0.3. The results of this test are reported in Table 1.

According to the rules discussed above, the finite element shows a number of zero eigenvalues equal to the number of rigid body modes. At the same time, the total number of positive eigenvalues is the same as the number of generalized stress d.o.f. and the total number of zero and negative eigenvalues is equal to the number of generalized displacement d.o.f. These conditions being satisfied in the test, the sufficient condition for solvability is passed by the present mixed element that thus can be applied to solution of other sample cases, in order to verify its behaviour in problems of practical interest.

Aiming at verifying the convergence rate of the present element, the sample case analysed by Zhen et al. [23] is considered, with a length-to thickness ratio of 4. The analysis is carried out for a plate that undergoes a bisinusoidal loading and is simply supported at the edges. The mechanical properties of the constituent material considered for this case are: E_L/E_T=25; G_{LT}/E_T=0.5; G_{TT}/E_T=0.2; υ_{LT}=0.2 and the stacking sequence is [15°/-15°]. Table 2 reports the through-the-thickness variation of the in-plane stress for different meshing schemes by the present element and by Zhen et al. [23], normalised as follows:

$$\bar{\sigma}_x = \frac{\sigma_x\left(\frac{L_x}{2}, \frac{L_y}{2}, z\right) h^2}{p^0 L_x^2}; \tag{38}$$

The results of Table 3 show that the present element is as accurate as the 3D solutions reported in Ref. [23], and even with rather coarse meshing the accuracy is satisfactory. This confirms that mixed elements are accurate without requiring a very fine discretization as already focused in the literature.

As a further assessment of the convergence rate, the laminated [0°/90°/0°] plate for which Vel and Batra computed the exact 3D solution in Ref. [42] is considered. The plate is square and has a length to thickness ratio (L_x/h) of 5. The mechanical properties of the constituent material are the same as in the previous case. For what concerns boundary and loading conditions, the plate is simply supported on two opposite edges, clamped on the other two and it is undergoing a bi-sinusoidal normal load with intensity p^0 on the upper face, whereas the bottom one is traction free. It could be noticed that the structural model can treat clamped edges because a non-vanishing transverse shear resultant can be obtained with all displacement d.o.f. vanishing with an appropriate choice of variable kinematics contribution Δ^i. The results of Table 3 are normalized according to [42] as:

$$\bar{\sigma}_{xz} = \frac{10 \cdot H \cdot \sigma_{xz}\left(\frac{L_x}{8}, \frac{L_y}{2}, z\right)}{p^0 L_x}; \quad \bar{w} = \frac{100 E_T \cdot h^3}{p^0 L_x^4} w(0,0,z) \tag{39}$$

Like in the previous case, the numbers in square brackets represent the computational time required to perform the analysis on a laptop computer with a 1800 GHz double-core processor and 2.96 GB RAM. The numerical results show that the present finite element provides very accurate results as compared to the exact 3D solution. Also in this case it is shown that even with a rather coarse discretization the accuracy is good.

4.2 Laminates and sandwiches with different boundary conditions

Hereafter different cases of analysis available in the literature are considered in order to exhaustively verify the accuracy of the present mixed element.

4.2.1 Simply supported sandwich beam

Aiming at assessing the capability of present element to smoothly represent the through-the-thickness stress and displacement distributions even when material properties of constituent layers abruptly change, it is considered an extremely thick, simply supported sandwich beam loaded by a sinusoidal transverse loading. Using the present element, the cellular structure of core could be discretized into details, but this is not done because the results used for comparisons have been determined considering the sandwich beam as a sandwich-like, multi-layered, homogenized structure where the core is described as a quite compliant intermediate thick layer and faces as thin, stiff layers. Therefore, it represents for the finite element a laminate having distinctly different properties of layers. Of course, this approach can be considered whenever it is supposed that local buckling phenomena do not occur in the cellular structure, as they cannot be accounted for by the homogenized description adopted. This approach will be used in all the following applications to sandwiches, since it was used also to obtain the reference solutions.

Faces are laminates with stacking sequence (MAT 1/2/3/1/3), where the constituent material have the following mechanical properties: MAT 1: E_1=E_3=1 GPa, G_{13}=0.2 GPa, υ_{13}=0.25; MAT 2: E_1=33 GPa, E_3=1 GPa, G_{13}=0.8 GPa, υ_{13}=0.25; MAT 3: E_1=25 GPa, E_3=1 GPa, G_{13}=0.5 GPa, υ_{13}=0.25. The core is made of MAT4, whose mechanical properties are as follows: MAT 4: E_1=E_3=0.05 GPa, G_{13}=0.0217 GPa, υ_{13}=0.15. The length to thickness ratio of the beam is 4 and the thickness ratios of the constituent layers are $(0.010h/0.025h/0.015h/0.020h/0.030h/0.4h)_s$. Due to the different thickness of constituent layers and to their distinctly different material properties, strong 3D effects rise for this case. However, in order to introduce the further complication of a strong unsymmetry, cases are presented with E_3 modulus of the core and upper face layers reduced by a 10^2 factor. As shown by the exact solution computed in [43] using the technique described in [41], this produces an opposite variation of the transverse shear stress across the upper and lower faces that is problematic to capture in the simulations.

The results for this case reported in Figure 2 are normalized as follows:

$$\bar{\sigma}_{xz} = \frac{\sigma_{xz}(0,z)}{p^0}; \quad \bar{\sigma}_z = \frac{\sigma_z\left(\frac{L_x}{2}, z\right)}{p^0}; \quad \bar{u} = \frac{u(0,z)}{hp^0}; \quad \bar{w} = \frac{w\left(\frac{L_x}{2}, z\right)}{hp^0}; \tag{40}$$

Figure 2 a represents the through-the-thickness variation of the shear stress $\bar{\sigma}_{xz}$ while Figure 2b represents $\bar{\sigma}_z$, and Figure 2c and 2d represent, respectively, the through-the-thickness variation of the in-plane displacement $\bar{u}$, and of the transverse displacement $\bar{w}$. All the results are obtained considering 150 elements over the beam, as shown by the inset reported in Figure 2. In this case, the analysis requires 16 s. The results of Figure 2 show that the present mixed element can obtain results as accurate as the exact 3D solutions even when the constituent material have abruptly changing mechanical properties that determine strong asymmetrical stress and displacement fields, using a reasonably fine mesh.

4.2.2 Simply supported sandwich plate

Still aiming at verifying the accuracy of the present mixed element in describing stress and displacement fields of structure with strong asymmetric effects, it is now considered the sandwich plate for which Brischetto et al. [44] compute the exact 3D solution. In this case, the asymmetry is due to differences between the thickness ratios of upper (symbol us) and lower (symbol ls) faces, which are respectively h_{ls} =h/10; h_{us} =2h/10 with respect to the thickness h of the plate. The thickness ratio of the core (symbol c) is h_c =7h/10. The constituent material has the following mechanical properties: E_{ls}/E_{us}=5/4, E_{ls}/E_c=10^5, ν_{ls}= ν_{us}=ν_c=ν= 0.34. For what concerns loading and boundary conditions, the plate is simply supported and it is undergoing bi-sinusoidal loading. The plate has a length to thickness ratio L_x/h=4 and a length-side ratio L_y/L_x=3. Figure 3

reports the comparison between the exact solutions presented in Ref. [44] and the numerical results for what concerns the in-plane displacement and the transverse shear stress computed using the present finite element, normalized as follows:

$$\bar{\sigma}_{xz} = \frac{\sigma_{xz}\left(0, \frac{L_y}{2}, z\right) h}{q^0 L_x}; \quad \bar{u} = \frac{u\left(0, \frac{L_y}{2}, z\right) E_c h^2}{q^0 L_x^3} \tag{41}$$

The results of Figure 3 have been obtained considering 300 elements and modelling only a quarter of the plate (see inset in Figure 3). Also in this case, despite the asymmetry of the structure, the present mixed element can obtain results in a very good agreement with the exact 3D solution at any point with the right gradients at the interfaces, requiring just 35 s to perform the analysis.

4.2.3 Cantilever sandwich beam

In order to more deeply assess whether the present finite element can accurately describe the stress field also with clamped edges, the cantilevered sandwich beam subjected to a uniform transverse loading of Ref. [45] is considered. The beam has laminated faces made of unidirectional Carbon-Epoxy laminates (E_1= 157.9 GPa, E_2=E_3= 9.584 GPa, G_{12}= G_{13}= 5.930 GPa, G_{23}= 3.277 GPa, ν_{12}= ν_{13}= 0.32, ν_{23}= 0.49), while the core is made with a PVC foam core (E= 0.1040 GPa, ν= 0.3). According to [45], a length-to-thickness ratio of 10 is assumed, while the thickness ratios of the constituent layers are 0.1h/0.8h/0.1h.

Figure 4 reports the through-the-thickness distribution of the transverse shear stress and the meshing scheme adopted. The stress is normalised as follows:

$$\bar{\sigma}_{xz} = \frac{2h}{L_x p^0} \sigma_{xz}\left(\frac{L_x}{5}, \frac{L_y}{2}, z\right) \tag{42}$$

The results of Figure 4 confirm the accuracy of the present mixed element as it obtains results in good agreement with those by the 3D finite element of Ref. [45]. For what concerns the computational times, only 17.5 s are required to perform the analysis. Thus, even if the model of Eqs. (1) and its EM counterpart have as functional d.o.f. the displacements and the transverse shear rotations at the middle plane, it does not give poor results for clamped structures like the equivalent single-layer models with classical five mid-plane d.o.f., because enforcing the vanishing of displacements at the clamped edges does not necessarily mean that the transverse shear stress resultant also vanishes. Also in this case, quite accurate results are obtained with a not extremely refined meshing.

4.2.4 Cantilever piezo-actuated beam

With the goal of verifying the accuracy of the present mixed element for clamped structure with abruptly changing material properties, the cantilever piezoactuated beam formerly studied by Robbins and Reddy [46] is considered. The structure is made of an underlying aluminium beam substructure (thickness 15.2 mm), an adhesive film (thickness 0.254 mm) and a piezoactuator (thickness 1.52) bonded on the upper face. The material properties of the constituent materials are: E_{alum}=69 GPa, G_{alum}=27.5 GPa, υ_{alum}=0.25; E_{ad}=6.9 GPa, G_{ad}=2.5 GPa, υ_{ad}=0.4; E_{1piezo}=69 GPa, E_{3piezo}=48 GPa, G_{piezo}=21 GPa, $\upsilon_{13piezo}$=0.25, $\upsilon_{31piezo}$=0.175. Piezoactuator, adhesive and aluminium substructure form an unsymmetrical three material laminate that exhibits bending/extension coupling. The only acting loads for this case are the self-equilibrating loads induced by the piezoactuator. A bending deformation is provided by applying an actuation strain of 0.001 to the piezoelectric layer via an applied electric field. The length of the beam is 152 mm.

Figure 5a shows the spanwise variation of membrane, transverse shear and transverse normal stresses near the top of the aluminium substrate (z1= 6.61 mm) and at the centre of the adhesive layer (z2= 6.84 mm), while Figure 5b represents the stress fields across the thickness close to the free edge. The stress distributions are presented in the following normalized form, according to [46], where the exact solution for this case is presented:

$$\bar{\sigma}_x = \frac{A_{tot} \cdot \sigma_x \cdot 10^3}{(E_1 A)_{alum} + (E_1 A)_{ad} + (E_1 A)_{piezo}};$$

$$\bar{\sigma}_z = \frac{A_{tot} \cdot \sigma_z \cdot 10^3}{(E_3 A)_{alum} + (E_3 A)_{ad} + (E_3 A)_{piezo}}; \tag{43}$$

$$\bar{\sigma}_{xz} = \frac{A_{tot} \cdot \sigma_{xz} \cdot 10^3}{(G_{13} A)_{alum} + (G_{13} A)_{ad} + (G_{13} A)_{piezo}};$$

the subscripts *alum*, *ad*, *piezo* and *tot* being used to indicate the cross sectional area and the elastic moduli of the substrate structure, of the adhesive and of the piezoactuator layer, respectively, which are considered as isotropic materials.

The results of Figure 5 show that the present mixed element is accurate also for this case in which a singular-like stress filed arise. In details, in Figure 5a it can be noticed that the element accurately describes the unwanted dangerous stress concentrations that appear at the free end of the beam that could cause debonding of the piezoactuator in service, without showing erroneous oscillating results close to the edge. Also the through-the-thickness distribution of the stresses is well described as shown in Figure 5b, in particular the mixed element is capable to capture the sharp variation of the bending stress that can be seen near the bonding layer also in this case with a reasonably refined meshing. For this case of analysis the present element required 47 s.

4.2.5 Double lap joint with aluminum adherents

As an application to a practical case, it is now considered the joint with aluminium 2024 T3 adherents analysed by Nemes and Lachaud [47]. The adhesive is epoxy resin REDUX 312/5 (E=27 GPa, G=1 GPa, υ=0.35) and it is 0.1 mm thick. The outer layer is 2 mm thick, the inner one is 4 mm thick, and the overlap length is 50 mm. A pressure load in *x* with intensity 1 N/mm is applied to the inner adherent, while the lower and the upper adherents are clamped at right and left bounds.

This case is treated as a plate with step variable properties in the finite element analysis, the adherents being constituted by a homogeneous and isotropic medium, while the overlap is constituted by and a three-layer laminate. Of course, all continuity functions vanish in the adherents, while they exist at the two interface between adhesive and lower adherent, adhesive and upper adherent. The piecewise contributions of Eqs. (13) – (13') are considered in this case in order to make continuous the stresses and their gradients at the interface of adherents and overlap, where properties vary from a single layer to a three-layer plate. Specifically, the terms of first order are aimed at fulfilling the continuity of the stresses; those of second order are aimed at satisfying the continuity of the stress gradients. The variable kinematic contributions across the thickness (3) in this case are aimed at satisfying also the stress boundary conditions at the ends of the overlap Ω_1, Ω_2:

$$N = \int_{\Omega_i} \sigma_{xx} dz = -\int_{\Omega_i} \sigma_{xz} dx; \quad M = \int_{\Omega_i} z\, \sigma_{xx} dz; \quad Q = \int_{\Omega_i} \sigma_{xz} dz; \tag{44}$$

N, *M*, *Q* being the in-plane, bending and shear resultants, respectively, along with the stress-free boundary conditions

$$\begin{aligned} &\sigma_{xz} = 0; \quad \int_{\Omega_i} \sigma_{xz} dz = 0; \quad \sum\nolimits_k \int_{\Omega_k} \sigma_{xz} dz = 0; \\ &\sigma_{xx} = 0; \quad \int_{\Omega_i} \sigma_{xx} dz = 0; \quad \sum\nolimits_k \int_{\Omega_k} \sigma_{xx} dz = 0; \end{aligned} \tag{45}$$

at the free edges of the overlap. The results for this case are presented in Figure 6, where the in-plane variations of the peel stress and of the shear stress are reported. They are obtained requiring 69 s to perform the analysis and modelling the whole joint with 600 elements with 2 concentrations of elements across the variation of adherents, as shown by the inset. Also this case confirms the accuracy of the mixed element, which correctly describes the stress peaks near the end of the overlap, which can have detrimental effects on the service life of the joint.

V. CONCLUDING REMARKS

A quadrilateral, eight-node, mixed plate element for analysis of laminates with general lay-up and sandwich composites with high face-to-core stiffness ratios and distinctly different properties of top and bottom faces, was developed. It has the displacements and the interlaminar stresses at the reference mid-plane as nodal d.o.f. Its structural model is a 3D physically based zig-zag one with fixed functional d.o.f. (the three displacements and the two transverse shear rotations at the mid-plane), whose representation can be refined across the thickness without increasing the unknowns. This model also allows the material properties to suddenly vary in the in-plane directions. A piecewise variable transverse displacement is assumed, since it has a significant bearing for certain problems, e.g. when temperature gradients cause thermal stresses, for the crushing behaviour of sandwiches, around geometric and material discontinuities and close to loading points. The expressions of continuity functions and higher-order coefficients of displacements incorporated in order to a priori satisfy all the physical constraints are determined once for all in closed-form as expressions of the five d.o.f. and of their spatial derivatives using a symbolic calculus tool.

The energy updating technique (SEUPT) is used to convert the d.o.f. derivatives without resulting in an increased number of variables. It allows obtainment of an equivalent C^0 version of the zig-zag model that is used to develop the finite element. The three displacements and the three interlaminar stresses at the mid-plane are assumed as nodal d.o.f. All these quantities are interpolated using the same standard serendipity shape functions

because this simplifies the development of the element without resulting in any accuracy loss, as shown by the comparison with exact solutions of sample cases. Consequently, equilibrium equations are satisfied just in approximate integral form.

Accuracy, solvability and convergence were assessed considering multi-layered monolithic structures with cross-ply and angle-ply lay-up and sandwich-like structures with also abruptly changing properties of faces, with different loading and boundary conditions, for which exact solutions are available. The structural model and the mixed formulation make easier the enforcement of stress-boundary conditions, either because the coefficients of higher-order terms can be determined from enforcement of these conditions, or the stresses are nodal variables. An application was presented also to an adhesively bonded joint, which represents a case with step varying properties, the adherents and the overlap being seen as interfaced plates with a different lay-up. The element was shown to be fast convergent and its results were not affected by the mesh configuration, as accurate predictions were obtained also with rather coarse meshes. It appears as a good alternative to the ones to date available in the literature, as it offers a good accuracy with the minimal number of unknown nodal variables at an affordable cost.

REFERENCES

[1]. J. Sliseris, K. Rocens K. Optimal design of composite plates with discrete variable stiffness. Composite Structures, 98: 15 – 23, 2013.

[2]. J. Barth. Fabrication of complex composite structures using advanced fiber placement technology. In Proc. 35th International SAMPE Symposium, 35, pages 710-720Anaheim, CA 1990.

[3]. C.S. Sousa, P.P. Camanho, A. Suleman. Analysis of multistable variable stiffness composite plates. Composite Structures, 98: 34 – 46, 2013.

[4]. S. Honda, T. Igarashi, Y. Narita, Multi-objective optimization of curvilinear fiber shapes for laminated composite plates by using NSGA-II. Composites: Part B, 45: 1071 – 1078, 2013.

[5]. D. Càrdenas, H. Elizalde, P. Marzocca, F. Abdi, L. Minnetyan, O. Probst. Progressive failure analysis of thin-walled composite structures. Composite Structures 95: 53-62, 2013.

[6]. A. Chakrabarti, H.D. Chalak, M.A. Iqbal, A.H. Sheikh, A new FE model based on higher order zig-zag theory for the analysis of laminated sandwich beam soft core. Composite Structures 93: 271-279, 2011.

[7]. M.S. Qatu, R.W. Sullivan, W. Wang, Recent research advances on the dynamic analysis of composite shells: 2000-2009, Composite Structures 93: 14-31, 2010.

[8]. Y. Zhang, C. Yang, Recent developments in finite element analysis for laminated composite plates. Composite Structures 88: 147-157, 2009.

[9]. H. Matsunaga, A comparison between 2-D single-layer and 3-D layerwise theories for computing interlaminar stresses of laminated composite and sandwich plates subjected to thermal loadings. Composite Structures 64: 161-177, 2004.

[10]. W.J. Chen, Z. Wu, A selective review on recent development of displacement-based laminated plate theories. Recent Pat. Mech. Eng., 1: 29–44, (2008).

[11]. I. Kreja, A literature review on computational models for laminated composite and sandwich panels. Central European Journal of Engineering, 1: 59 – 80, 2011.

[12]. M. Tahani, Analysis of laminated composite beams using layerwise displacement theories. Composite Structures, 79: 535-547, 2007.

[13]. M. Gherlone, On the use of zigzag functions in equivalent single layer theories for laminated composite and sandwich beams: a comparative study and some observations on external weak layers. J. of Appl. Mech., 80, 2013.

[14]. E. Carrera, F. Miglioretti, M. Petrolo, Accuracy of refined finite elements for laminated plate analysis. Composite Structures, 93: 1311-1327, 2011.

[15]. R.P. Shimpi, A.V. Ainapure, A beam finite element based on layerwise trigonometric shear deformation theory. Composite Structures, 53: 153-162, 2011.

[16]. D. Elmalich, O. Rabinovitch. A higher-order finite element for dynamic analysis of soft-core sandwich plates. J. Sandwich Struct. & Mat., 14: 525-555, 2012.

[17]. F. Dau, O. Polit, M. Touratier. C^1 plate and shell elements for geometrically nonlinear analysis of multi-layered structures. Composite Structures, 84: 1264-1274, 2006.

[18]. S.V. Hoa, W. Feng. Hybrid finite element method for stress analysis of laminated composites. Kluwer Academic Publ., 1998.

[19]. W. Feng, S.V. Hoa. Partial hybrid finite elements for composite laminates. Finite Elements in Analysis and Design, 30: 365-382, 1998.

[20]. Y.M. Desai, G.S. Ramtekkar, A.H. Shah. Dynamic analysis of laminated composite plates using a layer-wise mixed finite element model. Composite Structures, 59: 237-249, 2003.

[21]. G.S. Ramtekkar, Y.M. Desai, A.H. Shah. Application of a three-dimensional mixed finite element model to the flexure of sandwich plate. Comp. & Struct., 81: 2183-2198, 2003.

[22]. C.W.S To, M.L. Liu. Geometrically nonlinear analysis of layerwise anisotropic shell structures by hybrid strain based lower order elements. Finite Elements in Analysis and Design, 37: 1-34, 2001.

[23]. W. Zhen, S.H. Lo, K.Y. Sze, C. Wanji. A higher order finite element including transverse normal strain for linear elastic composite plates with general lamination configurations. Finite Elements in Analysis and Design, 48 :1346 – 1357, 2012.

[24]. C. Cao, A. Yu, Q.-H. Qin. A novel hybrid finite element model for modelling anisotropic composites, Finite Elements in Analysis and Design 64: 36 – 47, 2013.

[25]. P. Dey, A.H. Sheikh, D. Sengupta. A new element for analysis of composite plates. Finite Elements in Analysis and Design, 82: 62 – 71, 2014.

[26]. J.N. Reddy. Mechanics of Laminated Composite Plates and Shells: Theory and Analysis. CRC Press, 2003.

[27]. M. Di Sciuva. Development of an Anisotropic, Multilayered, Shear-Deformable Rectangular Plate Element. Composite Structures, 21: 789–796, 1985.

[28]. C.N. Phan, Y. Frostig, G.A. Kardomateas. Free vibration of unidirectional sandwich panels, Part II: Incompressible core. J. Sandwich Struct. & Mat., 15: 412-428, 2013.

[29]. V.R. Aitharaju, R.C. Averill. C0 zig-zag finite element for analysis of laminated composites beams. J. of Eng. Mech., 125: 323-330, 1999.
[30]. X.Y. Li, D. Liu. Generalized laminate theories based on double superposition hypothesis. Int. J. Num. Meth. Eng., 40, 1197–212, 1997.
[31]. W. Zhen, C. Wanji. A C0-type higher-order theory for bending analysis of laminated composite and sandwich plates. Composite Structures, 92: 653–661, (2010).
[32]. M. Cho, K.O. Kim, M.H. Kim. Efficient higher-order shell theory for laminated composites. Composite Structures, 34: 197–212, 1996.
[33]. R. Sahoo, B.N. Singh. A new shear deformation theory for the static analysis of laminated composite and sandwich plates. Int. J. of Mech. Sci., 75: 324-336, 2013.
[34]. U. Icardi, F. Sola. Development of an efficient zig-zag model with variable representation of displacement across the thickness. J. Eng. Mech., 140: 531-541, 2014.
[35]. U. Icardi. Multilayered plate model with "adaptive" representation of displacements and temperature across the thickness and fixed d.o.f. Journal of Thermal Stresses, 34: 958–984, 2011.
[36]. U. Icardi. C^0 plate element based on strain energy updating and spline interpolation, for analysis of impact damage in laminated composites. International Journal of Impact Engineering, 34: 1835–1868, 2007.
[37]. U. Icardi. Extension of the Strain Energy Updating Technique to a multilayered shell model with adaptive displacements and fixed DOF. J. Aerosp. Eng., 26: 842-854, 2013.
[38]. U. Icardi, F. Sola. C0 layerwise model with fixed d.o.f. and variable in and out-of-plane kinematics by SEUPT. Int. J. of Research Studies in Science, Engineering and Technology (IJRSST) IN PRESS
[39]. C. Loubignac, C. Cantin, C. Touzot. Continuous stress fields in finite element analysis. AIAA Journal, 15: 1645-1647, 1978.
[40]. S. Nakazawa. Mixed finite elements and iterative solution procedures. Iterative Methods in Non-Linear Problems. Pineridge, 1984.
[41]. N.J. Pagano. Exact solutions for composite laminates in cylindrical bending. J. Compos. Mater. 3, 398–411, 1969.
[42]. S.S. Vel, R.C. Batra. Analytical solution for rectangular thick laminated plates subjected to arbitrary boundary conditions. AIAA J., 11: 1464-1473, 1999.
[43]. U. Icardi. Higher-order zig-zag model for analysis of thick composite beams with inclusion of transverse normal stress and sublaminates approximations. Composites: Part B, 32: 343-354, 2001.
[44]. S. Brischetto, E. Carrera, L. Demasi. Improved response of asymmetrically laminated sandwich plates by using Zig-Zag functions. J. of Sand. Structures and Materials, 11: 257- 267, 2009.
[45]. A. Tessler, M. Di Sciuva, M. Gherlone. Refined zig-zag theory for laminated composite and sandwich plates. Technical Report No. TP-2009-215561, NASA, Langley, VA, 2009.
[46]. D.H. Robbins, J.N. Reddy. Analysis of piezoelectrically actuated beams using a layer-wise displacement theory. Comp. & Struct., 41: 265–279, 1991.
[47]. O. Nemes, F. Lachaud. Double-lap adhesive bonded-joints assemblies modeling. Int. J. of Adhesion and Adhesives, 30: 288-297, 2010.
[48]. U. Icardi. A. Atzori. Simple, efficient mixed solid element for accurate analysis of local effects in laminated and sandwich composites. Advances in Eng. Software, 32: 843-849, 2004.
[49]. U. Icardi. Layerwise mixed element with sublaminates approximation and 3D zig-zag field, for analysis of local effects in laminated and sandwich composites. Int. J. for Num. Meth in Eng, 70: 94-125, 2007.
[50]. I. Babuska. The finite element method with Lagrange multipliers. Numerical Mathematics, 20: 179-192, 1973.
[51]. F. Brezzi. On the existence, uniqueness and approximation of saddle point problems arising from Lagrangian multipliers. Revue Francaise D'Automatique, Informatique, Recherche Operationelle, Analyse Numerique, 8: 129-151, 1974.
[52]. M.D. Olson. In Hybrid and mixed finite element methods, Atluri SN, Gallagher RH, Zienkiewicz OC, John Wiley & Sons, 1983, 19-49.
[53]. D. Mijuca. A new primal-mixed 3D finite element. The Scientific Journal Facta Universitatis, Mechanics, Automatic, Control and Robotics, 3: 167–178, 2001.

Mode	Eigenv.	Mode	Eigenv.	Mode	Eigenv.	Mode	Eigenv.
1	2	5	0.2142	9	0	13	-0.3015
2	0.8999	6	0.1795	10	0	14	-0.6435
3	0.6364	7	0.1445	11	0	15	-0.6988
4	0.456	8	0.0557	12	-0.2326	16	-2.0244

Table 1. Solvability test for an isotropic material

z/h	-0.5	-0.2	0.0^-	0.0^+	0.2	1
3D [23]	-0.9960	-0.0373	0.4526	-0.4719	0.0260	1.0446
Zhen et al. [23] 4x4	-1.0292	-0.0371	0.4719	-0.4926	0.0240	1.0812
Present 4x4 [2.33]	-1.0291	-0.0371	0.4721	-0.4924	0.0250	1.0791
Zhen et al. [23] 8x8	-0.9992	-0.0356	0.4582	-0.4771	0.0235	1.0481
Present 8x8 [8.51]	-0.9991	-0.0362	0.438	-0.4751	0.0239	1.0465
Zhen et al. [23] 12x12	-0.9925	-0.0353	0.4552	-0.4738	0.0234	1.0411
Present 12x12 [17.1]	-0.0995	-0.0372	0.4531	-0.4729	0.0249	1.0451
Zhen et al. [23] 14x14	-0.9910	-0.0353	0.4546	-0.4732	0.0234	1.0396
Present 14x14 [20.2]	-0.9961	0.0374	0.4525	-0.4718	0.0261	1.0446

Table 2. Normalised in plane stress for a [15°/-15°] square plate by Zhen et al. [23]and by the present mixed element with progressively refining meshing.

	z/h	-0.50	-0.40	-0.30	-0.20	-0.10	0.00	0.10	0.20	0.30	0.40	0.50
$\bar{\sigma}_{xz}$	Ref. [42]	0.000	2.609	3.227	2.643	2.113	2.093	2.100	2.668	3.340	2.734	0.000
	Present (3x3) [1.97]	0.000	2.720	3.830	2.949	2.450	2.360	2.450	2.950	3.950	2.920	0.000
	Present (5x5) [2.70]	0.000	2.650	3.450	2.734	2.325	2.248	2.299	2.750	3.430	2.805	0.000
	Present (9x9) [9.26]	0.000	2.607	3.227	2.643	2.114	2.094	2.099	2.668	3.340	2.735	0.000
$\bar{w}$	Ref. [42]	1.152	1.158	1.162	1.167	1.173	1.180	1.188	1.198	1.208	1.218	1.227
	Present (3x3)	1.613	1.545	1.450	1.406	1.375	1.340	1.333	1.388	1.398	1.415	1.443
	Present (5x5)	1.234	1.288	1.291	1.299	1.304	1.306	1.309	1.295	1.299	1.305	1.312
	Present (9x9)	1.153	1.158	1.161	1.168	1.172	1.180	1.188	1.197	1.207	1.217	1.228

Table 3. Normalised shear stress and transverse displacement for a [0°/90°/0°] square plate by Vel and Batra [42] (exact 3D solution) and by the present mixed element with progressively refining meshing.

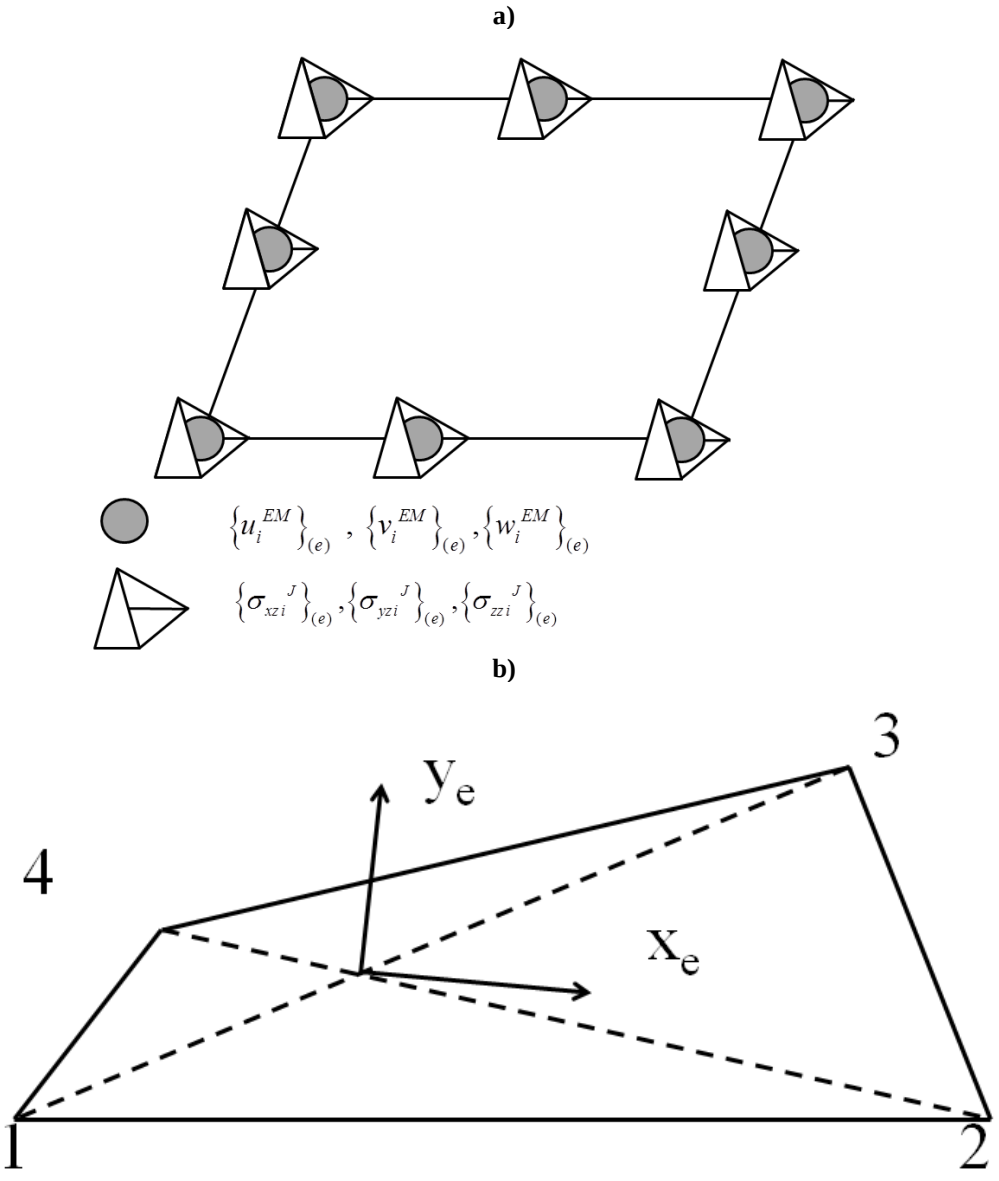

Figure 1. Reference system for the element in: a) the natural plane and b) the physical plane.

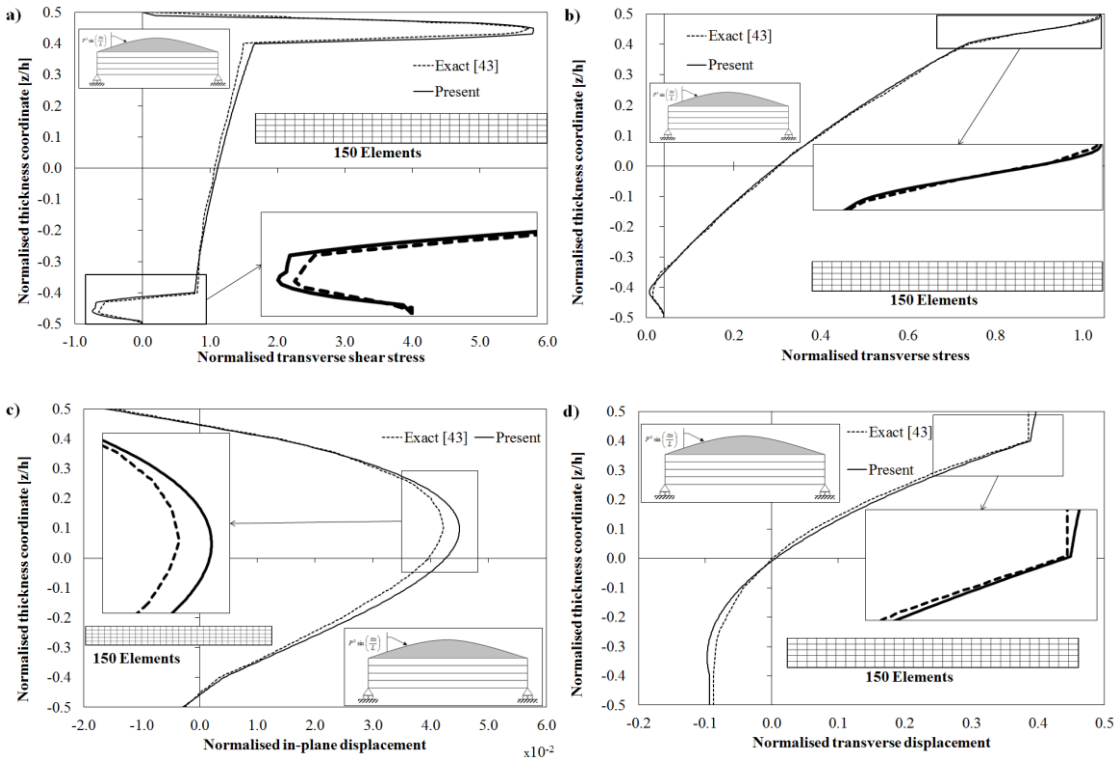

Figure 2. Stress and displacement field by the present mixed element and exat 3D solution [43] for a sandwich beam.

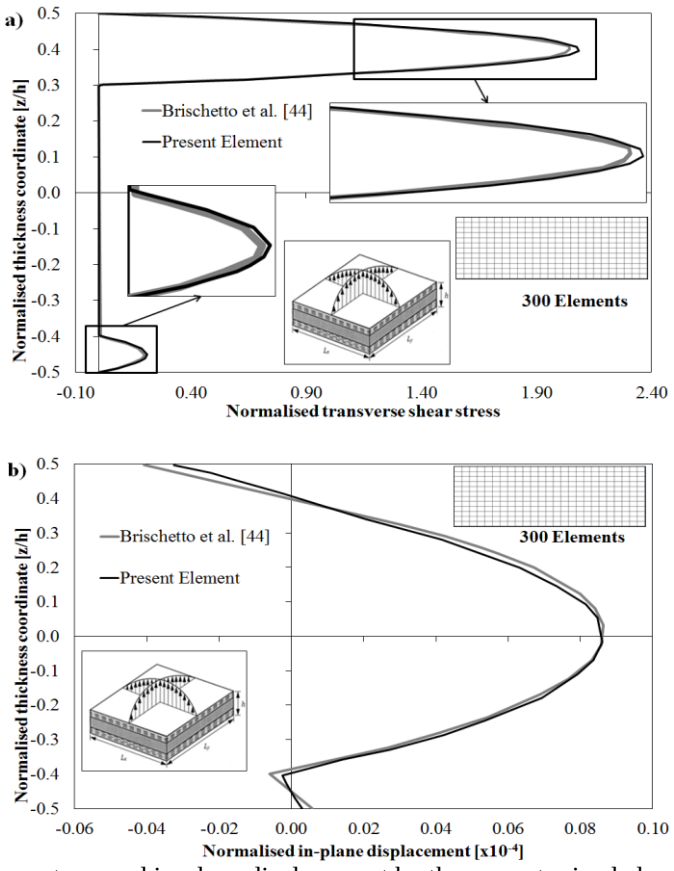

Figure 3. Transverse shear stress and in-plane displacement by the present mixed element and by Brischetto et al. [44] (Exact solution) for a simply supported sandwich plate.

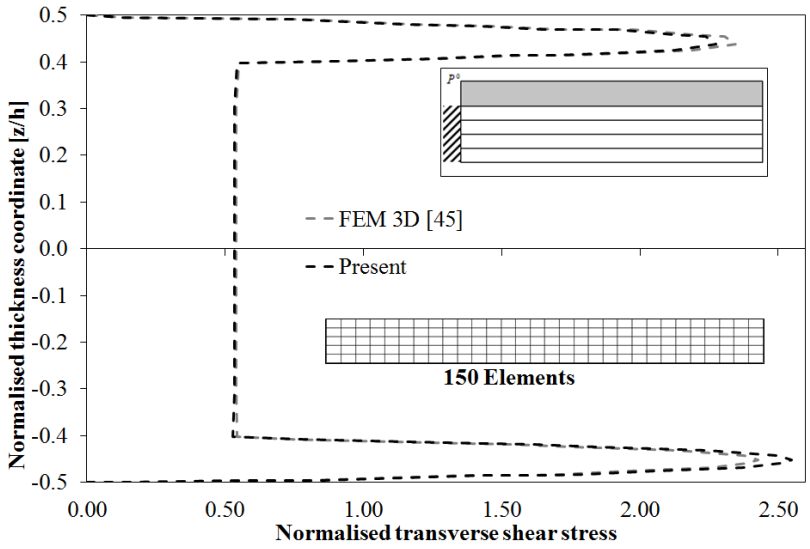

Figure 4. Normalised transverse shear stress by the present mixed element and by the 3D finite element by Tessler at al. [45]

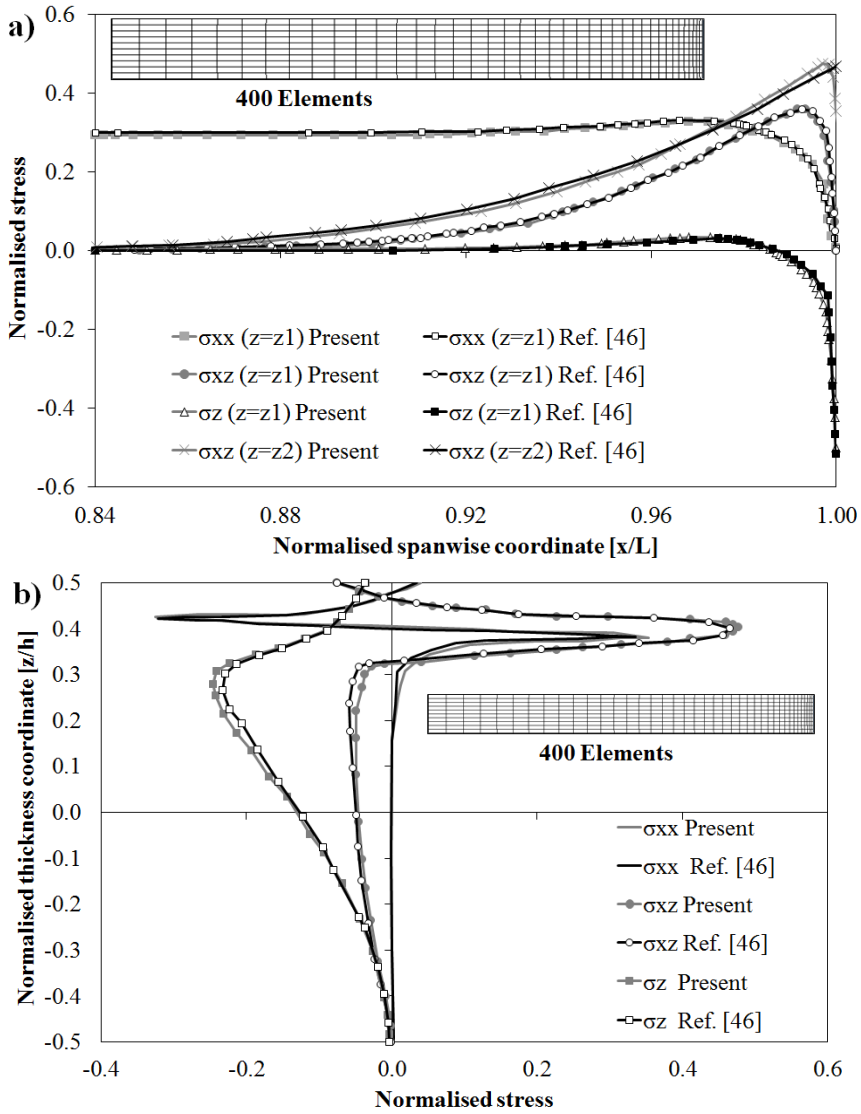

Figure 5. Normalised variation of the stress field for a cantilever piezoactuated beam a) along the span and b) across the thickness

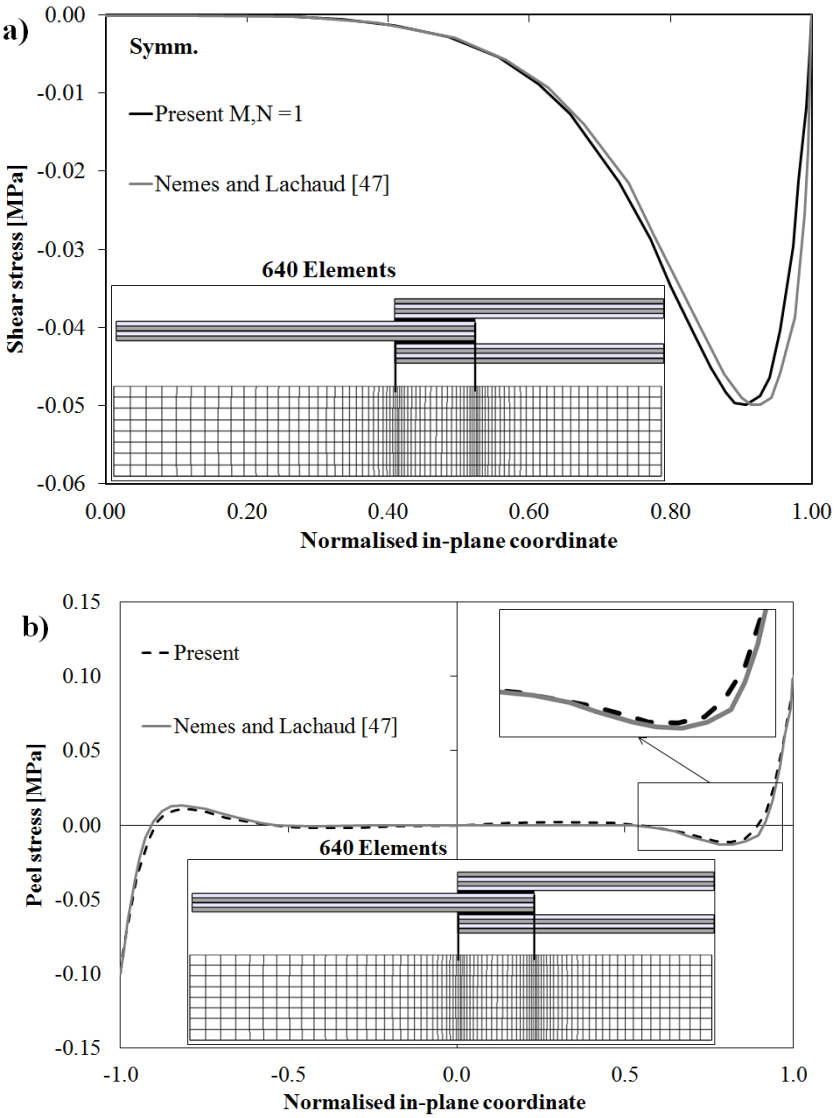

Figure 6. Span-wise distribution of a) shear stress and b) peel stress by Nemes and Lachaud [47] and by the present model

ISSN (e): 2250 – 3005 || Vol, 05 || Issue, 01 || January – 2015 ||
International Journal of Computational Engineering Research (IJCER)

Random Key Pre-distribution Schemes using Multi-Path in Wireless Sensor Networks

Si-Gwan Kim
Kumoh Nat'l Institute of Technology, Korea

ABSTRACT:
Low-cost, small-size and low-power sensors that incorporate sensing, signal processing and wireless communication capabilities is becoming popular for the wireless sensor networks. Due to the limited resources and energy constraints, complex security algorithms applied to ad-hoc networks cannot be employed in sensor networks. In this paper, we propose a node-disjoint multi-path hexagon-based routing algorithm with a key pre-distribution scheme in wireless sensor networks. We describe the details of the algorithm and compare it with other works. Simulation results show that the proposed scheme achieves better performance in terms of security, efficiency and message delivery ratio.

Keywords: *key pre-distribution, multi-path, routing, security, wireless sensor networks*

I. INTRODUCTION

Wireless sensor network (WSN) is becoming popular in critical applications. Composed of tens and thousands of sensor nodes, sensor network can work in the environment to which human cannot easily approach. Security issue is very important for WSNs applications, such as military applications. In these applications, each sensor node is highly vulnerable to many kinds of attacks due to each node's energy limitation, wireless communication, and exposed location, which make the task of incorporating security in WSNs a challenging problem. Because of resource limitations and secure applications in WSNs, key management emerges as a challenging issue for WSNs. In WSNs security, the key management problem is one of the most important issues.

Traditional schemes in ad hoc networks using asymmetric keys are expensive due to their storage and computation cost. These limitations make key pre-distribution schemes a good choice to provide low cost secure communication between sensor nodes [1-3]. The main drawback of key pre-distribution schemes is that the capture of a single sensor node allows adversary easily access to all keys stored in the node. This may not only lead to compromise of the links established by the captured node but also to compromise of links between two non-captured nodes, since these two nodes may have used one of the captured keys to secure their communication.

Establishing single-path routing between the source and destination nodes is more common study topics in WSNs. However, compromise of nodes along the path would lead to failure of the path and loss of data. Furthermore, if routing path is compromised then the entire WSN is endangered. In sensitive applications, establishing reliability and availability is very important for an application to serve its objectives successfully. To offer multiple paths in order to enhance the availability, resilience and reliability of the network, many studies suggest various mechanisms. However, the use of multiple paths introduces additional security problems, since it makes data available at more locations, giving more opportunities to adversaries to compromise the data. Therefore, in sensitive environments it is important to protect the network from malicious actions in order to enhance and maintain the availability and reliability of the network.

As most of the routing protocols in WSNs have not been designed with security requirements, secure routing protocols are studied recently [4-7]. The key management problem has been extensively studied in the WSNs. However, applying the public key management scheme used in the wired networks is impractical due to the resource constraints of sensor nodes. The key pre-distribution scheme using symmetric encryption techniques is another form of solution. Eschenauer and Gligor [3] proposed a random key pre-distribution scheme. Before deployment, each sensor node receives a random subset of keys from a large key pool. Two neighbor nodes find one common key within their subsets and use that key as their shared secret key. If no common key is found, they need to exchange a secret key via a multi-hop path.

The rest of the paper is organized as follows. In section 2, we introduce the related works. In section 3, we describe our multi-path routing algorithm. In section 4, simulation results are shown and compare our algorithm with previous works. Finally, we summarize our results in section 5.

II. RELATED WORKS

Key management involves various techniques that support the establishment and maintenance of key relationships between authorized parties [7][8][13]. An effective key management scheme is essential for the secure operations in wireless sensor networks. In recent years, key pre-distribution scheme has been widely studied. Many random key pre-distribution schemes have been suggested. Eschenauer and Gligor [3] proposed the basic probabilistic key pre-distribution, in which each sensor is assigned a random subset of keys from a key pool before the deployment of the network. In these techniques [3], a small number of keys are selected from a key pool and stored into a sensor before the deployment of the network. After deployment, two neighboring sensors can establish a secure single-hop path if they share a common key. Otherwise they need to exchange a secret key via a multi-hop path. Many subsequent schemes are mainly based on the improvement on the E-G scheme. For example, the random pairwise keys scheme [4] pre-distributes random pairwise keys between a particular sensor and a random subset of other sensors, and has the property that compromised sensors do not lead to the compromise of pairwise keys shared between non-compromised sensors. Chan proposes a q-composite random key pre-distribution scheme [9] to increase the network resilience at the cost of processing overhead. This allows neighbors to have a secure communication only when they share at least $q > 1$ common keys. This scheme can efficiently improve the resilience against node capture attack, in which attackers can capture sensors and derive the preinstalled information still used by uncompromised nodes. In [12], combinatorial properties of the set systems are used to distribute keys to sensors prior to deployment, which improves connectivity of two neighboring sensors when the network size is large.

Path key establishment is widely used in key pre-distribution schemes. Establishing keys between two neighbor nodes without pre-installed common keys through a secure path must be solved. The key called path key is transmitted using secure communication channel through several intermediate nodes. However, if one of the nodes along the path is compromised, the key may be exposed. To solve this problem, some multipath key establishment schemes [8, 9] were proposed. These schemes can effectively stop revealing the key, but they have some drawbacks in forward attacks.

Shamir's secret sharing [11] based path key establishment mechanism is proposed to improve the security of path key establishment. Path key is treated as a secret need to share, which will be divided into several key segments. The key segments will be transmitted through a node-disjoint path respectively. Whenever the network encounter the stop forwarding attacks, the destination node can reconstruct the path key so long as the received key segments are no less than the threshold set in the scheme.

Some multi-path key establishment schemes were studied to solve the path key exposure problem [13]. The basic idea behind multi-path key establishment schemes is first studied by Perrig [14]. In [8], multiple node-disjoint paths were used for the end to end pairwise key establishment. In this scheme, the path key will be divided into n parts and each part is transmitted on a node-disjoint paths. When the destination node receives all the n parts of the key, it can reconstruct the path key. Another path key establishment scheme [9] use multiple one-hop paths instead of node-disjoint paths to enhance the security of path-key establishment. But if the captured node is on the intersect point of several paths between these proxies and drops all the key shares passing through it [10], the entire system is endangered.

After the completion of the shared-key discovery phase, many direct links are protected by a same key K_i, which may be known by many nodes in the network. Thus, the capture of a single node chain will compromise all those links. These problems are studied in multi-path key establishment schemes [14][15]. In these schemes, the source sensor node finds a multi-hop secure path toward the destination node. Each pair of neighboring nodes on the secure path shares at least one common key, which could be different along the path. Then a secret key is generated by the source node and sent toward the destination through the multi-hop secure path. This scheme works quite well when no nodes on the path are compromised and all sensor nodes forward the secret key honestly. But, these sensor nodes are susceptible to many kinds of attacks, such as eavesdropping, stop forwarding and distorting.

In [15], Huang and Mehdi propose a multiple key establishment scheme based on error-correct coding scheme. This scheme is resilient to $t = (n - k) / 2$ faulty paths with the use of the (n, k) RS codes. But it uses too

more redundancy of parity code. Deng and Han [12] decrease the transmission overhead than [15] by sending redundant symbols when necessary.

In ad hoc networks, multi-path routing algorithms are based on the flooding mechanism, and need the centralized processing at the destination node. This flooding mechanism is not appropriate for large-scale sensor networks. Ye et al [10] presented a multi-path algorithm for sensor networks. But, the multi-path is not node-disjoint, and the flooding mechanism is be used. D. Ganesan et al [16] evaluated the relative performance of disjoint and braided multi-paths in sensor networks, but concrete multi-path algorithms are not presented.

III. OUR ALGORITHMS

In this section, we propose our algorithms based on multi-path routes. In our system, we use hexagon-based coordinates as well as grid-based ones. A hexagon-based coordinate system has more advantages over a grid-based one in wireless sensor networks. First, when a sensor node transmits data over wireless links, its signal range would form a circle that is centered around its deployment location with the radius being the distance of signal propagation. And, a hexagon can be used to describe equal distance between two neighboring sensor nodes. In a grid-based coordinate system, the distance between two neighboring sensor nodes differs. When the neighboring node is located directly adjacent or diagonally in the grid-based system, its distance is one unit and square root of two units, respectively.

In our systems, nodes are place in the grid form n x n as in Fig. 1. We assume that transmission range is two hops for each node. So the number of neighbor nodes within transmission range for each node is 16. Nodes within transmission range for node S is shown in black nodes in Fig. 1. Label of each node is numbered using two dimensional matrixes.

$\{N(i,j) \mid i=0,1,2, \ldots, n-1, j=0,1,2, \ldots, n-1\}$
, where, n is the size of the network.

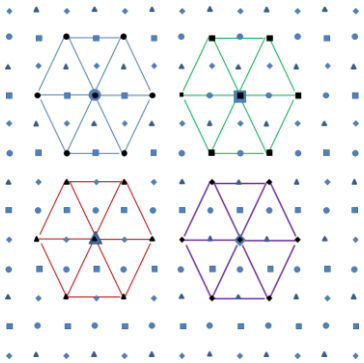

Figure 1. Example of source nodes

Four overlapping networks, G_0, G_1, G_2 and G_3, can be organized using the hexagon-based scheme as follows.

- $G_0 = \{N(i,j) \mid i=0,2,4, \ldots, 2m-2, j=0,2,4, \ldots, 2m-2\}$
- $G_1 = \{N(i,j) \mid i=0,2,4, \ldots, 2m-2, j=1,3,7, \ldots, 2m-1\}$
- $G_2 = \{N(i,j) \mid i=1,3,7, \ldots, 2m-1, j=0,2,4, \ldots, 2m-2\}$
- $G_3 = \{N(i,j) \mid i=1,3,7, \ldots, 2m-1, j=1,3,5, \ldots, 2m-1\}$

A node can be identified as a member of G_0, G_1, G_2 and G_3 according to the following rules.

- i and j value of node $N(i,j)$ are all even numbers : a member node of G_0
- i and j value of node $N(i,j)$ are even and odd number, respectively : a member node of G_1
- i and j value of node $N(i,j)$ are odd and even number, respectively : a member node of G_2
- i and j value of node $N(i,j)$ are all odd numbers : a member node of G_3

In Fig. 1, example source nodes of four networks are shown. An example member node in G_0, G_1, G_2 and G_3 is drawn as circle, rectangle, triangle and diamond, respectively. In this figure, an example of hexagon-based routing path is shown for each G_0, G_1, G_2 and G_3, with each source node drawn as big circle, big rectangle, big triangle and big diamond, respectively.

Our scheme has two kinds of hops, one-hop delivery and two-hop delivery. Hexagon-based two-hop delivery is used for the routing where a destination node is more than three hops away. On the other hand, one-hop delivery is used for the distribution of message segments to the neighbor nodes, or final hop of the segments to the destination node. This one-hop is routed using grid-based coordinates.

When a node wants to send some messages to the destination node, we first check the number of nodes (denoted as c) which shares keys with the two-hop range neighbor nodes. Then given message is divided into c segments, i.e. w_0, w_1, …, and w_{c-1}. Each segment except w_0 is delivered to c neighboring nodes. This delivery takes just one hop for each segment. Then each segment is routed to the destination node. This routing is hexagon-based coordinate system and uses two-hop delivery. Fig. 2 shows our routing algorithms.

Step 1. By transmitting hello packets to two-hop range nodes, find the number of nodes (denoted as c) which shares keys with neighbor nodes. Then a given message is divided into c segments, i.e. w_0, w_1, w_2, … , w_{c-1}.
Step 2. Each segment w_i is delivered to its corresponding key sharing node (S_i), which is one-hop or two-hop away neighbor node.
Step 3. When each segment w_i is arrived in the node Si, each segment decides its corresponding G_i (i=0,1,2,3).
Step 4. Each segment is forwarded to the destination node based on hexagon-based routing.
Step 5. When each segment is arrived at the intermediate node, each segment is routed to the next intermediate node according to the pre-determined G_i.
Step 6. As each segment gets closer to the destination node, the last hop may be one-hop or two-hop routing for the destination node depending on the position of that node.
Step 7. After receiving all the segments in the destination node, original messages can be constructed.

Figure 2. Outline of the proposed routing algorithms

Fig. 3 shows an example of our routing. In this example, source node 'S' has some messages for the destination node 'D'. Node S tries to find the neighbor nodes that share the key within two-hop distance. There can be sixteen nodes within two-hop distance. This is shown in Fig. 3(a). Assume the source node found that six neighbor nodes share the key. This is shown in Fig. 3(b). So it divides a message into six segments, and these six segments are forwarded to the neighbor nodes using one-hop or two-hop routing. These six segments are ready to be routed to the destination node using two-hop routing. For the two-hop routing, nodes that share the key are found among two-hop distant neighbor G_i nodes. As two-hop routing is based on the hexagon system, the maximum number of nodes that share the key is six. Among these six nodes, only one node that shares the key is needed for further routings. After finding the node that share the key, current segment message is routed to that node. The final hop to the destination node D may use one-hop delivery. This is shown in Fig. 3(b)

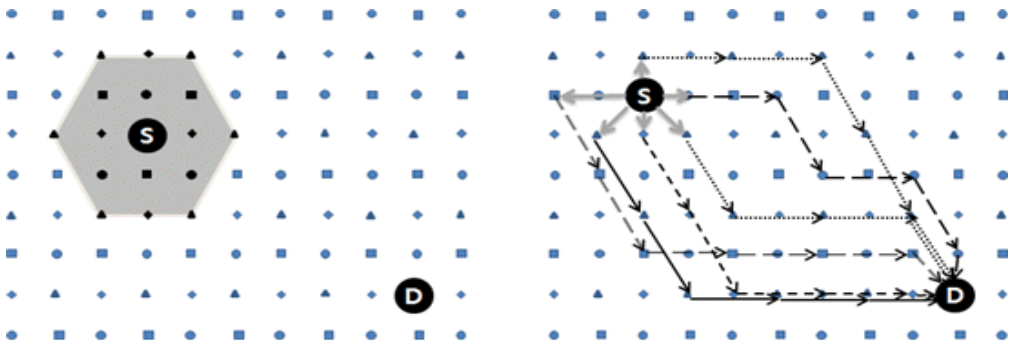

(a) Finding key share **(b) Routing**

Figure 3. Example routing

IV. SIMULATIONS

The performance of suggested algorithm is simulated and analyzed in this section. NS-2 is used to perform simulation to compare and analyze performance with the previous works. Performance metrics are message delivery ratio, the quantity of received data in comparison with the consumed energy and overhead of cluster composition. The size of network is 100m × 100m and sink is located outside of network. Simulation environments are as follows: simulation time is 900 sec, packet size is 50 bytes, communication range is 15 m, initial energy is 2 J, aggregation energy is 5 nJ, transmitter energy is 600 mW, receiver energy is 300 mW and idle energy is 120 mW. The performance of algorithm is observed with various network densities by increasing the number of message generating nodes from 20 to 60. We have performed three simulations to evaluate our protocols as follows.

4.1. Number of hops to reach the destination node for each node

We measured the average number of hops to reach the destination node for each node. As the message for a given node is routed to the intermediate nodes, the number of neighboring node that shares the key is very important. The more the number of key sharing nodes, the less the number of hops to reach the destination node. Fig. 4 shows the results of our algorithms. As the number of key pool(KP) is increased, the number of hops is decreased by about 1 hop. The size of key ring affects the number of hops too. As the number of key ring is increased, the number of hops to reach the destination is decreased by about 2.5 hops.

4.2. Number of available multi-path for a node

The number of multi-path for each node is one of the important factors that affect the performance of the networks. For a given node, the number of neighbor node for two-hop range is 16, which is the maximum number of multi-path. But key-sharing between the neighbors nodes may not be existed, the number of key-sharing is less than this number. We measured the average number of multi-path for a given node. Fig. 5 shows the results. As the number of key pool is increased from 1000 to 2000, the number of multi-path is by about 2. And if we vary the size of key ring, the number of multi-path is increased up to 13(KP=2000).

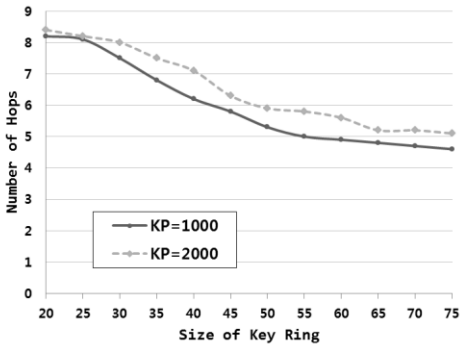

Figure 4. Number of hops

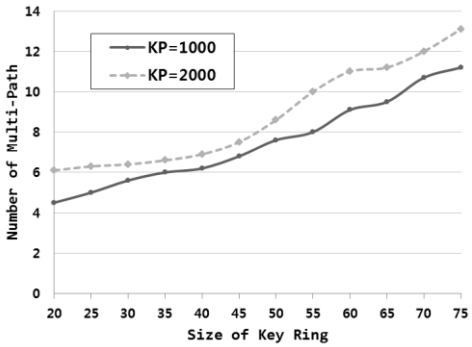

Figure 5. Number of available multi-path

4.3. Message Delivery Ratio

Message delivery ratio of member node to sink was simulated. Packet delivery ratio is the percentage of packets sent by the source which reaches the sink depending on the number of source nodes. The message delivery ratio was measured when the number of node was 100, the number of message generating node is 20, 40 and 60 and the interval time between messages changes from 0 second to 100 seconds.

Fig. 6, Fig. 7 and Fig. 8 show message delivery ratio when the number of message for each node is 20, 40 and 60 and the suggested algorithm was found to have the transmission ratio higher than that of SecLEACH [17] algorithm by about 4%. This is because the numbers of orphan nodes are generated more for the SecLEACH, where there may not exists share keys between head node and its member node. In addition, the message collected in the member node cannot be sent to the destination, i.e., sink node, since the route to cluster head is lost by wireless link error between the head node and its member node in the case of SecLEACH. However, the ratio of successful transmission to sink node is high, because the suggested algorithm can selectively transmit the message generated in member node to two cluster heads in each cluster.

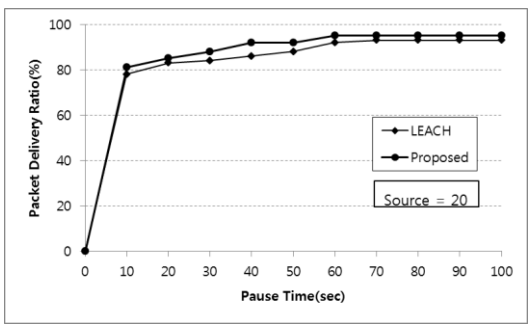

Figure 6. Message Delivery Ratio (sources=20)

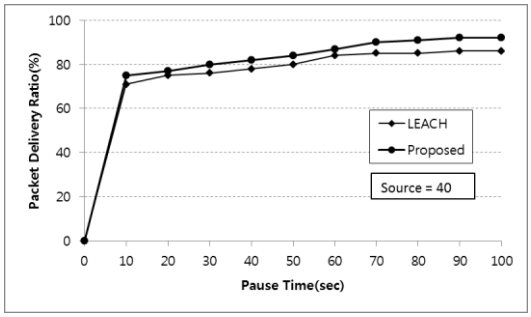

Figure 7. Message Delivery Ratio (sources=40)

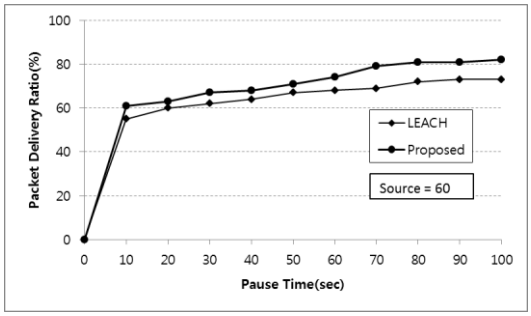

Figure 8. Message Delivery Ratio (sources=60)

V. CONCLUSIONS

Sensor network is limited by the energy resources of sensor node that composes network, computation ability and the memory capacity. This paper suggests key pre-distribution routing algorithm based on multi-path routes in sensor network. Simulation was performed in terms of number of multi-path, average number of hops to reach the destination node and message delivery ratio to compare the performance of suggested algorithm with that of the previous method. Due to the more routing paths, the suggested algorithm shows higher message delivery ratio than that of the existing method by some 4%.

ACKNOWLEDGEMENTS

This work was supported by Kumoh National Institute of Technology, Korea.

REFERENCES

[1] I. Akyildiz, S. Weilian, Y. Sankarasubramaniam, and E. Cayirci, "A survey on sensor networks," IEEE Communications Magazine, vol.40, no.8, pp.102-114, 2002.

[2] W. Du, J. Deng, Y. S. Han, S. Chen, and P. K. Varshney. A key management scheme for wireless sensor networks using deployment knowledge. IEEE INFOCOM, 2004.

[3] L. Eschenauer and V. Gligor, "A key management scheme for distributed sensor networks," in Proc. of the 9th ACM Conf. on Computer and Communications Security, New York: ACM Press, pp. 41-47, 2002.

[4] H. Chan, A. Perrig, and D. Song, "Random Key predistribution schemes for sensor networks", in IEEE Symposium on Security and privacy, Berkeley, California, May 11-14, 2003, pp. 197-213.

[5] M. Li, S. Yu, D. Guttman, W. Lou, and K. Ren, "Secure ad hoc trust initialization and key management in wireless body area networks," ACM Trans. Sen. Netw. 9, 2, pp. 1-35, 2013.

[6] W. Du, J. Deng, Y. Shan, S. Chen, and P. Varshney, "A Key Management Scheme for Wireless Sensor Networks Using Deployment Knowledge," in INFOCOM 2004, Volume 1, 7-11 March, 2004.

[7] W. Du, et al, "A pairwise key pre-distribution scheme for wireless sensor networks," in Proc 10th ACM Conference on Computer and Communications Security (CCS), Washington, DC., pp. 42-51, 2003.

[8] D. Liu and P. Ning, "Establishing pairwise keys in distributed sensor networks," ACM Transactions on Information and System Security, Volume 8(1), pp.41-77, 2005.

[9] [y2] H. Chan, A. Perrig, and D. Song, "Random key predistribution schemes for sensor networks," in IEEE Symposium on Research in Security and Privacy, 2003, pp. 197-213.

[10] Ye Ming Lu and Vincent W. S. Wong. 2007. An energy-efficient multipath routing protocol for wireless sensor networks: Research Articles. Int. J. Commun. Syst. 20, 7 (July 2007), 747-766.

[11] Ronald L. Rivest, Adi Shamir, and Yael Tauman. How to Leak a Secret. In Proceedings of the 7th International Conference on the Theory and Application of Cryptology and Information Security: Advances in Cryptology (ASIACRYPT '01), Colin Boyd (Ed.). Springer-Verlag, London, UK, UK, 552-565, 2001.

[12] J. Deng, R. Han, S. Mishra. Limiting DoS Attacks During Multihop Data Delivery In Wireless Sensor Networks. International Journal of Security and Networks, Special Issue on Security Issues in Sensor Networks, vol. 1, nos. 3/4, 2006, pp. 167-176.

[13] Stavrou, Eliana, and Andreas Pitsillides. "A survey on secure multipath routing protocols in WSNs." Computer Networks 54.13 (2010): 2215-2238.

[14] Xin Zhang and Adrian Perrig, "Correlation-Resilient Path Selection in Multi-Path Routing." In Proceedings of the IEEE Global Communications Conference (Globecom), December 2010.
[15] D. Huang and Deep Medhi, "A Byzantine Resilient Multi-Path Key Establishment Scheme and Its Robustness Analysis for Sensor Networks," in Proceedings of 19th IEEE International Parallel and Distributed Processing Symposium (IPDPS), 2005, pp. 4-8.
[16] Deepak Ganesan, Ramesh Govindan, Scott Shenker, and Deborah Estrin. 2001. Highly-resilient, energy-efficient multipath routing in wireless sensor networks. SIGMOBILE Mob. Comput. Commun. Rev. 5, 4 (October 2001), 11-25.
[17] Leonardo B. Oliveira, Adrian Ferreira, Marco A. Vilaça, Hao Chi Wong, Marshall Bern, Ricardo Dahab, Antonio A.F. Loureiro, SecLEACH—On the security of clustered sensor networks, Signal Processing, Volume 87, Issue 12, December 2007.

ISSN (e): 2250 – 3005 || Vol, 05 || Issue, 01 || January – 2015 ||
International Journal of Computational Engineering Research (IJCER)

Development of Seakeeping Test and Data Processing System

Fei Yu-Ting[1], HouGuo-Xiang[1*], Wang Kai[1], Zhang Yao[1]
School of Naval Architecture and Ocean Engineering, Huazhong University of Science and Technology, Wuhan 430074, P.R.China

ABSTRACT:
A seakeeping test and data processing system is developed for towing tanks. This system includes two main procedures: wave-generating and data processing. In the wave-generating procedure, the linear filtering method is used to generate irregular waveswith the full consideration of the actual efficiency of the machine and the compensation for the actual stroke of piston. Furthermore, groups of piston motion data meeting the requirements of target spectrum are afforded. To ensure the normal operation of a wave machine, the above data within the range of the rated strokes of piston should be chosen. In the data processing procedure, the correlation function method is used to handle the time domain signals which contain irregular waves, ship swaying motion, hull stress and so on. Then the spectrum curve of these test data can be drawn and some statistical values can be obtained based on the narrow-band spectrum theory. According to these statistical values, the frequency response function can be derived, and the predicted value of ship motion in irregular waves can be calculated. By comparing the predicted and experimental results, the reliability of this system can be evaluated. On the basis of the movement of a boat in irregular waves and a series of dynamic responding experiments, this paper proves that thedeveloped system has many advantages, such as succinctness, completeness, accurate data process, reliability, accurate simulation from actual spectrum to target spectrum and so on.

***KEY WORD**: Wave generator; irregular wave; seakeeping test; software*

I. INTRODUCTION

Wave loadsare the main external loads of ship and ocean structure, which directly affects their sailing, performance and operation in the sea. At present, we mainly predict ship and ocean structure's seakeeping performance in real ocean waves through experiment[1, 2]. In the laboratory, waves can be divided into regular, irregular and short-crested wave [3]. Irregular wave test of ship and marine structures mainly includes the following contents: the simulation of irregular waves; the movement of marine structures on wave; collection and analysis of test data. At present, the regular wave linear superposition and energy halving of ocean wave spectrum method are mainly adopted to simulate two-dimensional irregular waves. Luo Chao-lin and He Qi-lian have designed a set of multi-directional irregular wave generator system using the regular wave linear superposition[4]. Using the method of equal energy, Jiang Man-song has developed an AC servo 16 cells rocker-flap wave making system [5]. The analytical methods of test data include spectrum analysis [6, 7] and statistical analysis [8].In this paper, we develop a seakeeping test and data processing system combining the modern sensor technology, data acquisition technology, and computer technology, which adopts the linear filtering method and spectrum analysis to produce two-dimensional irregular waves and deal with the experimental data.

Simulation of two-dimensional irregular waves

The basic principles of using linear filtering method to generate two dimensional irregular waves are expressed in this section. In order to generate wave signals meeting the requirements, we make a white noise with

Foundation item: Project(51475179) is supported by National Natural Science Foundation of China
Corresponding author: HouGuo-xiang, Prof.; Tel: +8615327194313; Email: houguoxiang@163.com

normal distribution to get through a designed filter according to the given target spectrum in advance. Then we could simulate any number of irregular wave signals meeting the requirements of target spectrum on the computer, which can control the movement of the wave machine and without periodically repeating two-dimensional irregular waves [9]. For a fixed point, the wave high ηchanging with time can be expressed as:

$$\eta(t_i) = \sum_{i=1}^{\infty} a_i \cos(\omega_i t_i + \varepsilon_i) \tag{1-1}$$

where a_i representsthe wave amplitude of the ith component wave; ω_i represents the circular frequency of the ith component wave; t_i represents the time; ε_i represents initial phase of ith component wave, which is uniformly distributed random numbers within$(0\sim2\pi)$. Changing the equation (1-1) in discrete form with equal time interval, we obtain

$$\eta(n\Delta t) = \sum_{i=1}^{L} a_i \cos(\widehat{\omega_i} n\Delta t + \varepsilon_i) \tag{1-2}$$

whereΔtrepresents the time interval; $n = 1,2,3,4,5,6,\cdots,N$, $N$is the wave signal points determined by the duration of wave, L representsthe number of component waves within spectrum scope; $\widehat{\omega_i}$ represents the frequency in the frequency increment. To prevent cyclical repeat of two-dimensional irregular wave signal, its value can be calculated by the following equation.

$$\widehat{\omega_i} = \omega_{i-1} + q\Delta\omega \tag{1-3}$$

where$q$is arandom number within $0\sim1$; $\Delta\omega$ stands for the frequency increment,which is constant when using the frequency to divide the whole spectrum range.According to the theory of waves, the amplitude of irregular wave and wave spectrum has the following relationship:

$$a_i = \sqrt[2]{2S(\widehat{\omega_i})\Delta\omega} \tag{1-4}$$

where$\widehat{\omega_i}$=$(\omega_{i-1} + \omega_i)/2$.

According to the Eq. (1-2) and the transfer function of wave machine $M(\omega)$, the irregular wave signals $e(n\Delta t)$ can be expressed as:

$$e(n\Delta t) = \sum_{i=1}^{L} \frac{\sqrt[2]{2S(\widehat{\omega_i})\Delta\omega}}{M(\omega_i)} \cos(\widehat{\omega_i} n\Delta t + \varepsilon_i) \tag{1-5}$$

where

$$M = -0.00002\lambda^3 + 0.0022\lambda^2 - 0.0841\lambda + 1.0427 \tag{1-6}$$

whereλrepresents the wave length. This transfer function is obtained by the way of experiment. For different wave tanks, their transfer functionsare not the same.

The main advantages of this method is that we can fully consider the actual efficiency of wave machine, and can make some compensation for the actual stroke of electric cylinder, which will generate the actual irregular waves signal meeting the requirements of the target spectrum.

II. PROCESSING METHOD OF TEST DATA

2.1.The time domain processing method

The time domain analysis is the most basic method to process the test date of the seakeeping experiment. It not only reflects the essence of the problem, but also verifies the frequency domain analysis of seakeeping test. Through the experimental data collected from various channels, this system visually displaysthe spectrums of irregular waves, ship swaying motion and hull stress in the time domain. In addition, sincethe test data collected by one experiment is insufficient, this system provides a function to link test data from experiments with same condition. To exclude the interference of high frequency concussion signal, the system also provides high frequency filtering and smoothing function. Moreover, this system provides some auxiliary function to eliminate the unrepresentative data.

According to the time domain curves and the test data, we can examine the test results and obtain the various statistics results of irregular waves, the ship swaying motions and the hull stresses.

2.2.The Frequency processing method

Using the correlation function, we can convert the time domain data collected by sensors into oscillation spectrum curve in frequency domain and displays this curve on the screen.According to the theory of narrow band spectrum, the statistics value and the amplitude response function of amplitude can be calculated. The basic theory of correlation function can be expressed as follows:

Considering the test data collected by sensors with equal time intervals as a sample, the correlation function$R(\tau)$can be solved through the following formula [10]:

$$R(\tau) = \frac{1}{N_0 - \nu} \sum_{n=0}^{N_0-\nu} \xi(t_n) \cdot \xi(t_n + \tau) \tag{2-1}$$

where$\tau = \nu\Delta t, \nu = 0, 1, 2, \cdots, m; N_0, m, \Delta t$ represents respectively the simple size, maximum slip multiplied and sampling interval. $\xi(t_n)$is the experimental data at time sequence of n . Since the covariance function is an even function, one-sided spectrum of the volatility process can be obtained by the numerical integration of the following formula.

$$S'(\omega) = \frac{2}{\pi}\int_0^{\infty} R(\tau)\cos(\omega\tau)d\tau \tag{2-2}$$

There is obvious vibrating of the spectrum curve obtained directly from the above method. The spectral values are not very accurate. Therefore, to improve the accuracy, in this system, we uses the Hamming method to fair this spectrum curve, which means we multiplies the correlationfunction by a weighting function$D(\tau)$.

$$D(\tau) = \begin{cases} 0.54 + 0.46\cos\dfrac{\pi\tau}{T_m}, & |\tau| \le T_m \\ 0, & |\tau| > T_m \end{cases} \tag{2-3}$$

where$T_m = m\Delta t$.

III. SEAKEEPING EXPERIMENT

3.1.Main parameters

The main parameters of the real ship and model are shown in table 3-1.

ÕËI

Main dimension	Symbol	Unit	Model	Real ship
Overall Length	L_{oa}	m	3.000	60
Waterline length	L_{wl}	m	2.844	56.888
Breadth	B	m	0.420	8.4
Draft	T	m	0.102	2.046
Drainage volume	Δ	t	0.0489	400
Wet area	S	m^2	1.085	434
Scale	λ	20		

3.2. Spectrum of experiment

In this experiment, we select the limited wind area spectrum which was recommended by the 15Th international towing tank conference (ITTC) as the given target spectrum. Its expression can be written as.

$$S(\omega) = 0.658 S_\xi(\omega) 3.3^{exp\left[-\left(\frac{206\omega T_1 - 1}{2\sqrt{\sigma}}\right)^2\right]} \tag{3-1}$$

where$S_\xi(\omega)$represent the wave spectrum of 12thITTC, $\sigma = 0.07,\ \text{when}\ \omega \le 4.85/T_1$,
$\sigma = 0.09,\ \text{when}\ \omega > 4.85/T_1$.

Before the experiment we need to verify the accuracy of the waves generated by our wave machine. As shown in 3.1, the blue and red curves represent the target spectrum and generated spectrum obtained from our wave machine respectively.Fig 3.1shows that the generated wave fully satisfy the experimental requirements.

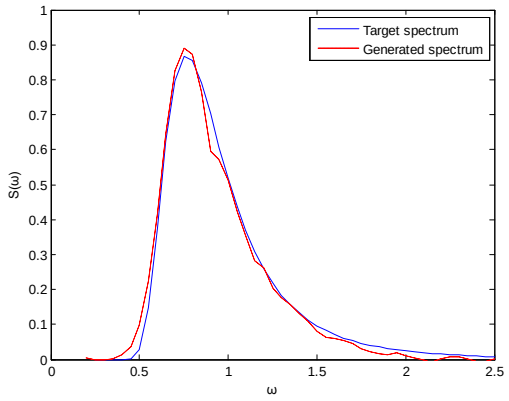

Figure3.1. Target spectrum v. s. Generated spectrum

3.3. Data processing

In this experiment, the speed of model is $2.0\ m/s$, which is corresponding to $18Kn$ of the real ship.The classification of wave is IV, the significant wave heigh$H_1 = 1.85m$, characteristic period $T_1 = 6.34$s. Besides in this experiment, we mainly collect the data ofheaving and acceleration and adopt two ways the time domain processing and frequency processing method to deal with the data. Fig 3.2 shows the heaving curve of model in time domain, and its spectrum curve frequency is shown in Fig 3.3.

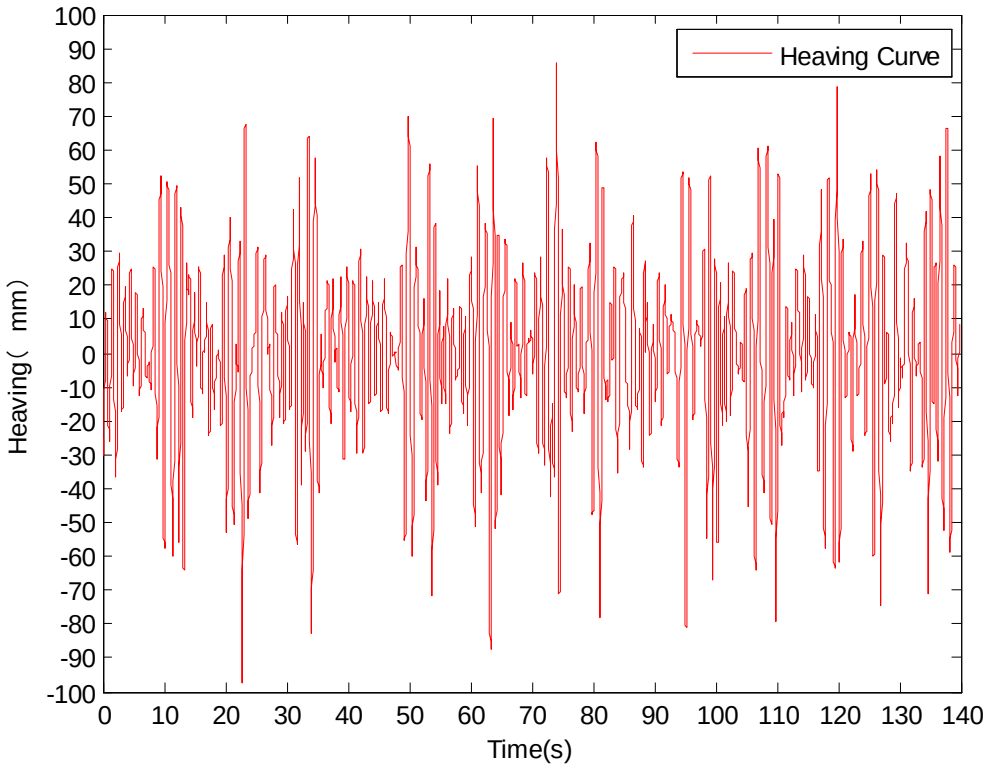

Figure3.3. The heaving curve of model in time domain

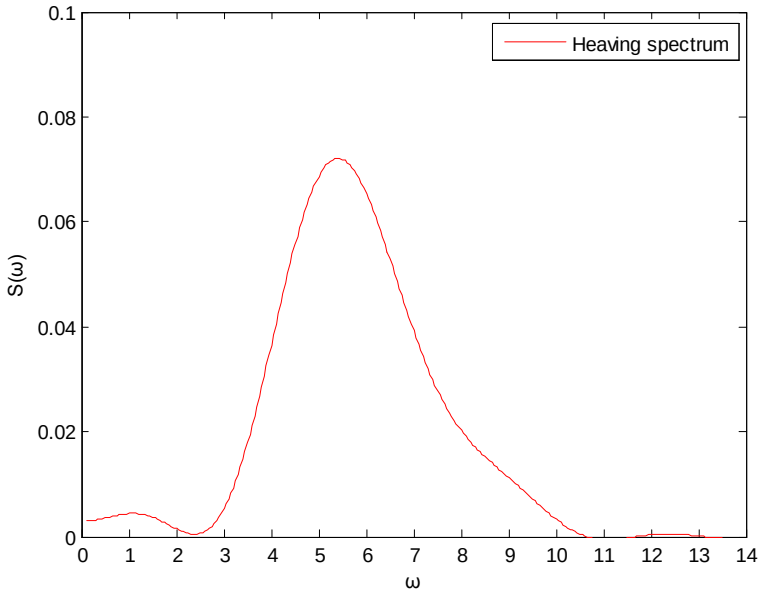

Fgiure3.3 The spectrum curve of model

The acceleration curves of model in time domain and its spectrum curve are shown in Fig 3.4 and Fig3.5 respectively.

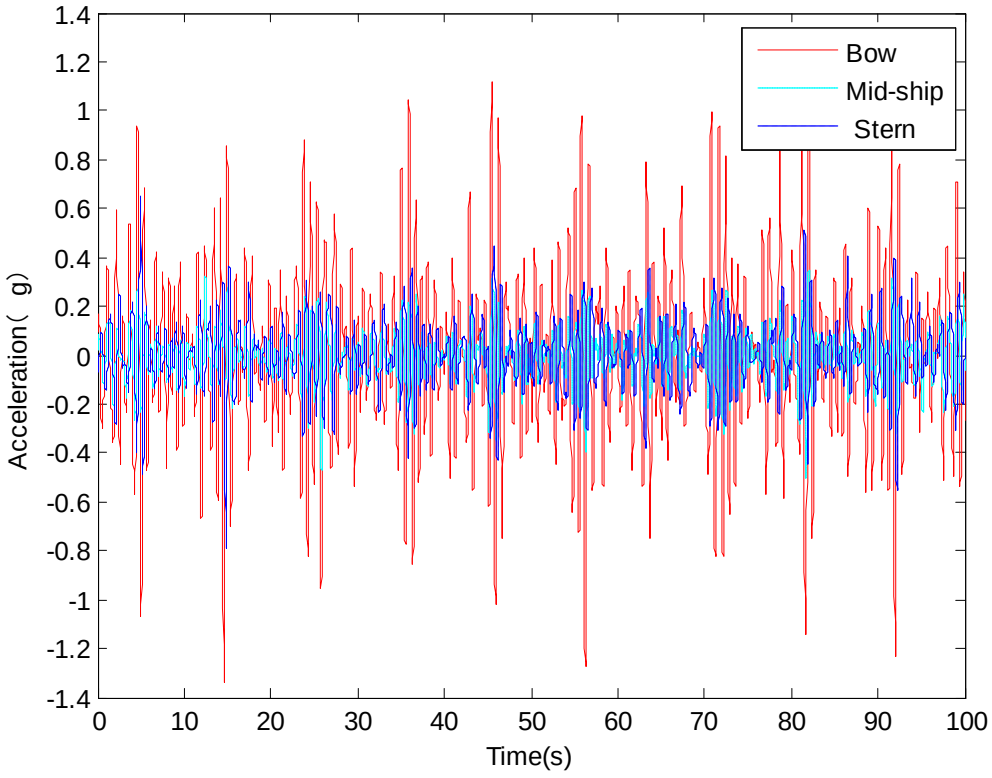

Figure3.4. The acceleration curve of model

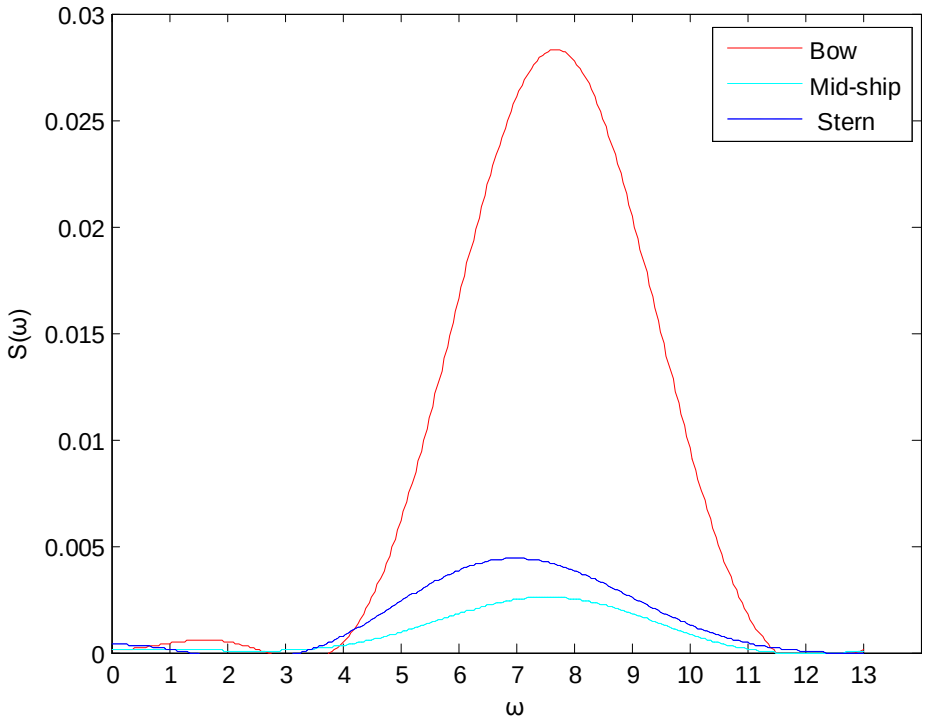

Figure3.5 The spectrum curve of modle

In figure 3.4 and 3.5, the red, yellow and blue curves respectively represents the acceleration of model on the bow, mid-ship and stern.

3.4. Experimental result

Before the irregular wave experiment, we have carried out the regular wave experiment of model. Basis on the data of the regular wave test, we forecasted the irregular wave result. In table 3-2, the forecast value and experimental value are shown.

Table 3-2 .Forecast value and Irregular experimental value

Forecast project		Significant shaking value			
		Heaving(*m*)	Acceleration		
			Bow (g)	Mid-ship(g)	Stern(g)
18*kn*	Irregular experimental value	0.796	0.552	0.170	0.233
	forecast values of regular wave	0.764	0.507	0.155	0.250

IV. CONCLUSION

Fromtable 3-2, theforecast value is very close to the irregular experimental value, whichindicates that it is reasonable to adopt these basic method and principle, and this system can be used for our wave machine.In addition, this system can also produce some commonly used spectrum in the seakeeping test, such as12th ITTC standard spectrum, north Atlantic spectrum, JONSWAP spectrum, China ocean wave spectrum. Because the system provides 16 data channels, we can visually select the data processing channels to set the minimum and maximum coordinate value for each channel.

REFERENCES:

[1] Synolakis, C.E., Generation of long waves in laboratory. 1990. p. 252-266.
[2] Madsen, O.S., Onthe generation of long waves. journal of geophysical research, Vol 76, No 36, P 8672-8683, 1971.
[3] ChenJing-pu and Zhu De-xiang, Numerical simulations of nonlinear ship motions in wavesby a Rankine panel method. Chinese journal of hydrodynamics, 2010(06): P.830-836.

[4] Luo Chao-lin, Design of Multi-directional Irregular Wave Generator System Monitoring Software. Pearl River, 2011(03): P.56-59.
[5] Jiang Man-song, The AC Servo 16 Cells Rocker-Flap Wave Making System. Shipbuilding of
[6] Yu YU-xiu and Liu Shu-xue, Observation and estimations of directional spectra of sfa waves. Ocean Engineering, 1994(02): P.1-12.
[7] Yu YU-xiu and Liu Shu-xue, The Field Observation and the statistical Characteristics of sea wavs. China Offshore Platform, 1994(Z1): P.488-493.
[8] Zhang Ya-qun, The Control and Realization of WaveMake, 2007, Wuhan University of Technology,P.74.
[9] Wang Yang, Power Matching of Motor-driven Shock Tank Type Wave Maker. 2005,Huazhong University of Science and Technology. P. 60.
[10] Yang Bing-zheng, The Estimation of wave spectra by Co-variance function method. Journal of Chongqing Jiaotong University, 1983(01): P.97-105.

ISSN (e): 2250 – 3005 || Vol, 05 || Issue, 01 || January – 2015 ||
International Journal of Computational Engineering Research (IJCER)

Emotion Recognition based on audio signal using GFCC Extraction and BPNN Classification

Shaveta Sharma[1], Parminder Singh[2]
[1] Assistant Professor, Department of Electronics and Communication, GCET, PTU
[2] Assistant Professor, Department of Electronics and Communication, DIET, PTU

ABSTRACT:
For automatic speech recognition (ASR) there is a big challenge which deals with momentous presentation reduction in high noisy environments. This paper presents our emotion classification based on Gammatone frequency cepstrum coefficient used for feature extraction along with Back propagation neural network and the experimental results on English speech data. Eventually, we obtained significant presentation gains with the new feature in various noise conditions when compared with traditional approaches. In our proposed work we considered two emotions SAD and HAPPY which are used to show the implementation results. The simulation environment taken to implement the whole process is in MATLAB

Keywords: *Back propagation neural network, GFCC, audio signals, filter banks*

I. INTRODUCTION

Emotional speech recognition aims at involuntarily identifying the emotional or physical condition of a human being via his or her voice [1]. A speaker has dissimilar stages throughout speech that are recognized as emotional aspects of speech and are integrated in the so named paralinguistic aspects. The database considered for emotion recognition is based on audio signals based on emotions. The features extracted from these speech samples are, the energy, pitch, linear prediction cepstrum coefficient (LPCC), Gammatone frequency cepstrum coefficient (GFCC) [2] etc. Among them GFCC is widely used for speech related studies with a simple calculation and good ability of the distinction. So, in the proposed work GFCC will be used. There are some factors that make difficult the speech [3] recognition and are discussed as:

1. Orator Sound- Identical word is pronounced another way by diverse people since gender, age, swiftness of speech, expressiveness of the speaker and vernacular variations.
2. Surrounding Noise- It is the disturbance added because of environment or surrounding noise as well as speaker's voice too adds to this facto.

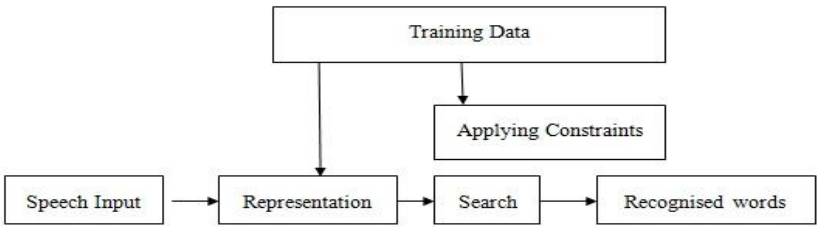

Figure 1. Speech Recognition System

In this proposed work, we are going to use Back Propagation neural network technique [4] on speech that is extract by GFCC. The classification performance is features extraction method using GFCC extraction method. In this paper we have taken two emotions i.e. SAD and HAPPY. Eventually we achieve on a conclusion on the basis of emotion having accuracy that will be achieved by classifying using Back Propagation Neural Network method.

Lasting part of this paper is discussed as following: Section I defines the introduction to the basic topic, Section II shows the introduction to speech features of emotion detection, Section III shows the proposed flowchart of the proposed methodology, Section IV shows the pseudo code of the implementation algorithm, Section V shows the results and discussion. Finally Section VI contains the conclusion part of the proposed work.

1. GFCC (Gamma Tone Frequency Cepstrum Coefficient)

Gammatone cepstral coefficients computation process is equivalent to MFCC extraction scheme. The audio signal is first windowed into short frames; usually of 10–50 ms. This process is based on two processes: The typical audio signals which are non stationary can be assumed to be stationary for such a short interval, thus facilitating the spectro temporal signal analysis. The efficiency of the feature extraction process is increased. Next, the GT filter bank which is composed of the frequency responses of the several Gamma Tone filters is applied to the signal's fast Fourier transform (FFT), emphasizing the perceptually meaningful sound signal frequencies. The design of the Gamma Tone filter bank which is composed of array of band pass filters is the object of study in this work, taking into account characteristics such as: total filter bank bandwidth, GT filter order, ERB model and number of filters.

II. PROPOSED FLOWCHART

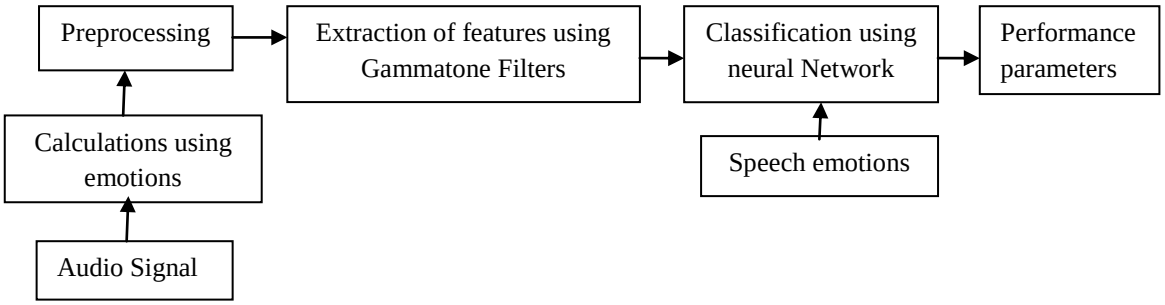

Figure 2. Flow diagram of the proposed work

1. Firstly we need speech file for emotion detection. So the basic step is to upload speech file which is in .wav format in MATLAB software
2. Now progression of some steps to make it compatible with MATLAB platform and ready for further process through training of the audio files[7], used to familiarizing the arrangement with characteristics of the emotions of the speech.
3. Apply Gamma Tone Frequency Cepstrum algorithm for feature extraction based on audio files like min value, max value etc.
4. Now testing process will be implemented using classifier which is Back Propagation Neural Network and then accuracy [8] is measured.
5. Evaluate results.

III. Pseudo code for GFCC Technique

1. Pass input signal through a 64-channel filter bank which contains array of band pass filters [9].
2. At each channel, fully rectify the filter response (i.e. take absolute value) and decimate it to 100 Hz as a way of time windowing.
3. Creation of time frequency (T-F) representation to convert the time domain signal to frequency domain
4, Apply logarithms for finite sequence data set
5. Apply DCT transformation for compression of speech signal and convolution computations.

IV. Simulation and Discussion

Results simulation is taken place in MATLAB environment. Firstly we will upload the file emotion set like happy sad fear etc randomly. Then we set the noise level because we assume that the speech signal is not noise free signal. Then we will extract the features using GFCC algorithm [10] which is used for feature extraction. It includes Fast Fourier transformation used to convert the time domain signal to frequency domain for spectral analysis, filtration process like hamming window which is a type of filter to attenuate the unwanted frequencies and accepts the required frequency to boost up the frequencies and Error rectangular bandwidth which is the process of bandwidth approximation and to increase the strength of the signal in noisy environment. GFCC also includes filter bank which is an array of Band Pass Filter that separates the input signal into multiple components, each one carrying a single frequency sub-band of the original signal. Then we train the system for the emotion detection so that it will perform better for further use then we will test the uploaded file using neural network which act as a classifier to classify the speech emotion and then on the basis of that detection the accuracy will be measured.

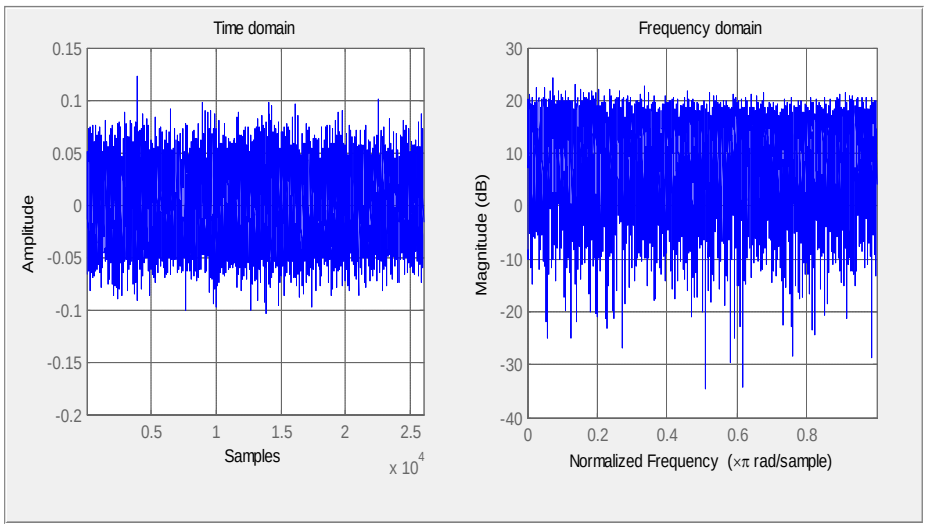

The above figure shows the GFCC based graph in which signal is converted from time domain to frequency domain after applying fast Fourier transform because the signal is having no frequency component in the time domain so we apply FFT to boost up the frequency and for conversion of signal to frequency domain from time domain to have frequency component in the audio signal.

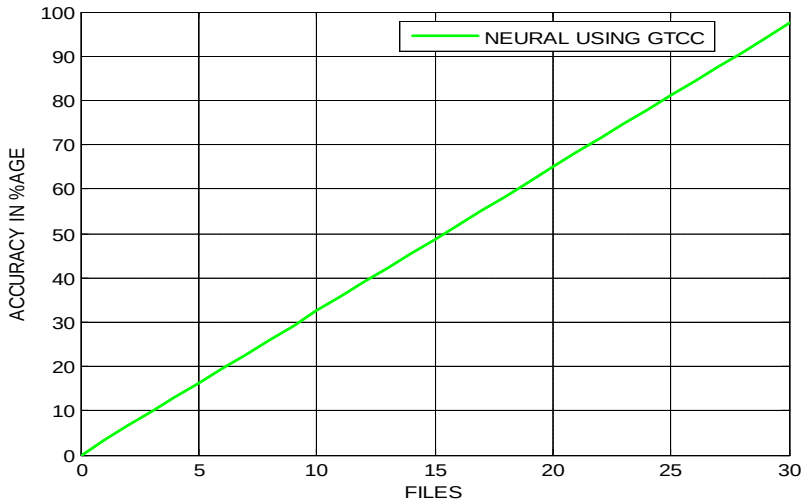

Figure.3 GFCC Performance

The above figure shows the accuracy rate in which emotion is detected

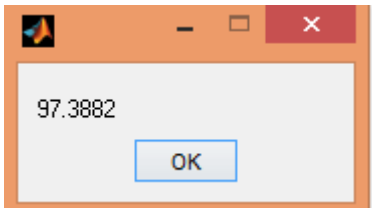

The above figure shows the message box used in MATLAB which shows the accuracy value which is 97.3882

V. Conclusion and Future scope

In proposed work, eventually we conclude about recognition of speech using BPA (Back Propagation Algorithm) that belongs to neural networks. Classifier [11] perform better it conclude by testing of speech data with classifier. We apply BPA classifier on selected speech data. Each classifier has different theory for implementation. From all the above calculations we come to the conclusion that detection of speech emotion by using BPA (Back Propagation Algorithm) that belongs to neural networks with GFCC feature extraction method performs better.

In future, we can apply this proposed algorithm on different languages to make this proposed algorithm more practical .i.e. Punjabi, Hindi, Bengali speech etc. We can also replace the BPA classifier by the MLP Classifier to get differentiate accuracy rate. Also we can increase the number of features extracted from speech data inputted like pitch, frequency range etc.

REFERENCES

[1] Md. Ali Hossain, Md. Mijanur Rahman, Uzzal Kumar Prodhan, Md. Farukuzzaman Khan "Implementation Of Back-Propagation Neural Network For Isolated Bangla Speech Recognition" In ijscit , 2013.

[2] Wouter Gevaert, Georgi Tsenov, Valeri Mladenov, "Neural Networks used for Speech Recognition", JOURNAL OF AUTOMATIC CONTROL, UNIVERSITY OF BELGRADE, VOL. 20:1-7, 2010.

[3] S. K. Shevade, S. S. Keerthi, C. Bhattacharyya, and K. R. K. Murthy, "Improvements to the SMO Algorithm for SVM Regression", IEEE Transactions on Neural Networks, Vol. 11, No. 5, September 2000.

[4] Ibrahim Patel, Dr. Y. Srinivas Rao, "Speech Recognition Using Hmm With GFCC- An Analysis Using Frequency Specral Decomposion Technique", Signal & Image Processing : An International Journal(SIPIJ) Vol.1, No.2, December 2010.

[5] Hitesh Gupta, Deepinder Singh Wadhwa, "Speech Feature Extraction and Recognition Using Genetic Algorithm", International Journal of Emerging Technology and Advanced Engineering, Vol. 4, Issue 1, January 2014.

[6] Jian Wang, Zhiyan Han, and ShuxianLun, "Speech Emotion Recognition System Based on Genetic Algoithm and Neural Network", Published in IEEE, Print ISBN No: 978-1-61284-881-5/11/$26.00, on 2011

[7] Richard P. Lippmann, "Speech recognition by machines and humans", 1997 Elsevier Science B.V.

[8] Kuo-Hau Wu, Chia-Ping Chen and Bing-Feng Yeh, "Noise-robust speech feature processing with empirical mode decomposition", EURASIP Journal on Audio, Speech, and Music Processing 2011.

[9] JozefVavrek, JozefJuhar and Anton Cizmar, "Emotion Recognition from Speech", Published in IEEE Transactions on Audio Speech Vol.21,No.12,on dec2013.

[10] M.A.Anusuya, S.K.Katti, "Speech Recognition by Machine: A Review" (IJCSIS) International Journal of Computer Science and Information Security, Vol. 6, No. 3, 2009

[11] Rahul.B.Lanjewar,D.S.Chaudhari,"SpeechEmotion Recognition:A Review" International Journal of Innovative Technology and Exploring Engineering, ISSN:2278-3075, Vol.2,Issue-4,March 2013.

ISSN (e): 2250 – 3005 || Vol, 05 || Issue, 01 || January – 2015 ||
International Journal of Computational Engineering Research (IJCER)

Analysis of Circular Patch Antenna Embeded on Silicon Substrate

Shaikh Haque Mobassir Imtiyaz[1], Sanjeev kumar Srivastava[2]
[1]Dept Of Electronics, Pillai Institute Of Information Technology, Engineering, Media Studies & Research, University Of Mumbai
[2]Professor,Dept of Electronics & Telecommunication Pillai Institute Of Information Technology, Engineering, Media Studies & Research, University Of Mumbai

ABSTRACT:
This paper presents the effect of changing the substrate thickness and path diameter on a circularly polarized linearly feed micro-strip antenna. The base is fabricated with silicon substrate having di-electric permittivity value as 9. The antenna we have simulated is having the centre frequency of 1.227ghz which makes it suitable even for gps satellite communication. The parameters we will be dealing here mainly are total gain, substrate thickness and patch diameter and its subsequent effect on radiation pattern.
KEYWORDS: *Antenna, silicon, gain, patch, diameter, substrate, thickness*

I. INTRODUCTION

Microstrip antennas, also called patch antennas, are very popular antennas in the microwave frequency range because of their simplicity and compatibility with circuit board technology. The circular patch has similar traits to the rectangular patch regarding gain, beam position and efficiency. Circular patch antennas are usually manufactured by etching the antenna patch element in a metalised dielectric substrate. Larger antennas are sometimes constructed by bonding metal cut-outs to a bare substrate.The pin-fed patch, which is simple to construct, is fed by making a circular hole in the substrate and ground plane and bringing the centre conductor of a coaxial connector or cable into ohmic contact with the patch at an appropriate point. The point of contact depends mainly on the required centre frequency and input impedance, typically 50 Ω, but also on the suppression of higher order resonant modes. Fringing fields act to extend the effective diameter of the patch. Thus, the diameter of the half-wave patch (dominant TM11 mode) is usually less than a half wavelength in the dielectric medium. The electric fringing fields are responsible for radiation. Fringing fields act to extend the effective diameter of the patch. Thus, the diameter of the half-wave patch (dominant TM11 mode) is usually less than a half wavelength in the dielectric medium. The electric fringing fields are responsible for radiation.

II. IMPEDANCE CHARACTERISTICS

The circular patch has an impedance bandwidth ranging from 0.3% to 15%. It is usually operated near resonance to obtain a real-valued input impedance. The position of the feed determines the input resistance of the patch. While the input resistance can be determined quite accurately by the position of the pin, the inductive reactance caused by the pin may affect the input match considerably when the substrate is electrically thick.

III. RADIATION CHARACTERISTICS

The dominant mode radiation pattern is a single lobe with maximum in the direction normal to the plane of the antenna

IV. SIMULATION PROCESS

The simulation has been carried in six different stages. In all the stages the relative permittivity of silicon layer has been kept constant to provide the uniformity during entire simulation. in first three steps substrate thickness have been varied with patch diameter constant and in remaining three substrate thickness has been varied keeping the patch diameter constant. The parameters of different stages have been provided in tabular form followed by the graph and respective radiation pattern

Tabulation of parameters for various step of simulation

Step	Substrate Thickness (mm)	Patch Diameter (mm)	Relative Permittivity
1	1.217	23.63	9
2	3.210	23.63	9
3	3.255	23.63	9
4	2.66	23.26	9
5	2.66	23.88	9
6	2.66	24.00	9

Resultant observation

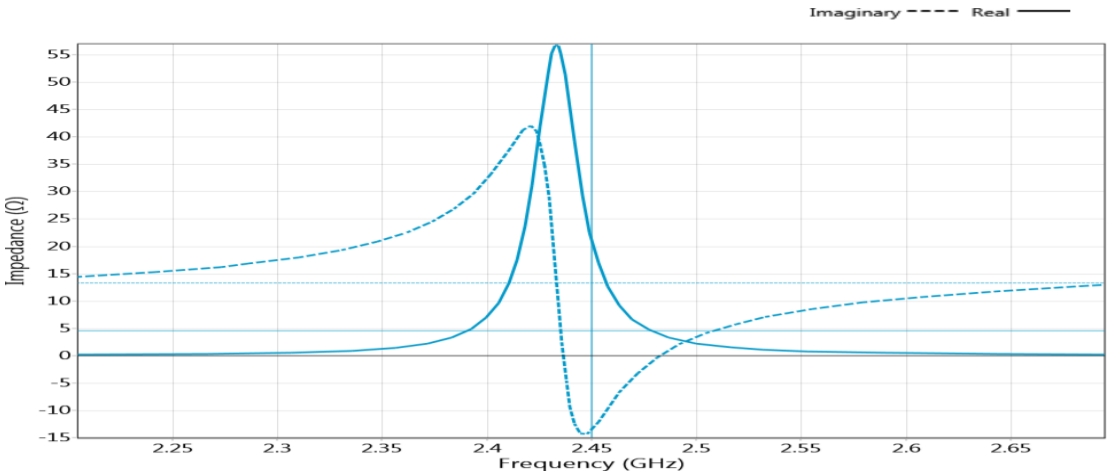

Fig1: Impedance Characteristics for step1

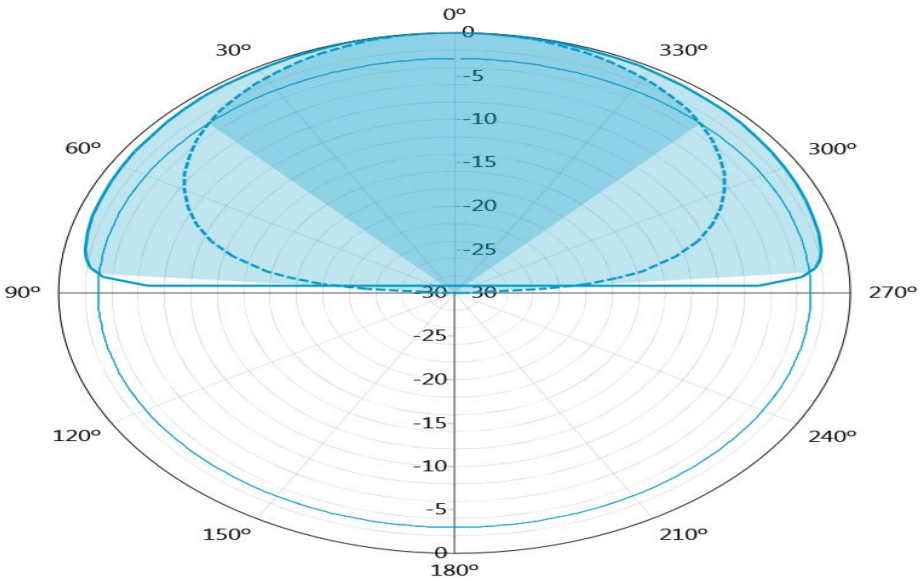

Fig2: Total gain for step 1

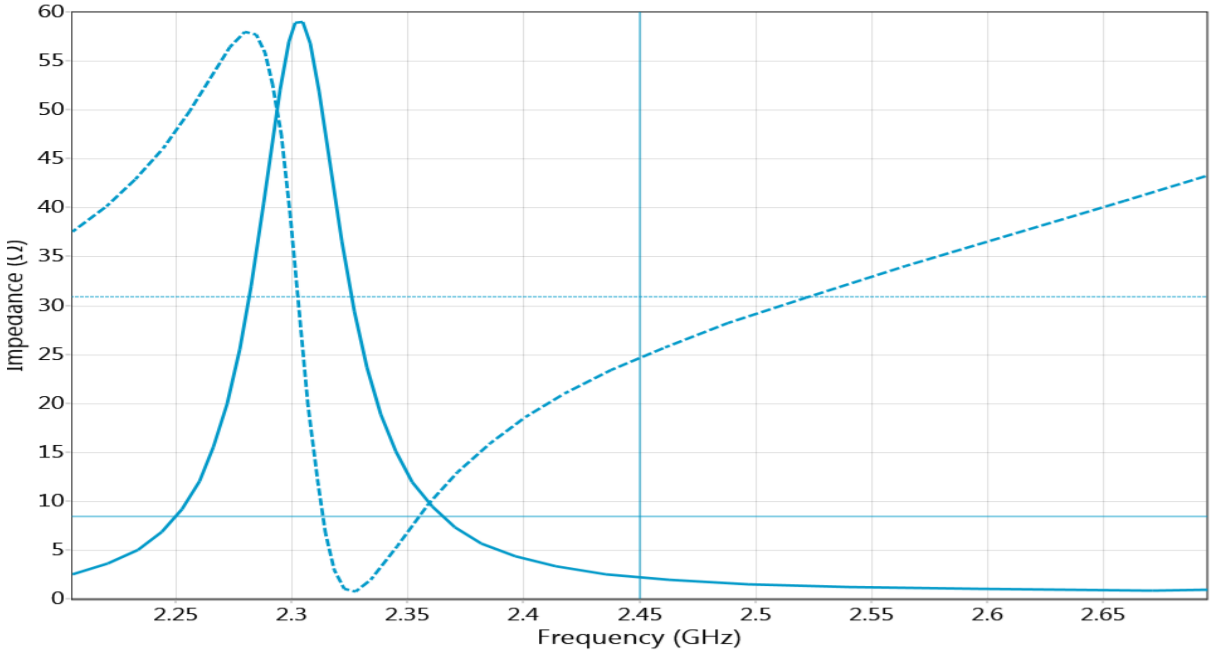

Fig3: Impedance characteristics for step2

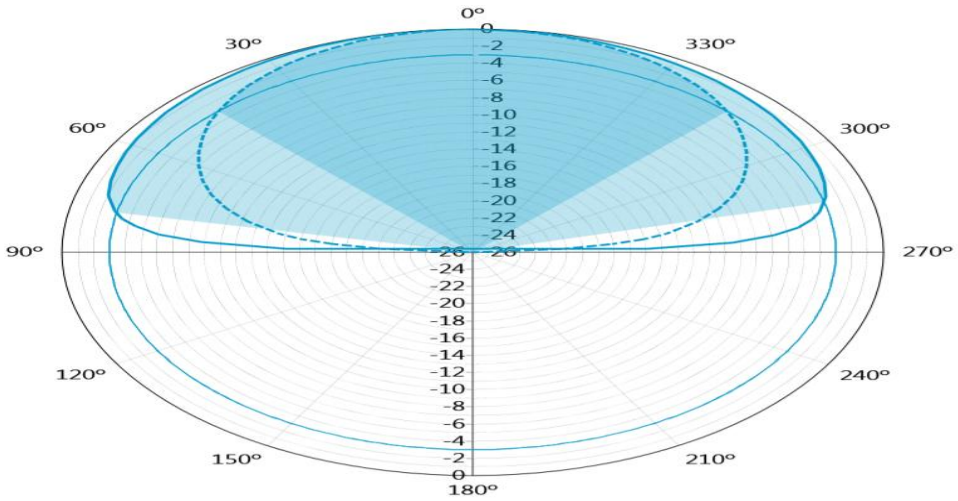

Fig4: Radiation pattern for step 2

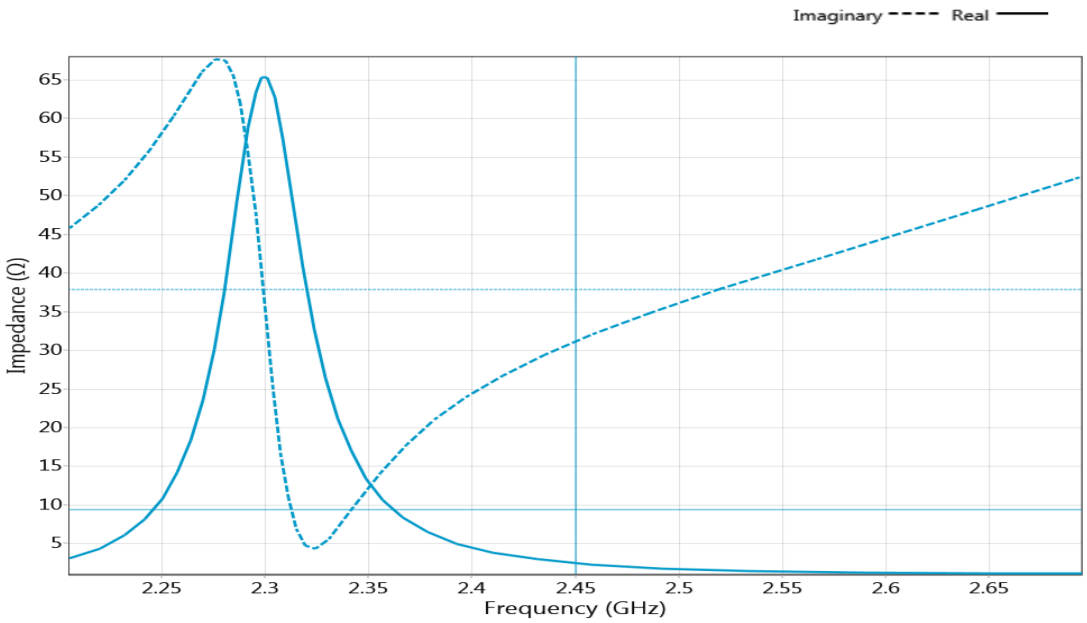

Fig5: Impedance Characteristics for step 3

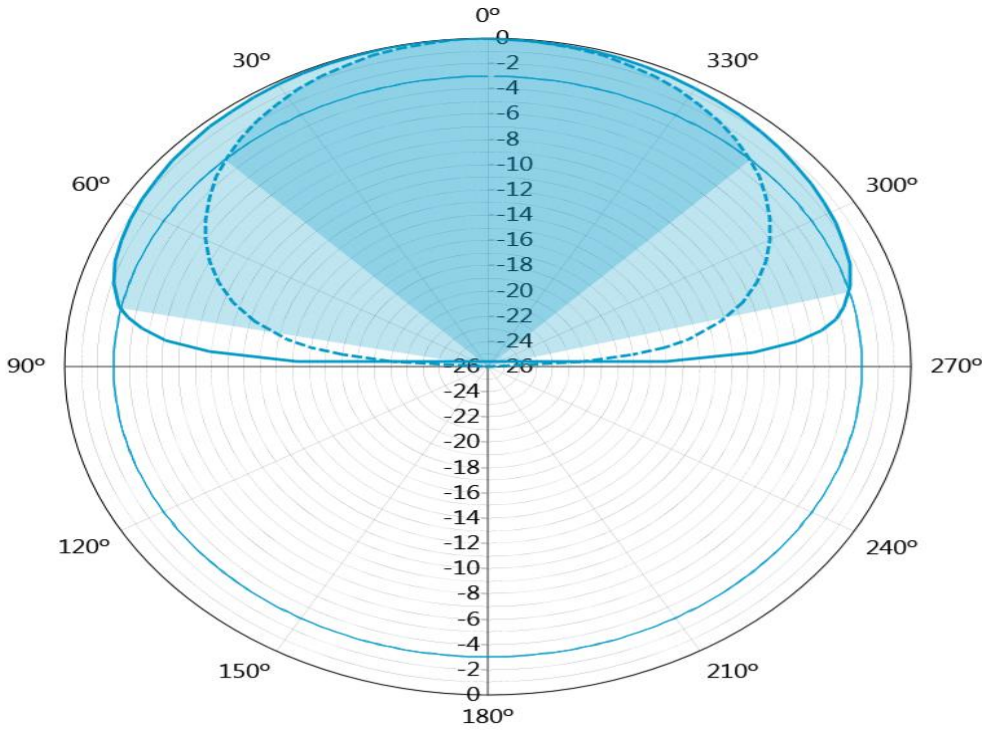

Fig6: Radiation Pattern for step 3

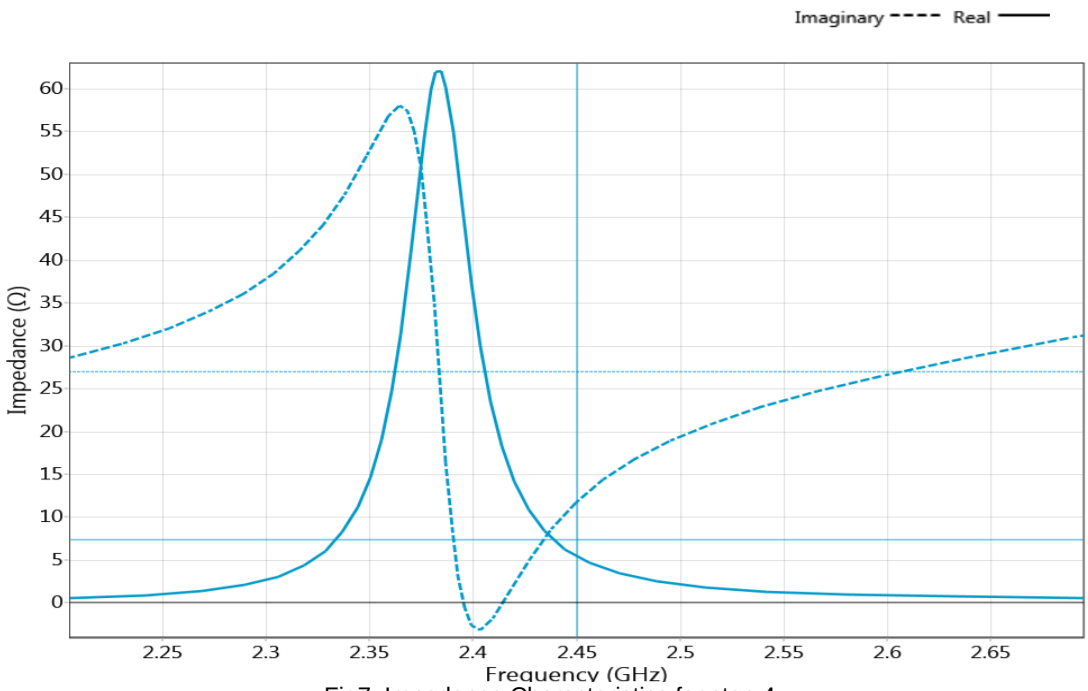

Fig7: Impedance Characteristics for step 4

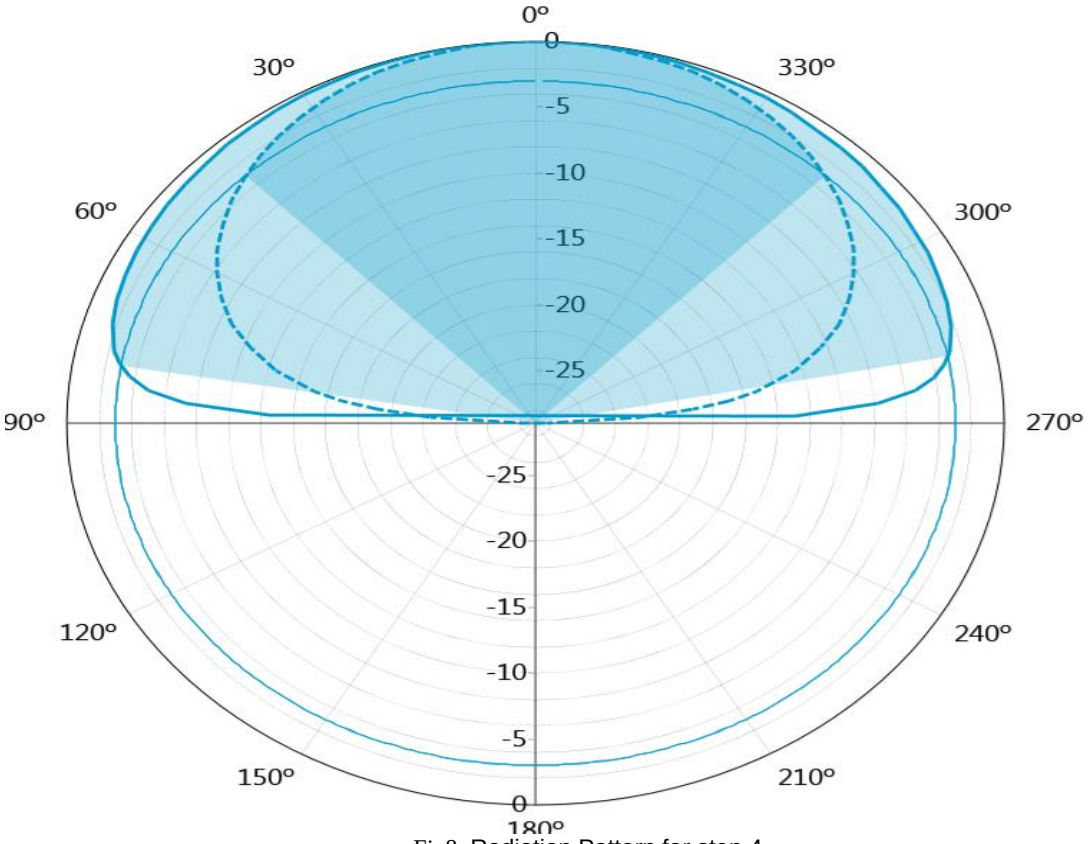

Fig8: Radiation Pattern for step 4

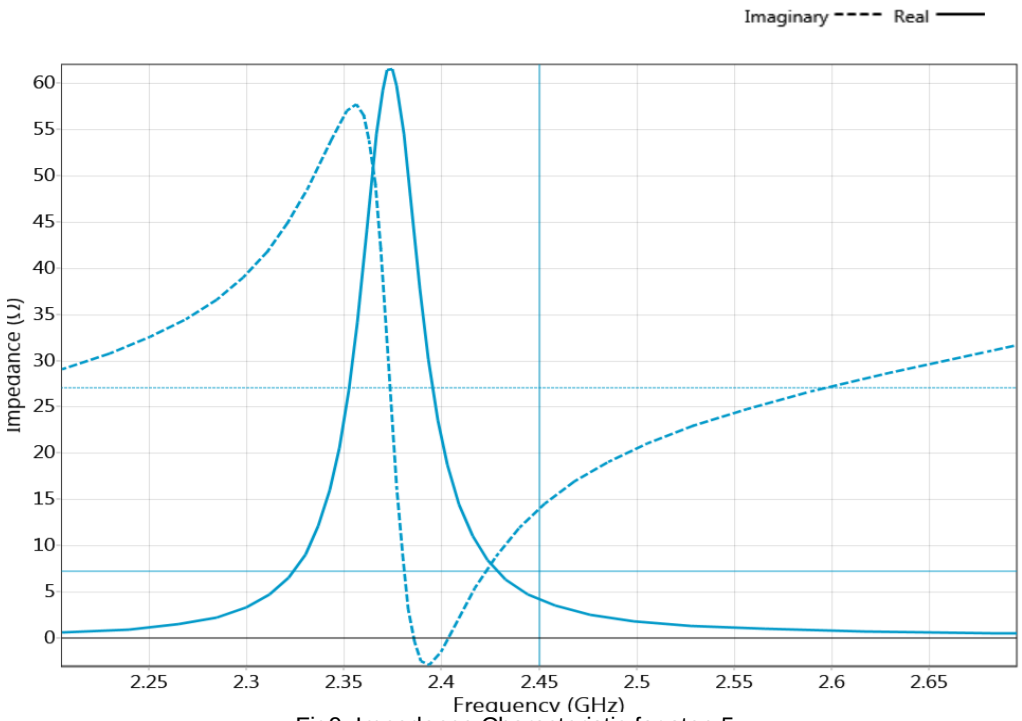

Fig9: Impedance Characteristic for step 5

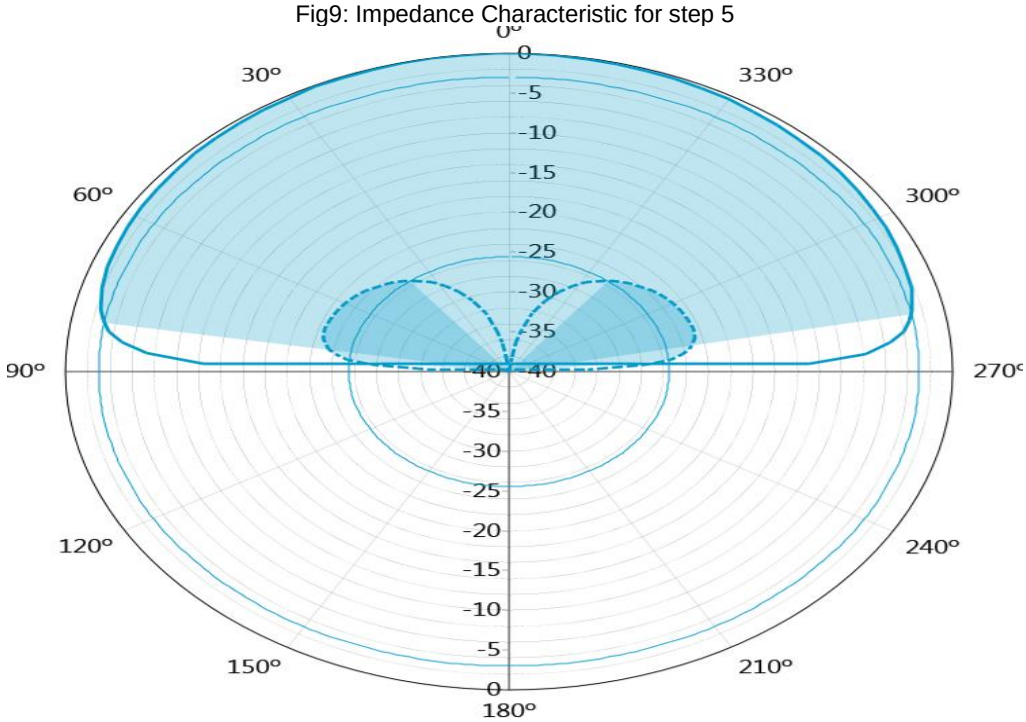

Fig10: Radiation Pattern for step 5

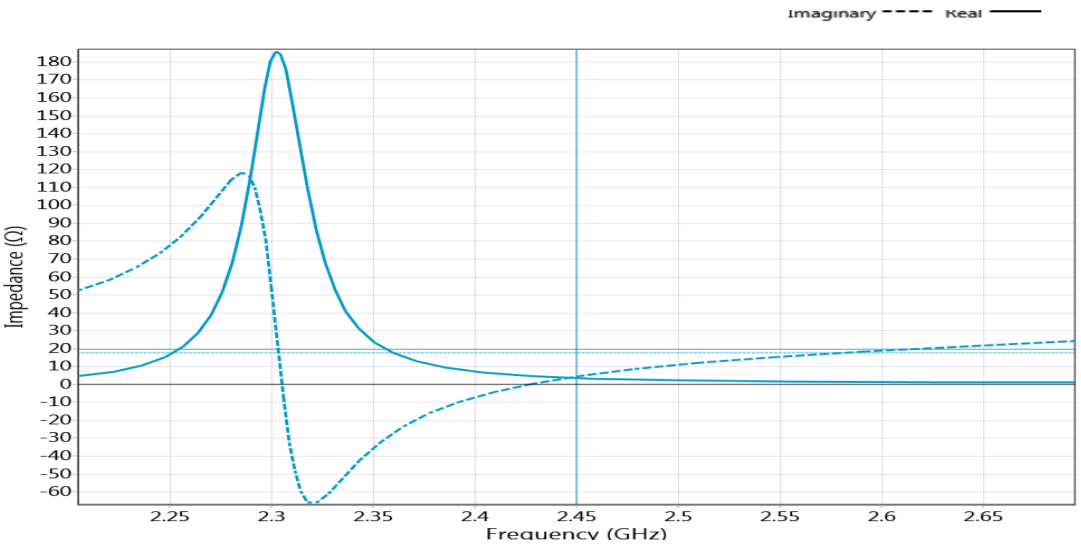

Fig11: Impedance Characteristics for step 6

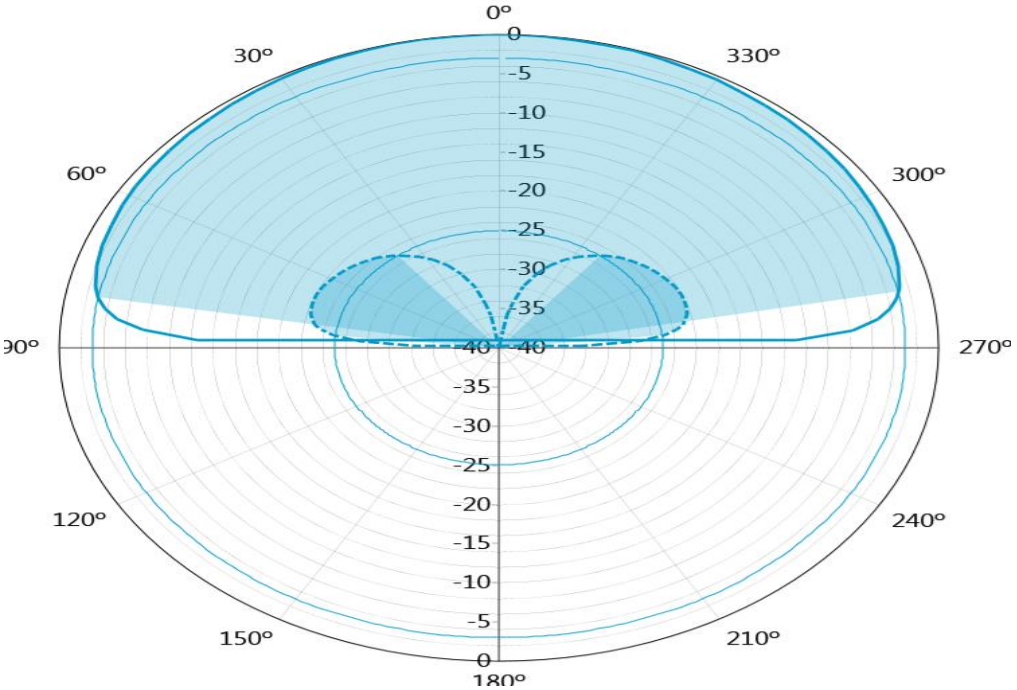

Fig12: Radiation Pattern for step 6

V. RESULT & DISCUSSION

Before discussing the results we have summarized the gain , impedance frequency, for the every above mentioned parameters

Fig	Angle Frequency(Degree)	Gain(DB) @ 2.45Ghz	Real Impedance
1,2	0	3.153	56.86 ohm @ 2.43 Ghz
	90	3.151	
3,4	0	4.507	59.18 ohm @ 2.30 Ghz
	90	4.487	
5,6	0	4.492	65.58 ohm @ 2.5Ghz
	90	4.470	
7,8	0	4.845	62.29 ohm @ 2.384 Ghz
	90	4.837	
9,10	0	4.484	61.70 ohm @ 2.37 Ghz
	90	-17.17	
11,12	0	4.883	186.1 ohm @ 2.37 Ghz
	90	-17.18	

The ideal gain of circular linearly fed patch antenna is 8db maximum from 4dbi which is minimum for wavelength greater $\frac{lambda}{6}$ upto $\frac{lambda}{2}$ and we observe that if we increase substrate thickness in spite of increase in inductive reactance the gain has not decreased and have maintained the minimum level of gain and the result have further improved while we have kept substrate thickness to minimum and have increased the patch diameter though it have affected the resonant frequency but all the gains have been measured at 2.45ghz so the results match the requirement of minimum gain.

VI. CONCLUSION

A high-performance microstrip patch antenna was fabricated on a normal low resistive silicon wafer The fabrication progress was fully compatible with MMCM packaging, without any additional process steps. The antenna resonated with a maximum gain of 4.9dbto minimum gain of 3.153db.

REFERENCES

[1] Tang J J, Ding X Y, Geng F, et al. Wafer-level multilayer integration of RF passives with thick BCB/metal interlayer connection in silicon-based SiP. Microsyst Technol, 2012, 18: 119

[2] Tang J J, Sun X W, Luo L. A wafer level multi-chip module process with thick photosensitive benzocyclobutene as dielectric for microwave application. J Micromech Microeng, 2011, 21: 065035

[3] Tang J J, Sun X W, Luo L. A wafer level multi-chip module process with thick photosensitive benzocyclobutene as dielectric for microwave application. J Micromech Microeng, 2011, 21: 065035

[4] Aoshima, Y., Y. Kimura, and M. Haneishi, \A microstrip antenna with variable reactance elements for polarization control and frequency control of circular polarization," *IEICE Trans. B*, Vol. J93-B, No. 9, 1177{1183, 2010 (in Japanese).

[5] Rao R T, Madhavan S. Introduction to system-on-package (SoP): miniaturization of the entire system. USA: McGraw-Hill Prof Med/Tech, 2008, 3: 81

[6] Ju C W, Park S S, Kim S J, et al. Effects of O2C2F6 plasma descum with RF cleaning on via formation in MCM-D substrate using photosensitive BCB. Electronic Components and Technology Conf. Orlando, FL, USA, 2001: 1216

AUTHOR INFORMATION

Shaikh HaqueMobassir I
M.E Electronics
P.I.I.T PANVEL

Sanjeev kumar Srivastava

Currently working as an associate professor in Dept of Electronics & Telecommunication Engineering, in pillai Institute Of Information Technology, Engineering, Media Studies & Research, New-Panvel, Mumbai University. He has completed his Bachelor & Master degree in E &TC Engg from Mumbai University. Presently he is pursuing PhD from Nagpur University(Maharashtra). He has more than 17years of teaching experience in various engineering colleges affiliated to Mumbai university. He has published more than 13 papers National, International conferences & International journals & has also attended several National International workshops and Seminars

ISSN (e): 2250 – 3005 || Vol, 05 || Issue, 01 || January – 2015 ||
International Journal of Computational Engineering Research (IJCER)

Performance Analysis of Bus Topology in Fiber Optic Communication

Lakshmi A Nair[1], Lakshmy G B[2]
[1] P G Scholar, Optoelectronics and Communication Systems, TKM Institute of Technology
[2] Assistant Professor, Electronics and Communication Department, TKM Institute of Technology

ABSTRACT:
Topology refers to the layout of connected devices in a network. It describes the way in which the elements of the network are mapped. Optical network topologies such as bus, star and tree reduce complexity by using minimum number of couplers, multiplexers, demultiplexers and optical amplifiers and can reduce cost in large network. The performance of bus topology is investigated and identified that, for bus topology the quality of signal goes on decreasing with increase in number of nodes. The performance of bus topology is investigated in presence of optical amplifiers such as Semiconductor Optical Amplifiers (SOA) and Erbium Doped Fiber Amplifier (EDFA) and photodiodes such as PIN and Avalanche photodiode (APD). By considering the signal quality factor and bit error rate it is investigated that bus topology using EDFA with PIN photodiode serves better.

KEYWORDS: *Avalanche photodiode (APD), data rate, Erbium Doped Fiber Amplifier (EDFA), LAN (Local area Network), Q factor, Semiconductor Optical Amplifiers (SOA), Topology*

I. INTRODUCTION

Optical fibers are essentially very thin glass cylinders or filaments which carry signals in the form of light (optical signals). An optical network connects computers using optical fibers. Optical networks have found widespread use because the bandwidth of such networks using current technology is 50 tera-bits per second. Optical network uses optical multiplexing and switching technique to increase its capacity. The implementation of time multiplexers, demultiplexers and encoders/decoders at terabits per second is very difficult in networks. Optical network topologies such as bus, star and tree reduces complexity by using minimum number of couplers, multiplexers, demultiplexers and optical amplifiers and can reduce cost in large networks. Also maximum number of users can be supported with minimum received power for a given bit error rate.

Bus is the network topology in which all of the nodes of the network are connected to a common transmission medium which has exactly two endpoints. All data that is transmitted between nodes in the network is transmitted over this common transmission medium and is able to be received by all nodes in the network virtually simultaneously. Star is the topology in which each of the nodes of the network is connected to a central node with a point-to- point link. All data that is transmitted between nodes in the network is transmitted to this central node, which is usually some type of device that then retransmits the data to some or all of the other nodes in the network. A tree topology combines characteristics of linear bus and star topologies. It consists of groups of star configured workstations connected to a linear bus backbone cable.

Optical fiber accommodates today's increasingly complex network architectures. Using optical fiber various topologies came into being. Each topology has its strengths and weaknesses, and some network types work better for one application while another application would use a different network type.

II. OPTICAL NETWORK TOPOLOGY

The optical networks can be configured in a number of topologies. These include a bus, a star network, a tree network, or some combination of these. Network topology is the study of the arrangement or mapping of the elements (links, nodes, etc.) of a network, especially the physical (real) and logical (virtual) interconnections between nodes. A local area network (LAN) is one example of a network that exhibits both a physical and a logical topology. Any given node in the LAN will have one or more links to one or more other nodes in the network and the mapping of these links and nodes onto a graph results in a geometrical shape that determines the physical topology of the network Likewise, the mapping of the flow of data between the nodes in the network determines the logical topology of the network. It is important to note that the physical and logical topologies might be identical in any particular network but they also may be different.

Network Topology is, therefore, technically a part of graph theory. Distances between nodes, physical interconnections, transmission rates, or signal types may differ in two networks and yet their topologies may be identical. In addition to its advantages (i.e., bandwidth, durability, ease of installation, immunity to EMI/RFI and harsh environmental conditions, long-term economies, etc.), optical fiber better accommodates today's increasingly complex network architectures than copper alternatives. Using optical fiber various topologies came into being. Each topology has its strengths and weaknesses, and some network types work better for one application while another application would use a different network type.

.

III. BUS TOPOLOGY

Bus network topology is a network architecture in which a set of clients are connected via a shared communications line, called a bus. This topology is easy to implement and install. It is well-suited for temporary or small networks not requiring high speeds, resulting in faster networks. Cost effective and easy identification of cable faults is possible. Moreover, Bus networks are the simplest way to connect multiple clients, but often have problems when two clients want to transmit at the same time on the same bus. Many active architectures can also be described as a bus, as they provide the same logical functions as a passive bus, for example, switched Ethernet can still be regarded as a logical bus network, if not a physical one. The advantage of bus topology is it is cheap, easy to handle and implement, require less cable and suitable for small networks. The disadvantage of using bus topology is, the cable length is limited and it limits the number of stations that can be connected.

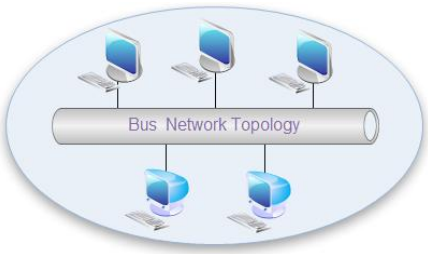

Figure 1: Bus Topology

Figure 2 given below shows the block diagram of bus topology having two users, the transmitter section is composed of data source, NRZ rectangular driver, CW Lorentzian laser, optical amplitude modulator and optical link section. The outputs from driver and laser source are passed to the optical amplitude modulator. The optical signal from the modulator is passed through the fixed gain amplifier and splitter. Each user in the bus is connected through the optical splitter; each user is connected to every other user by a Single Mode Fiber (SMF) and Dispersion Compensating Fiber (DCF) through an amplifier. The combination of SMF and DCF fibers for long distance scenario has been considered to mitigate the nonlinear effects. The placement of one amplifier is done at the start of each segment in order to continue broadcasting the information from transmitter users. A single user section is composed of optical raised cosine filter (Raised cosine1), PIN photodiode (IdealRX1) and low pass Bessel filter (Bessel5poles 1). At receiver measurements are made with the help of optical spectrum analyzer, optical probe and electrical scope. Electrical scope is used to obtain eye diagram and from the eye diagram Q factor can be determined.

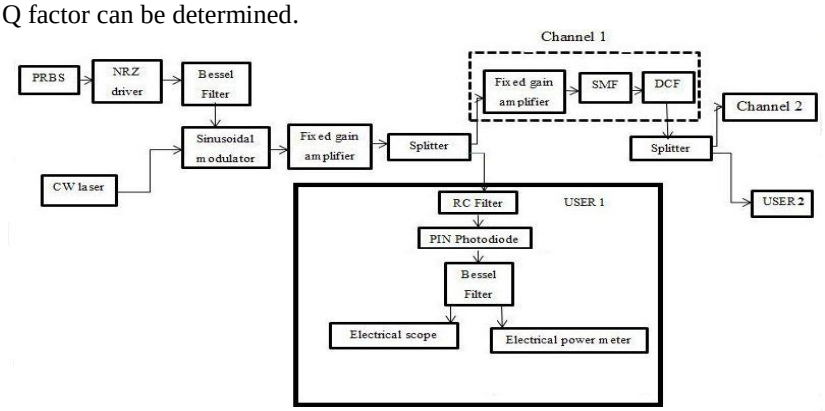

Figure 2: Block Diagram of bus topology

IV. SYSTEM DESIGN

The design model of bus topology shown in Figure 3, the transmitter section consists of data source with data rate 10Gbps, laser source (CW Lorentzian) and optical amplitude modulator (Sin2 MZI). Data source is customized by baud rate, sequence, logical signal level and the period length. In this transmitter set up NRZ modulation format is used. Laser source provides transmission at 1552.52nm laser emission frequency. Laser phase noise is taken into account by generating a lorentzian whose power spectrum width at half maximum is specified at 10 MHz The output from driver and laser source is passed to the optical amplitude modulator. The optical signal from the modulator is passed through a fixed gain amplifier where the optical signal is get amplified. Each user in the bus is connected through the optical splitter; every user is connected to every other user by a single mode fiber (SMF) and dispersion compensating fiber (DCF) with reference frequency 193.41449 THz. A single user section is composed of optical raised cosine filter (Raised cosine1), PIN photodiode (Ideal RX1) and low pass Bessel filter (Bessel 5 poles 1). At receiver measurements are made with the help of electrical scope and electrical power meter. Electrical scope is used to obtain eye diagram and from the eye diagram determines the values of Q factor. Electrical power meter is used to obtain the received power value. In the above simulation diagram different combinations of optical amplifiers and photodiodes can be used for comparison, they are SOA with PIN, SOA with APD, EDFA with PIN and EDFA with APD.

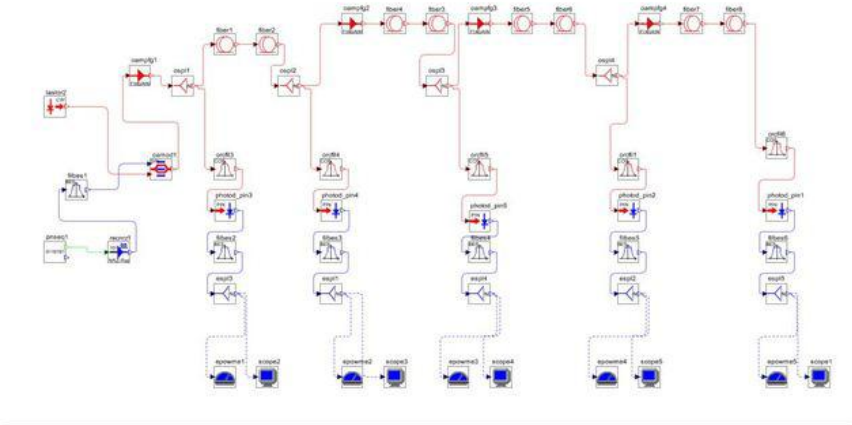

Figure 3: Simulation diagram of bus topology

V. RESULT AND DISCUSSION

Bus topology is designed and simulated using the Optsim software. The results of these simulations are obtained with the help of measurement tool such as Electrical scope. Eye diagram is the methodology used to evaluate the performance of the system.

5.1. Relationship between Q Factor with internode distance

As the internode distance increases the quality of signal received at the receiver section begins to fade and hence bus topology serves better for short distance communication.

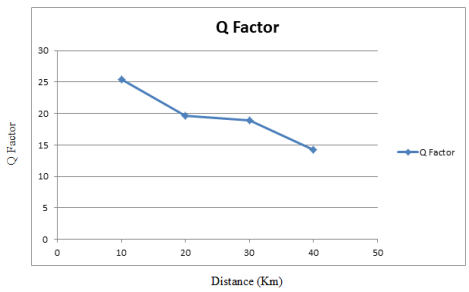

Figure 4: Relationship between Q Factor and internode distance

5.2. Eye diagram of different users with different internode distances

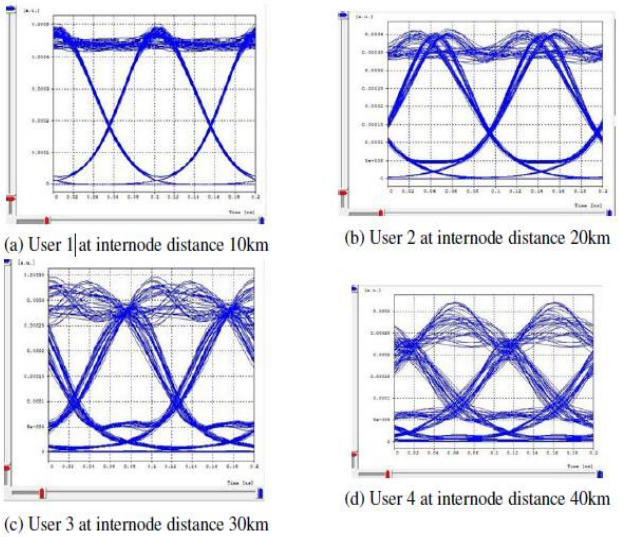

(a) User 1 at internode distance 10km

(b) User 2 at internode distance 20km

(c) User 3 at internode distance 30km

(d) User 4 at internode distance 40km

Figure 5: Eye diagram of different users with different Internode distances

5.3. Relationship between received power at different nodes with variable input power

The value of received power is observed at different nodes with variable input power and it is observed that with increase in input power, the received power also increases.

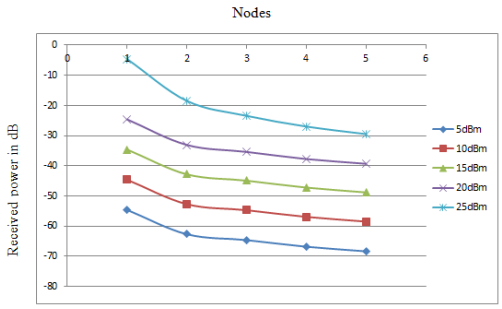

Figure 6: Relationship between received power at different nodes with variable input power

5.4. Relationship between data rate and Q factor

The value of Q Factor is observed at different nodes with variable data rate and observed that with increase in data rate the Q Factor get decreased.

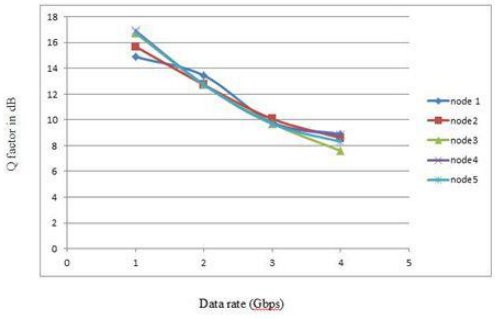

Figure 7: Relationship between data rate and Q factor

5.5. Comparison of Bus Topology using different Optical Amplifiers (SOA and EDFA) and different Photodiodes (PIN and APD)

By analyzing the results it is clear that bus topology using optical amplifier EDFA and photodiode PIN serves better because EDFA is having less noise figure and high gain and PIN serves better for longer wavelength region.

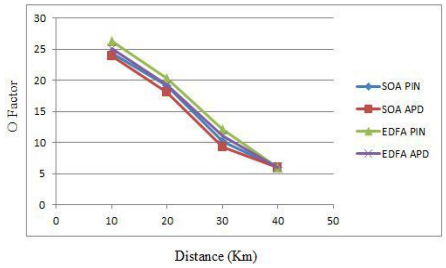

Figure 8: Comparison of bus topology using different Optical Amplifier and Photodiode in terms of Q factor

VI. CONCLUSION

The performance of bus topology is investigated and identified that, for bus topology the quality of signal goes on decreasing with increase in number of nodes. So it is used for short distance communication. As the internode distance increases Q factor decreases and as the data rate increases the Q factor decreases. The value of received power is observed at different nodes with variable input power and it is observed that with increase in input power, the received power also increases. Simulation and performance analysis of bus and star topology is done using different optical amplifier (SOA and EDFA) and different photodiodes (PIN and APD) and analyzed that bus topology using optical amplifier EDFA with PIN photodiode serves better.

REFERENCES

[1] Raghavee N.S, Gaurav H Kankaria, S. Sugumaran, S.Revathi,“ Comparative Analysis of Network Topologies Using Optical Amplifiers”, Int.J.Computer Technologyand Applications, Vol 5 (2),573-577 (2014).

[2] Chirag Saini, Gaurav Agarwal, Vikash Patnaik, Jabeena A ,“Performance Analysisof Different Hybrid-Optical Amplifiers”, SSRG International Journal of Electronics and Communication Engineering (SSRG-IJECE) , volume 1April 2014.

[3] Jitender kumar, Manoj Arora, R. S. Chauhan ,“Performance Analysis of WDM PON at 10 Gb/s”, International Journal of Engineering and Advanced Technology,(IJEAT) ISSN: 2249 - 8958, Volume-1, Issue-3, February 2012.

[4] Surinder Singh “Performance comparison of optical Network Topologies in the presence of optimized Semiconductor Optical Amplifiers ,”Journal of Optical Communications and Networking ,Vol.1, Issue 4, pp. 313-323 (2009).

[5] Senior John M, “Optical Fiber Communications ”,Pearson Education.

[6] Gerd Keiser, “Optical Fiber Communications”, 3e.Tata McGraw hill Publication.

ISSN (e): 2250 – 3005 || Vol, 05 || Issue, 01 || January – 2015 ||
International Journal of Computational Engineering Research (IJCER)

Special Double Sampling Plan for truncated life tests based on the Marshall-Olkin extended exponential distribution

D.Malathi[1] ,Dr.S.Muthulakshmi[2]
[1] *Assistant Professor (Sr.Gr), Department of Mathematics, Velalar College of Engineering & Technology, Erode.*
[2] *Professor, Department of Mathematics, Avinashilingam Institute for Home Science and Higher Education for Women, Coimbatore.*

ABSTRACT
In this study , we propose the designing of special double sampling plan for truncated life tests using percentiles under the assumption that the life time of the product follows Marshall-Olkin extended exponential distribution . The minimum sample sizes for the first and second samples are determined for the specified consumer's confidence level with minimum average sample number. The operating characteristics are analysed and the minimum percentile ratios of life time are obtained so as to meet the specified producer's risk. The efficiency of special double sampling plan is analysed with zero-one double sampling.

Keywords*: Special double sampling, Consumer's risk, Operating Characteristic function, Producer's risk, Truncated life tests, Average sample number.*

I. INTRODUCTION

The reliability of the product has become a vital factor in a global business market. Acceptance sampling ensures the quality of the product.The acceptance sampling for life tests is concerned with accepting or rejecting a submitted lot of products on the basis of life time of the sample units taken from the lot. The producer and the consumer are subject to risks due to decision based on sample results. By increasing the sample size, Consumer's risk of accepting bad lots and producer's risk of rejecting good lots may be minimized to a certain level but this will increase the cost of inspection. Truncation of life test time may be introduced to reduce the cost of inspection.

Many studies have been carried out for designing single sampling plan and double sampling plans for the truncated life tests under various statistical distributions for life time.

Epstein (1954) first introduced single acceptance sampling plans for the truncated life test based on the exponential distribution. Goode and Kao (1961) developed an acceptance sampling plan using the Weibull distribution as a lifetime distribution. Gupta and Groll (1961) derived the acceptance sampling plan for the gamma distribution and Gupta (1962) designed the plan for the lifetime of the product having Log-normal distribution. All these authors considered the design of acceptance sampling plans based on the population mean.

Duncan (1986) pointed out that double sampling plan reduce the sample size to attain the same result as compared to single sampling plan. Aslam and Jun (2010) introduced double acceptance sampling for the truncated life test based on percentiles of the generalized log-logistic distribution.

The purpose of this paper is to propose the special double acceptance sampling plan for the truncated life test assuming that the lifetime of a product follows Marshall-Olkin extended exponential distribution. This distribution plays a vital role , in studying the life time of electrical component such as memory disc, mechanical component such as bearings and systems such as aircraft, automobiles. The minimum sample sizes of special double sampling plan are determined to meet the specified consumer's confidence level by incorporating minimum average sample number. The operating characteristics are analysed and the minimum percentile ratio's of life time are obtained for the specified producers risk. The accomplishment of this plan is studied by comparing with zero-one double sampling plan.

Marshall- Olkin extended exponential distribution

Assume that the lifetime of a product follows Marshall- Olkin extended exponential distribution. The probability density function and cumulative distribution function of Marshall- Olkin extended exponential distribution are given by

$$f(t) = \frac{(a/\sigma)\exp(-t/\sigma)}{[1-(1-a)\exp(-t/\sigma)]^2}, \quad t > 0, a, \sigma > 0 \tag{1}$$

and

$$F(t) = \frac{1-\exp(-t/\sigma)}{1-(1-a)\exp(-t/\sigma)}, \quad t > 0, a, \sigma > 0 \tag{2}$$

where σ is the scale parameter and **a** is the shape parameter. The $100q^{th}$ percentile is given by

$$t_q = \sigma \ln[(1-(1-a)q)/(1-q)] \tag{3}$$

where 0<q<1. When *q=0.5*, t_q reduces to σln(1+a) which is the median of Marshall- Olkin extended exponential distribution. It is seen that, t_q depends only on **a** and **σ** .Also it is seen that t_q is increasing with respect to **a** for *q> 0.5* and decreasing with respect to **a** for *q< 0.5*.

Taking

$$\eta = \ln[(1-(1-a)q)/(1-q)]$$

and $\delta = t/t_q$,

equation (2) becomes

$$F(t) = \frac{1-\exp(-\delta\eta)}{1-(1-a)\exp(-\delta\eta)}, t > 0 \tag{4}$$

The designing of special double acceptance sampling plan using percentiles under a truncated life test is to set up the minimum sample sizes for the given shape parameter **a** such that the consumer's risk, the probability of accepting a bad lot, does not exceed 1- P* . A bad lot means that the true $100q^{th}$ percentile t_q , is below the specified percentile t_q^0 .

Design of the proposed sampling plan

Assume that the acceptable quality of a product is represented by its percentile lifetime t_q^0 . The lot will be accepted if the data supports the null hypothesis, H_0: $t_q \geq t_q^0$ against the alternative hypothesis, H_1: $t_q < t_q^0$. The significance level for the test, is 1−P*, where P*is the consumer's confidence level.

The operating procedure of special double sampling plan for the truncated life test has the following steps:

- Draw a sample of size n_1 from the lot and put on the test for pre-assigned experimental time t_0 and observe the number of defectives d_1. If $d_1 \geq 1$ reject the lot.
- If $d_1 = 0$, draw a second random sample of size n_2 and put them on the test for time t_0 and observe the number of defectives d_2.If $d_2 \leq 1$ accept the lot, Otherwise reject the lot.

In a special double sampling plan the decision of acceptance is made only after inspecting the second sample. This aspect differs from usual double sampling plan in which decision of acceptance can be made even before the inspection of the second sample.

It is more convenient to make a termination time interms of acceptable percentiles of lifetime t_q^0 which depend only on $\delta = t/t_q^0$. For a given P*, the proposed acceptance sampling plan can be characterized by $(n_1, n_2, a, \eta, \delta)$.

The minimum sample sizes n_1 and n_2 are determined for

$$P_a = (1-p)^{n_1+n_2}\left\lceil 1+\frac{n_2 p}{1-p}\right\rceil \le 1-P^* \quad (5)$$

where, p is the probability that an item fails before t_0, which is given by

$$p = \frac{1-\exp(-\delta\eta)}{1-(1-a)\exp(-\delta\eta)} \quad (6)$$

Equation (5) provides multiple solutions for sample sizes n_1 and n_2 satisfying the specified consumer's confidence level. In order to find the optimal sample sizes the minimum of ASN is incorporated along with the probability of the acceptance of the lot less than or equal to 1-P* and $n_2 \le n_1$.

Determination of the minimum sample sizes for special double sampling plan reduces to

Minimize $ASN = n_1 + n_2(1-p)^{n_1}$

subject to $(1-p)^{n_1+n_2}\left\lceil 1+\frac{n_2 p}{1-p}\right\rceil \le 1-P^*$ (7)

where n_1 and n_2 are integers.The minimum sample sizes satisfying the condition (7) can be obtained by search procedure. Table 1 is constructed for the minimum sample sizes of zero-one double sampling plan for q=0.05 and 0.1 with various values of a (=2,3,4,5), P*(=0.75,0.90,0.95,0.99) and δ (=0.5,0.7,1.0, 1.5,2.0,2.5,3.0,3.5) . Numerical values in Tables 1 reveals that

(i) increase in consumers confidence level increases the first and the second sample sizes quite rapidly, when the test time is short
(ii) increase in shape parameter **a** increases sample sizes for any P*.
(iii) increase in δ decreases the sample size for any P* .

Operating characteristics values of the sampling plan

OC values depict the performance of the sampling plan according to the quality of the submitted product. The probability of acceptance will increase more rapidly if the true percentile increases beyond the specified life .we need to know the operating characteristic values for the proposed plan according to the ratio of the true percentile to the specified life t_q/t_q^0. These plans are desirable since operating characteristic values increase more sharply to nearly one. Tables 2 and 3 are constructed to give the operating characteristic values corresponding to q=0.05 and 0.1 for fixed **a**.

Minimum Percentile ratio

Producer wants to know the minimum product quality level in order to maintain the producers risk at the specified level. At the specified producers risk α=0.05 the minimum ratio t_q/t_q^0 are obtained by solving $P_a \ge 1-\alpha$ and presented in table 4 by using the sample sizes in Table 1 for specified consumers confidence level. From Table 4 it is seen that with increase in consumers confidence level, decreases the ratio.

Comparitive study

The following table shows the gradual increase of OC values for the increase in the percentiles for special double sampling plan with confidence level P*=0.90, $t/t_q^0=3.5$ and $t_q/t_q^0=15$ with a=3 .

q	0.05	0.01	0.1	0.15	0.2	0.25
OC values	0.9738 (13,12)	0.9845 (47,46)	0.9901 (6,1)	0.9895 (4,1)	0.9888 (3,10)	0.9912 (2,1)

Also, the ASN values of zero-one double sampling plan and special double sampling plan for a=2,q=0.1 P*=0.75 are obtained as follows:

δ / plan	2	2.5	3	3.5
DSP(0,1)	10.366	8.2671	6.8	6.5171
SDSP	6.7981	5.2441	4.5018	4.1927

On comparing the values of life test plans,the zero-one double sampling plan using percentiles provides minimum sample size and hence economical.

References

[1] MuhammedAslam and Chi-Hyuck Jun, *A Double Acceptance Sampling Plan for generalized log-logistic distributions with known shape parameters*, Journal of Applied Statistics, Vol.37,No.3,March (2010),405-414.

[2] H.P.Goode and J.H.K Kao, *Sampling plans based on the Weibull distribution*,In proceedings of the Seventh National Symposium on Reliability and Quality Control, Philadelphia, (1961),pp.24-40.

[3] S.S.Gupta, *Life test sampling plans for normal and lognormal distributions*, Technometrics 4(1962),pp.151-175.

[4] A.J.Duncan, *Quality Control and Industrial Statistics* 5th ed., Richard D.Irwin, Homewood, Illinois,(1986).

[5] B.Epstein,*Truncated life tests in the exponential case*,Ann.Math.Statist.25(1954),pp.555-564.

[6] S.S Gupta and P.A.Groll, Gamma *Distribution in acceptance sampling based on life tests*,j.Am.Statist.Assoc.56(1961),pp.942-970.

[7] K.Govindaraju,(1985) *Contribution to the study of certain special purpose plan*, Disseration,Madras University, Madras, India.

Table-1 Minimum sample sizes for Special double sampling plan

q	a	δ P*							
			0.5	0.7	1	1.5	2	2.5	3
0.05	2	0.75	43,40	31,28	22,19	15,11	11,9	9,7	8,4
		0.9	66,63	47,45	33,31	22,20	17,14	13,12	11,10
		0.95	82,81	59,57	41,40	28,25	21,18	17,14	14,12
		0.99	119,118	85,84	60,57	40,37	30,27	24,22	20,18
	3	0.75	43,41	31,28	22,19	14,13	11,8	9,6	7,6
		0.9	66,65	47,46	33,31	22,20	16,15	13,11	11,8
		0.95	83,82	59,58	41,40	27,26	20,19	16,14	13,12
		0.99	121,119	86,84	60,57	39,38	29,27	23,21	19,17
	4	0.75	44,41	31,29	22,19	14,13	11,8	8,7	7,5
		0.9	67,66	48,45	33,31	22,19	16,14	13,10	10,9
		0.95	84,83	60,57	41,40	27,25	20,18	16,13	13,11
		0.99	122,121	86,85	60,57	39,37	28,27	22,21	18,17
	5	0.75	44,42	31,29	22,19	14,12	10,9	8,6	7,4
		0.9	68,66	48,46	33,31	22,19	16,13	12,11	10,8
		0.95	85,84	60,58	41,40	27,25	19,18	15,13	12,11
		0.99	124,121	87,85	60,57	39,37	28,26	21,20	17,16
0.1	2	0.75	21,20	15,14	11,9	8,4	6,3	5,1	4,2
		0.9	33,31	24,21	17,14	11,10	8,7	7,5	6,3
		0.95	41,39	29,28	21,18	14,12	10,9	8,7	7,5
		0.99	59,58	42,41	30,27	20,18	15,13	12,10	10,8
	3	0.75	22,20	16,13	11,9	7,6	6,2	4,3	4,1
		0.9	34,31	24,22	17,14	11,9	8,7	7,4	5,4
		0.95	42,40	30,28	21,18	14,11	10,8	8,6	7,4
		0.99	61,59	43,41	30,27	19,18	14,13	11,10	9,8
	4	0.75	22,21	16,14	11,9	7,6	5,4	4,3	4,1
		0.9	34,33	24,23	17,14	11,8	8,6	6,5	5,3
		0.95	43,41	30,29	21,18	13,12	10,7	8,5	6,5
		0.99	62,60	43,42	30,27	19,17	14,11	11,8	8,7
	5	0.75	23,20	16,14	11,9	7,5	5,4	4,2	3,2
		0.9	35,33	24,23	17,14	11,8	8,5	6,4	5,2
		0.95	44,42	30,29	21,18	13,11	9,8	7,6	6,4
		0.99	63,62	44,42	30,27	19,16	13,12	10,8	8,6

Table-2 Operating Characteristic values of special double sampling plan with a=2 & q=0.05

P*	t/t_q^0	n_1	n_2	t_q/t_q^0					
				3	6	9	12	15	18
0.75	0.5	43	40	0.6794	0.8342	0.8888	0.9164	0.9331	0.9442
	0.7	31	28	0.6833	0.8368	0.8907	0.9179	0.9343	0.9453
	1	22	19	0.689	0.8406	0.8935	0.9202	0.9361	0.9468
	1.5	15	11	0.7167	0.8578	0.9058	0.9297	0.9439	0.9533
	2	11	9	0.7001	0.8476	0.8985	0.9241	0.9393	0.9494
	2.5	9	7	0.7041	0.8506	0.9008	0.9258	0.9407	0.9507
	3	8	4	0.7679	0.8893	0.9281	0.9469	0.9579	0.9652
0.9	0.5	66	63	0.5279	0.7445	0.8268	0.8693	0.8951	0.9125
	0.7	47	45	0.5279	0.7446	0.8268	0.8693	0.8951	0.9125
	1	33	31	0.5316	0.7475	0.8291	0.8711	0.8966	0.9137
	1.5	22	20	0.5398	0.7536	0.8336	0.8747	0.8996	0.9163
	2	17	14	0.5544	0.7649	0.8422	0.8816	0.9053	0.9212
	2.5	13	12	0.5401	0.7541	0.8339	0.8749	0.8997	0.9164
	3	11	10	0.5377	0.7532	0.8334	0.8746	0.8996	0.9163
0.95	0.5	82	81	0.4345	0.6798	0.7804	0.8335	0.6611	0.8881
	0.7	59	57	0.4345	0.6827	0.7828	0.8355	0.8677	0.8897
	1	41	40	0.4341	0.6824	0.7825	0.8352	0.8675	0.8893
	1.5	28	25	0.4487	0.6952	0.7926	0.8435	0.8744	0.8952
	2	21	18	0.4594	0.7038	0.7992	0.8488	0.8788	0.899
	2.5	17	14	0.4648	0.7088	0.8032	0.8521	0.8816	0.9014
	3	14	12	0.4577	0.7034	0.7991	0.8487	0.8788	0.8991
0.99	0.5	119	118	0.2749	0.5565	0.6885	0.7614	0.8071	0.8382
	0.7	85	84	0.2754	0.5573	0.6892	0.7621	0.8076	0.8387
	1	60	57	0.2821	0.5648	0.6955	0.7674	0.8122	0.8427
	1.5	40	37	0.2881	0.5716	0.7012	0.7721	0.8162	0.8462
	2	30	27	0.2944	0.5785	0.7071	0.7769	0.8203	0.8498
	2.5	24	22	0.2884	0.5733	0.7029	0.7736	0.8175	0.8474
	3	20	18	0.2923	0.5778	0.7068	0.7768	0.8203	0.8497

Table-3 Operating Characteristic values of special double sampling plan with a=2 & q=0.1

P*	t/t_q^0	n_1	n_2	t_q/t_q^0					
				3	6	9	12	15	18
0.75	0.5	21	20	0.6798	0.8342	0.8888	0.9164	0.9331	0.9442
	0.7	15	14	0.6841	0.8371	0.8907	0.9181	0.9343	0.9452
	1	11	9	0.6993	0.8472	0.8982	0.9238	0.9391	0.9493
	1.5	8	4	0.7673	0.8891	0.9279	0.9468	0.9578	0.9651
	2	6	3	0.7673	0.8892	0.9281	0.9469	0.9579	0.9651
	2.5	5	1	0.8628	0.9428	0.9651	0.9751	0.9606	0.9842
	3	4	2	0.7676	0.8896	0.9283	0.9471	0.9581	0.9652
0.9	0.5	33	31	0.5306	0.7469	0.8286	0.8708	0.8963	0.9135
	0.7	24	21	0.5426	0.7561	0.8386	0.8764	0.9011	0.9175
	1	17	14	0.5534	0.7643	0.8418	0.8813	0.9051	0.9211
	1.5	11	10	0.5368	0.7526	0.8331	0.8744	0.8993	0.9161
	2	8	7	0.5576	0.7666	0.8431	0.8822	0.9057	0.9214
	2.5	7	5	0.5756	0.7821	0.8553	0.8921	0.9141	0.9286
	3	6	3	0.6457	0.8288	0.8892	0.9185	0.9356	0.9468
0.95	0.5	41	39	0.4404	0.6874	0.7864	0.8383	0.8701	0.8915
	0.7	29	28	0.4394	0.6867	0.7858	0.8378	0.8696	0.8911
	1	21	18	0.4583	0.7031	0.7987	0.8484	0.8785	0.8987
	1.5	14	12	0.4566	0.7027	0.7986	0.8483	0.8785	0.8987
	2	10	9	0.4614	0.7054	0.8001	0.8493	0.8792	0.8992
	2.5	8	7	0.4679	0.7111	0.8046	0.8529	0.8821	0.9017
	3	7	5	0.5021	0.7388	0.8259	0.8701	0.8964	0.9141
0.99	0.5	59	58	0.2786	0.5607	0.6919	0.7642	0.8095	0.8403
	0.7	42	41	0.2809	0.5635	0.6943	0.7662	0.8112	0.8416
	1	30	27	0.2933	0.5776	0.7063	0.7764	0.8199	0.8494
	1.5	20	18	0.2912	0.5769	0.7061	0.7763	0.8198	0.8494
	2	15	13	0.2993	0.5862	0.7138	0.7827	0.8253	0.8541
	2.5	12	10	0.3079	0.5956	0.7217	0.7892	0.8308	0.8589
	3	10	8	0.3169	0.6054	0.7297	0.7959	0.8364	0.8637

Table -4 Minimum percentile ratio of Special double sampling plan with a=2

q	a	P*	t/t_q^0						
			0.5	7	1	1.5	2	2.5	3
0.05	2	0.75	0.1999	0.1894	0.1871	0.2031	0.2105	0.2095	0.2089
		0.9	0.1198	0.1277	0.1295	0.1364	0.1368	0.1382	0.1357
		0.95	0.0987	0.0985	0.0971	0.0981	0.0982	0.0987	0.0995
		0.99	0.0693	0.0673	0.0663	0.0693	0.0683	0.0682	0.0681
	3	0.75	0.1921	0.1931	0.1899	0.1959	0.2009	0.2013	0.2093
		0.9	0.1278	0.1248	0.1258	0.1268	0.1277	0.1298	0.1339
		0.95	0.0992	0.0989	0.0984	0.0999	0.1028	0.1094	0.1108
		0.99	0.0732	0.0702	0.0714	0.0712	0.0782	0.0772	0.0724
	4	0.75	0.1985	0.1965	0.1952	0.1982	0.2079	0.2192	0.2299
		0.9	0.1238	0.1299	0.1278	0.1299	0.1329	0.1393	0.1391
		0.95	0.1053	0.0991	0.0999	0.1129	0.1168	0.1198	0.1212
		0.99	0.0691	0.0699	0.0736	0.0721	0.0792	0.0791	0.0993
	5	0.75	0.1949	0.1981	0.1982	0.2192	0.2312	0.2432	0.2391
		0.9	0.1291	0.1269	0.1299	0.1309	0.1392	0.1409	0.1463
		0.95	0.1094	0.1053	0.1099	0.1109	0.1172	0.1163	0.1193
		0.99	0.0717	0.0754	0.0783	0.0778	0.0784	0.0799	0.0873
0.1	2	0.75	0.1909	0.1899	0.1901	0.2099	0.2095	0.2395	0.2229
		0.9	0.1276	0.1277	0.1275	0.1274	0.1278	0.1272	0.1379
		0.95	0.1037	0.1085	0.1087	0.1091	0.1082	0.1077	0.1075
		0.99	0.0699	0.0672	0.0673	0.0693	0.0683	0.0691	0.0709
	3	0.75	0.1909	0.1991	0.1999	0.2099	0.2491	0.2283	0.2459
		0.9	0.1279	0.1262	0.1298	0.1398	0.1397	0.1398	0.1469
		0.95	0.1099	0.1089	0.1074	0.1062	0.1088	0.1124	0.1178
		0.99	0.0732	0.0762	0.0709	0.0729	0.0759	0.0772	0.0794
	4	0.75	0.1985	0.1965	0.2069	0.2099	0.2292	0.2312	0.2499
		0.9	0.1258	0.1279	0.1378	0.1429	0.1432	0.1493	0.1631
		0.95	0.1093	0.1045	0.1091	0.1139	0.1168	0.1298	0.1312
		0.99	0.0731	0.0791	0.0796	0.0799	0.0852	0.0891	0.0973
	5	0.75	0.1999	0.2099	0.2092	0.2292	0.2312	0.2592	0.2661
		0.9	0.1339	0.1329	0.1459	0.1499	0.1592	0.1663	0.1891
		0.95	0.1094	0.1053	0.1099	0.1189	0.1299	0.1293	0.1399
		0.99	0.0717	0.0754	0.0793	0.0899	0.0924	0.0973	0.0993

ISSN (e): 2250 – 3005 || Vol, 05 || Issue, 01 || January – 2015 ||
International Journal of Computational Engineering Research (IJCER)

Data Integration in Multi-sources Information Systems

Adham mohsin saeed
Computer Engineer Dept, Al-Rafidain University College,Iraq,Bagdad,

ABSTRACT

Data integration involves combining data coming from different sources and providing users with a unified view of these data. In this paper, we introduced the problem of integration of multi-source information systems with some focus on the heterogeneity and conflict issues at different levels .We have made some survey related the current implementations methods that have been used to solve the problems of data integration of multi sources IS which can be classified on three will established approaches, we have also discussed some of the limitations and advantages of such approaches, next we talked about the current trends in data integration such as warehousing, descriptive logic and ontology . Finally, we have presented some case studies that have been implemented using some of these approaches.

Key words: *Data integration, multi-source information systems, warehousing.*

I. INTRODUCTION

In recent years there is a tremendous growth for the need of a various application that can access, relate, use, and integrate of multiple disparate information sources and repositories including databases, knowledge bases, file systems, digital libraries, information retrievals systems and electronic mail systems. Data integration is a core issue in these applications, For instance, in the area of business intelligence (BI), integrated information can be used for querying and reporting on business activities, for statistical analysis, online analytical processing (OLAP), and data mining in order to enable forecasting, decision making, enterprise-wide planning, and in the end to gain sustainable competitive advantages. (1) A study by Forrest Research reported that 98% of companies it recently interviewed said that integration is either "extremely important" or "very important" to their firm's IT strategy and their integration projects have been running for an average of more than 20 months and involve an average of seven systems . (2) Ensuring Data integrity in the process of integration of heterogeneous data sources has proven to be very challenging task because of the "asymmetric "nature of the integration and a "seamless Integration" has been so far more of a wish than reality, due to the difficulties and challenges faced in dealing with the heterogeneity, technology obsolescence and semantic discrepancy associated with multiple source information systems. (3) More recently, research has focused on the Intelligent Integration of Information. Here the problem is to access the diverse data residing in multiple, autonomous, heterogeneous information sources, and to integrate, or fuse, that data into coherent information that can be used by decision makers. (4)

II. MULTI-SOURCES INFORMATION SYSTEM

A **Multi-Sources Information System** (MSIS) can be defined as an Information System where exist a set of different User Views and a set of distributed, heterogeneous and autonomous Information Sources (5). We briefly explain these concepts: (6) (7)

- **Distributed**: Nowadays most computers are connected to some type of network, especially the Internet, and it is natural to think of combining application and data sources that are physically located on different hosts, but that can communicate through the network.
- **Heterogeneous** information sources: are sources with possibly different data models, schemas, data representations, and interfaces.
- **Autonomous** information sources: are sources that were developed independently of each other, and are maintained by different organizations, that may wish to retain control over their sources.

Figure (1) shows the architecture of such a system. There are three layers: source, mediation and application. The source layer contains each source with its associated wrapper, which translates queries and queries' responses that pass through it. The mediation layer has in charge the transformation and integration of the information obtained from the sources, according to the requirements coming from the application layer. The application layer provides the user views to the user applications through execution of queries over the mediation layer. (5)

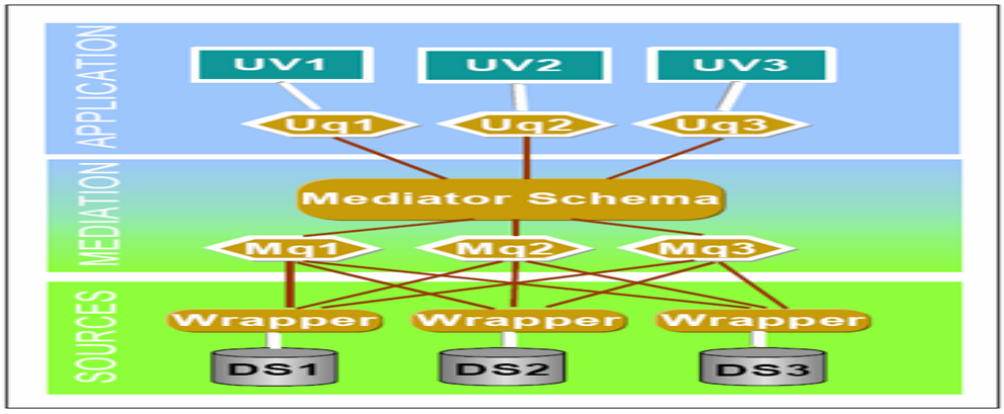

Figure (1) MSIS architecture

Some of the requirements that may be faced when designing a multi-source information system:

1. How to provide an integrated view of overlapping data sets from multiple sources.
2. How to support updates against such views.
3. How to identify the relationship between two or more institutions of replicated data.
4. How to keep replicated data "synchronized".

III. INFORMATION CONFLICTS IN DATA SOURCES

With the advent of the internet and web technologies, the focus shifted from integrating purely well-structured data to also incorporating semi- and unstructured data while architecturally, loosely-coupled mediator and agent systems became popular. (1) (9)

An important issue almost in every system of information integration is the possibility of information conflicts among the different data sources. These conflicts are at two different levels: (6)

1. **Intentional inconsistencies**: The sources are in different data models, or have different schemas within the same data model, or their data is represented in different natural languages or different measurement systems. Such conflicts have often been termed **semantic inconsistencies**.
2. **Extensional inconsistencies**: There are factual discrepancies among the sources in data values that describe the same objects. Such conflicts are also referred to as data inconsistencies. Extensional inconsistencies can only be observed after intentional inconsistencies have been resolved. That is, different attribute names in the schemas of different information sources must be mapped to each other and attribute values must be within the same measurement system, to conclude that these values indeed contradict each other.

In a broad sense, semantic inconsistencies or conflict can occur at two different levels: at the **data level** and at the **schema level**. Data-level conflicts are differences in data domains caused by the multiple representations and interpretations of similar data. Data-level conflicts may have different forms such as data-value conflicts, data representation conflicts , data-unit conflicts , and data precision conflicts. (2)
Schema-level conflicts are characterized by differences in logical structures and/or inconsistencies in metadata (i.e., schemas) of the same application domain. Examples of such conflicts are naming conflicts, entity-identifier conflicts, schema-isomorphism conflicts, generalization conflicts, aggregation conflicts, and schematic discrepancies.

IV. APPROACHES TO INFORMATION INTEGRATION IN MULTI-SOURCE INFORMATION SYSTEMS

Information Integration can be defined as a process of using data abstraction to provide a single interface for viewing all the data within an organization, or a part of it, and a single set of structures and naming conventions to represent this data. (10) Data integration can be either virtual or materialized. In the first case, the integration system acts as an interface between the user and the sources, and is typical of multi databases, distributed databases, and more generally open systems. In virtual integration query answering is generally costly, because it requires accessing the sources. In the second case, the system maintains a replicated view of the data at the sources, and is typical, for example, both in information system re-engineering and data warehousing. In materialized data integration, query answering is generally more efficient, because it does not require accessing the sources, whereas maintaining the materialized views is costly, especially when the views must be up-to-date with respect to the updates at the sources (view refreshment). (11)

4.1 Established approaches to data Integration

Over the past few years various approaches and techniques have been proposed and adopted in the search for achieving an ultimate information integration system. In this section, we provide a brief description of the well-known approaches that form the basis for the design of existing integration framework.

Early work on integration was carried out in the context of database design, and focused on the so-called **schema integration** or **Mapping based approach** by constructing a global unified schema for semantically related information sources starting from several sub schemata (local schema), each one produced independently from the others. Mappings are not limited to schema components (i.e., entity classes, relationships, and attributes), but may be established between domains and schema components. (11) (2)

More recent efforts have been devoted to data integration, which generalizes schema integration by taking into account actual data in the integration process. Here the input is a collection of source data sets (each one constituted by a schema and actual data), and the goal is to provide an integrated and reconciled view of the data residing at the sources, without interfering with their autonomy. We only deal with the so-called read-only integration, which means that such a reconciled view is used for answering queries, and not for updating information. (11)

The second approach to the data integration problem is the **procedural approach** or **Intermediary approach,** where data are integrated in an ad-hoc manner with respect to a set of predefined information needs. In this case, the basic issue is to design suitable software modules (e.g., mediators, agents, ontology's) that access the sources in order to fulfill the predefined information requirements. Several data integration (both virtual and materialized) projects follow this idea. They do not require an explicit notion of integrated data schema, and rely on two kinds of software components: **wrappers** that encapsulate sources, converting the underlying data objects to a common data model, and **mediators** that obtain information from one or more wrappers or other mediators, refine this information by integrating and resolving conflicts among the pieces of information from the different sources, and provide the resulting information either to the user or to other mediators.. (11) (2).

The third approach is called **declarative approach** or **query-oriented approach**, here the goal is to model the data at the sources by means of a suitable language (either declarative logic-based languages or extended SQL) to construct a unified representation and to refer to such a representation when querying the global information system, and to derive the query answers by means of suitable mechanisms accessing the sources and/or the materialized views. This approach typically requires users to engage in the detection and resolution of semantic conflicts since it provides little or no support for identifying semantic conflicts (11) (2).

Note that research approaches classified into these three categories may not be mutually exclusive. For example, the intermediary-based approach may not necessarily be achieved only through intermediaries. Some approaches based on intermediaries also rely on mapping knowledge established between a common ontology and local schemas. It is also often the case that mapping and Intermediaries are involved in query-oriented approaches.

4.2 Current trend in data Integration

4.2.1 Warehousing

The Warehousing approach derives its basis from traditional data warehousing techniques. Data from heterogeneous distributed information sources is gathered, mapped to a common structure and stored in a centralized location. Warehousing emphasizes data translation, as opposed to query translation in mediator-based systems. In fact, warehousing requires that all the data loaded from the sources be converted through data mapping to a standard unique format before it is stored locally. In order to ensure that the information in the warehouse reflects the current contents of the individual sources, it is necessary to periodically update the warehouse. (12)

4.2.2 Description Logic

Description Logic provides a way to manipulate the semantics of data. It has the advantage that most of the data models developed so far can be represented using Description Logic. Systems based on Description Logics tend to focus on conjunctive queries i.e. these queries provide an integrated view, which hold a subset of data. This approach has been very successful in manipulating the meanings associated with data and the approach is also very flexible as the formalizations are based on concepts and roles. The basic essence of concepts and classes comes from Object Oriented (OO) Methodology. The strengths associated with OO approach can be utilized in this approach as well. This allows the developers to add new roles and reuse the already developed components. Some research material refers to these concepts as "classes". These concepts/classes provide the framework for managing meaning associated with data. (11)

4.2.3 Ontological

In the last decade, semantics (which are an important component for data integration) gained popularity leading to the inception of the celebrated ontology-based integration approach. The Semantic Web research community has focused extensively on the problem of semantic integration and the use of ontology's for blending heterogeneous schemas across multiple domains. Their pioneering efforts have provided a new dimension for researchers to investigate the challenges in information integration. A number of frameworks designed using ontology-based integration approaches have evolved in the past few years.

There are a lot of advantages in the use of ontologies for data integration. Some of them are : the ontology provides a rich, predefined vocabulary that serves as a stable conceptual interface to the databases and is independent of the database schemas; the knowledge represented by the ontology is sufficiently comprehensive to support translation of all the relevant information sources; the ontology supports consistent management and the recognition of inconsistent data. (7) (12)

V. CASE STUDIES

5.1 Infomaster: Mapping based approach

Infomaster is an information integration system that provides integrated access to multiple distributed heterogeneous information sources on the Internet, thus giving the illusion of a centralized, homogeneous information system. We can say that Infomaster creates a virtual data warehouse. Infomaster handles both structural and content translation to resolve deference's between multiple data sources and the multiple applications for the collected data. Infomaster connects to a variety of databases using wrappers, such as for Z39.50, SQL databases through ODBC, EDI transactions, and other World Wide Web sources. (13)

The core of Infomaster is a facilitator that determines which sources contain the information necessary to answer the query efficiently, designs a strategy for answering the query, and performs translations to convert source information to a common form or the form requested by the user. Formally, Infomaster contains a model-elimination resolution theorem prove as a workhorse in the planning process. There are wrappers for accessing information in a variety of sources. For SQL databases, there is a generic ODBC wrapper. There is also a wrapper for Z39.50 sources. For legacy sources and structured information available through the WWW, a custom wrapper is used.

Infomaster uses rules and constraints to describe information sources and translations among these sources. These rules and constraints are stored in knowledge. For efficient access, the rules and constraints are loaded into Epilog, a main memory database system from Epistemic.

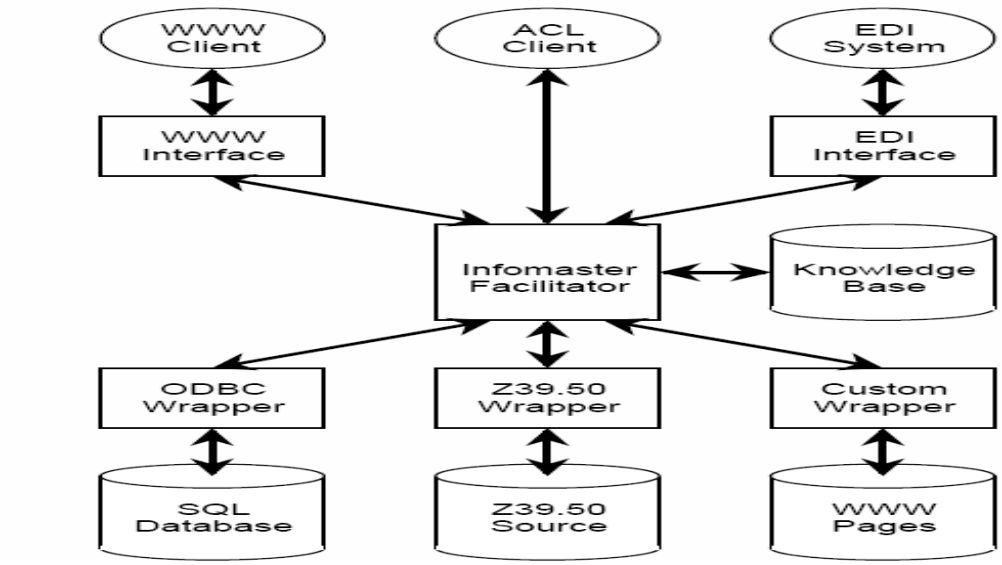

Figure 2: Infomaster Architecture

Infomaster includes a WWW interface for access through browsers. This user interface has two levels of access: an easy-to-use, forms-based interface and an advanced interface that supports arbitrary constraints applied to multiple information sources. However, additional user interfaces can be created without affecting the core of Infomaster. Infomaster has a programmatic interface called Magenta, which supports ACL (Agent Communication Language) access. ACL consists of KQML (Knowledge Query and Manipulation Language), KIF (Knowledge Interchange Format), as well as vocabularies of terms.

5.2 The TSIMMIS Project: an Intermediary approach to data integration

TSIMMIS is a mediator system being developed by the Stanford database group, in conjunction with IBM. The goal of the TSIMMIS project is to develop tools to rapidly accessing in an integrated fashion multiple information sources that may include both structured and semi-structured data and to ensure that the information obtained is consistent. (14)

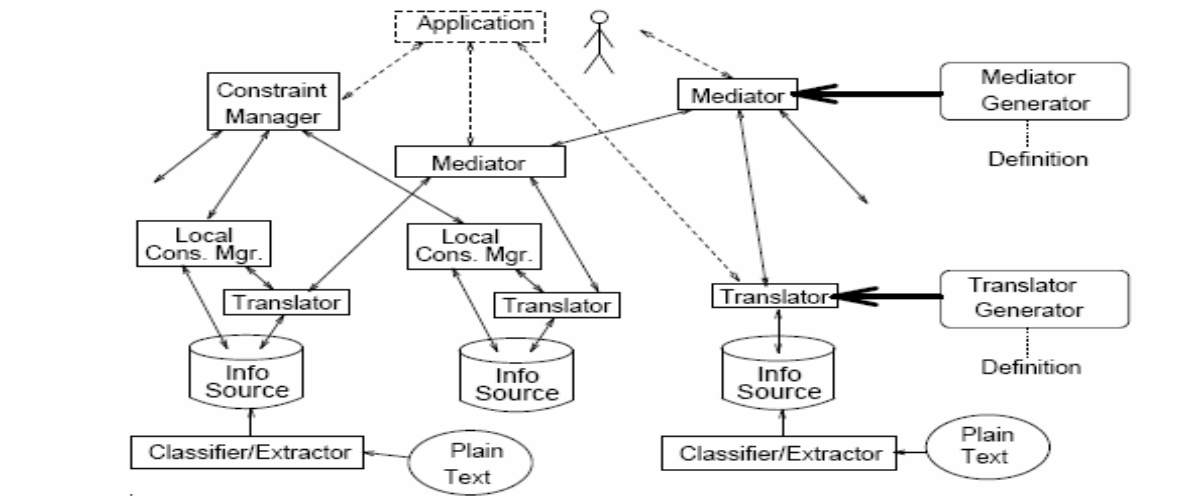

Figure 3: TSIMMIS Architecture

TSIMMIS employs classifiers/extractors, wrappers/translators, mediators, and constraint managers to achieve system integration. The above figure shows a collection of (disk-shaped) heterogeneous information sources. The classifiers/extractors attempt to identify simple patterns in unstructured sources and then export this information to the entire TSIMMIS system through a wrapper. Above each source is a translator (or wrapper) that logically converts the underlying data objects to a common information model. To do this logical translation, the translator converts queries over information in the common model into requests that the source can execute, and it converts the data returned by the source into the common model. For the TSIMMIS project they have adopted a simple self-describing (or tagged) object model called the Object Exchange Model, or OEM. One of the goals of this project was to automate the development of wrappers. To this end, a wrapper implementation toolkit was developed. The toolkit allows for the semi-automatic creation of wrappers through the use of predefined templates.

Above the translators in Figure 3 lie the mediators. A mediator is a system that refines in some way information from one or more sources. A mediator embeds the knowledge that is necessary for processing a specific type of information. The mediator may also process answers before forwarding them to the user, say by converting dates to a common format, or by eliminating articles that duplicate information.

Mediators export an interface to their clients that is identical to that of translators. End users can access information either by writing applications that request OEM objects, or by using one of the generic browsing tools that have been developed. Finally, there are the constraint managers which attempt to ensure semantic consistency across integrated resources.

5.3 Information Integration Wizard (IWIZ): Hybrid Approaches

Information Integration Wizard combines the data warehousing and mediation approaches. IWIZ allows end-users to issue queries based on a global schema to retrieve information from various sources without knowledge about their location, API, and data representation. However, unlike existing systems, queries that can be satisfied using the contents of the IWIZ warehouse are answered quickly and efficiently without connecting to the sources. In the case when the relevant data is not available in the warehouse or its contents are out-of-date, the query is submitted to the sources via the IWIZ mediator; the warehouse is also updated for future use. An additional advantage of IWIZ is that even though sources may be temporarily unavailable, IWIZ may still be able to answer queries as long as the information has been previously cached in the warehouse.

Due to the popularity of the Web and the fact that much of the interesting information is available in the form of Web pages, catalogs, or reports with mostly loose schemas and few constraints, IWIZ have focused on integrating semi structured data. The following figure show Schematic description of the IWIZ architecture and its main components. (8)

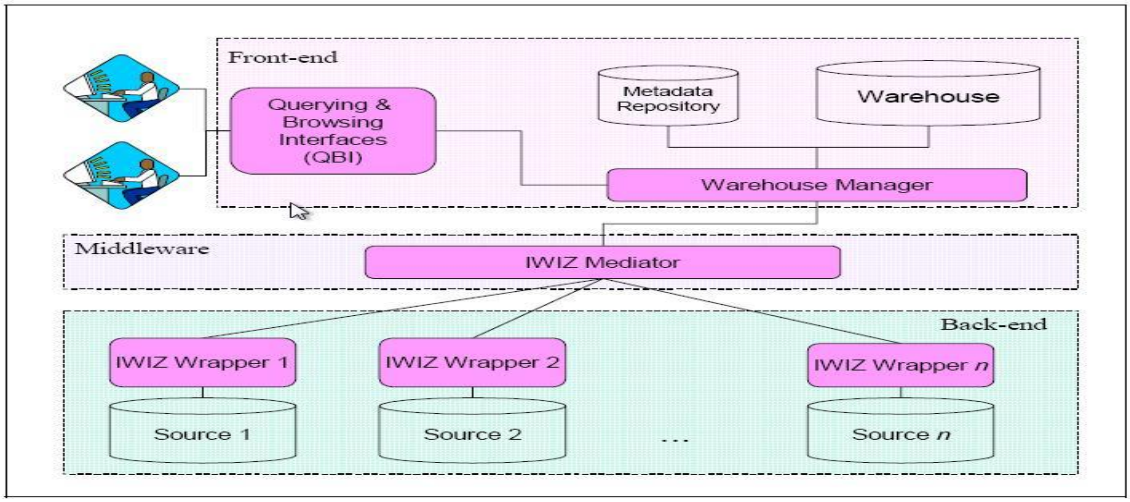

Figure 4: IWIZ Architecture

A conceptual overview of the IWIZ system is shown in the above Figure. System components can be grouped into two categories: Storage and control. Storage components include the sources, the warehouse, and the metadata repository. Control components include the querying and browsing interface (QBI), the warehouse manager, the mediator, and the wrappers. In addition, there is information not explicitly shown in the figure, which includes the global schema, the queries and the data. The global schema, which is created by a domain expert, describes the information available in the underlying sources and consists of a hierarchy of concepts and their definitions as well as the constraints. Internally, all data are represented in the form of XML documents, which are manipulated through queries expressed in XML-QL. The global schema, which describes the structure of all internal data, is represented as a Document Type Definition (DTD), a sample of which is shown later in the paper. The definition of concepts and terms used in the schema is stored in the global ontology.

As indicated in Figure 4, users interact with IWIZ through QBI, which provides a conceptual overview of the source contents in the form of the global IWIZ schema and shields users from the intricacies of XML and XML-QL. QBI translates user requests into equivalent XML-QL queries, which are submitted to the warehouse manager. In case when the query can be answered by the warehouse, the answer is returned to QBI. Otherwise, the query is processed by the mediator, which retrieves the requested information from the relevant sources through the wrappers. The contents of the warehouse are updated whenever a query cannot be satisfied or whenever existing content has become stale. Our update policy assures that over time the warehouse contains as much of the result set as possible to answer the majority of the frequently asked queries.

VI. CONCLUSIONS

Integration of multiple information sources aims at combining selected sources so that they form a unified new whole and give users the illusion of interacting with one single information sources. In this paper, we briefly introduced the problem of integration of multi-source information systems with some focus on the heterogeneity and conflict issues at different levels that may affect such a design of such systems and should be considered when designing such systems. We have made some survey related the current implementations methods that have been used to solve the problems of data integration of multi sources IS which can be classified on three will established approaches, we have also discussed some of the limitations and advantages of such approaches, next we talked about the current trends in data integration such as warehousing, descriptive logic and ontologies. Last, but not least, we have presented some case studies that have been implemented using some of these approaches.

REFERENCES

[1]. **Patrick Ziegler, Klaus R. Dittrich.** *Three Decades of Data Integration - All Problems Solved ,2004.* s.l. : In 18th IFIP World Computer Congress, 2004. Vols. Volume 12, Building the Information Society , 2004.

[2]. **PARK, JINSOO and RAM, SUDHA.** *Information Systems Interoperability:What Lies Beneath?* s.l. : ACM Transactions on Information Systems, Vol. 22, No. 4, 2004.

[3]. **Y. Tang, J. B. Zhang, C. H. Tan and M. M. Wong.** *A Five-step Approach to Multi-source Information Infusion with Guaranteed Data Integrity.* s.l. : Singapore Institute of Manufacturing Technology (SIMTech) web site , 2003.

[4]. **Weishar, Larry Kerschberg and Doyle J.** *Conceptual Models and Architectures for Advanced Information Systems.* s.l. : Applied Intelligence, vol. 13, pp. 149-164, 2000.

[5]. **Marotta, Adriana.** *Quality Management in Multi-Source Information Systems.* s.l. : Instituto de Computación. Facultad de Ingeniería.Universidad de la República. Montevideo, Uruguay., 2004.
[6]. **Motro, Amihai and Anokhin, Philipp.** *Fusionplex: resolution of data inconsistencies in the integration.* Department of Information and Software Engineering, George Mason University, University Drive, Fairfax, VA 22030-4444, USA : Information Fusion 7 176–196, 2006.
[7]. **Agustina Buccella, Ra Cechich, Nieves R. Brisaboa.** *An Ontology Approach to Data Integration.* s.l. : Journal of Computer Science and Technology , Vol 3,No. 2, 2003.
[8]. **Hammer, Joachim and Pluempitiwiriyawej, Charnyote.** *Overview of the Integration Wizard Project for Querying and Managing Semistructured Data in Heterogeneous Sources.* s.l. : Proceedings of the Fifth National Computer Science and Engineering Conference , Thailand, , November 2001.
[9]. **Wood, Peter.** *Semi-Structured Data.* Birkbeck College at the University of London : http://www.dcs.bbk.ac.uk/~ptw/, 2003.
[10]. **Michiels, Eric.** *New Trends in Information Integration.* s.l. : IBM corporation ,http://www.econ.kuleuven.be/, 2008.
[11]. **Calvanese, Diego.** *Description Logic Framework for Information Integration.* s.l. : Proc. of the 6th Int. Conf. on the Principles of Knowledge Representation and Reasoning , 1998.
[12]. **Chakravarthy, Aditya Telang and Sharma.** *Information Integration across Heterogeneous Domains: Current Scenario, Challenges and the InfoMosaic Approach.* s.l. : Department of Computer Science and Engineering, University of Texas at Arlington, 2007.
[13]. **Genesereth, Michael R., Keller, Arthur M. and Duschk, Oliver M.** *Infomaster:An Information Integration System.* s.l. : proceedings of 1997 ACM SIGMOD Conference , 1997.
[14]. **Chawathe, S., Garcia-Molina, H., Hammer, J., Ireland, K., Papakonstantinou, Y., Ullman, J., and Widom j.** *The TSIMMIS project: Integration of heterogeneous information sources.* Tokyo : 10th Anniversary Meeting of the Information Processing Society of Japan, 1994.

ISSN (e): 2250 – 3005 || Vol, 05 || Issue, 01 || January – 2015 ||
International Journal of Computational Engineering Research (IJCER)

Aluminum Foaming For Lighter Structure

Prof. Sunil M Mahajan[1], Ganesh A Jadhav[2]
[1] Assistant Professor, SITRC,Sandip Foundation,Nashik,
[2] Student of SITRC, Sandip Foundation, Nashik

ABSTRACT:

Aluminum foaming for light weight construction has become an attractive research field both from the scientific viewpoint and the prospect of industrial applications. Various methods for making such foams are available. Some techniques start from specially prepared molten metals with adjusted viscosities. Such melts can be foamed by injecting gases or by adding gas-releasing blowing agents which decompose in-situ, causing the formation of bubbles. A further way is to start from solid precursors containing a blowing agent. Alternatively, casting routes can be used to make such precursors. The properties of aluminum foams promise a variety of applications in vehicle design ranging from light-weight construction, impact energy absorption to various types of acoustic damping and thermal insulation. Aluminum Foaming is not implemented in India. In these seminar a over view of various term like concept, process, properties, advantages, disadvantages and practical applications of it are explained.

Keywords: *Aluminum foam; cellular structure; production; lightweight; incombustible; sound absorption; energy absorption.*

I. INTRODUCTION

Foams are two phase system and thermodynamically unstable. This is new technique to make a material even more ductile, with more shear strength along with light weight by foaming. In the last 40 years many metallic foam structures were produced, but they were not successful, because of their relatively high costs. There are various methods for making foams. Some techniques start from specially prepared molten metals with adjusted viscosities. Foamed aluminum is in stable form. Aluminum foam is very efficient for sound absorption, electromagnetic shielding, impact energy absorption and vibration damping. It is nonflammable and stable at elevated temperature. Aluminum foam is recyclable and thus environmentally friendly. Metallic foams have become an attractive field from the scientific viewpoint and the industrial applications. In many industrial applications, new materials are required for the production of light weight structures. Metal foams with porosities exceeding 50% can meet this requirement. In recent years, there has been a strongly growing demand for the use of metallic foams, particularly aluminum foam for automotive, railway and aerospace applications where weight reduction and improvement in safety is needed. For future industrial applications it is helpful for saving material, energy and environment.

II. MANUFACTURING PROCESS

Aluminum foam produced by following two basic methods:

2.1 Foaming of liquid melt

2.2 Foaming of powder compact.

2.1 Foaming Liquid Metals

Aluminum foam can be produced by creating gas bubbles in the liquid provided that the melt has been prepared such that the emerging foam is fairly stable during foaming process. This can be done by adding fine ceramic powders or alloying elements to the melt which form stabilizing particles. There are three methods of foaming metallic melts: gas injecting into the liquid metal, gas releasing blowing agent's addition into the molten metal.

2.1.1 Foaming Melts by Gas Injection

In this process, Sic, aluminum oxide or magnesium oxide particles are used to increase the viscosity of the liquid metal and adjust its foaming properties because liquid metals cannot easily be foamed by air bubble into it. The drainage of the liquid down the walls of the bubbles occurs too quickly and the bubbles collapse. If a small percentage of these particles are added to the melt, the flow of the liquid metal is impeded sufficiently to

stabilize the bubbles. After these, the gas (air, argon or nitrogen) is injected into molten aluminum by using special rotating impellers or air injection shaft, which emerges gas bubbles in the melt and uniformly distributes through the melt. The base metal is usually an aluminum alloy.

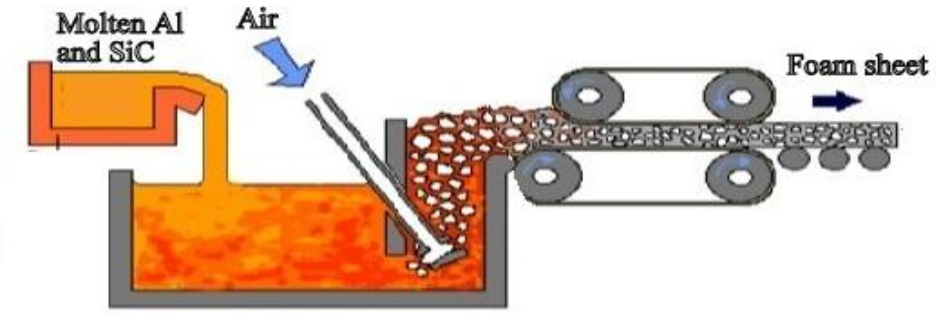

Fig.1 Schematic diagram of manufacturing of aluminum foam by melt gas injection.

The foam is relatively stable to the presence of ceramic particles in the melt. The mixture of bubbles and metal melt floats up to the surface of the liquid where it turns into fairly dry liquid foam as the liquid metal drains out. A conveyor belt is used to pull the foam off the liquid surface and then left to cool and solidify. Foaming of melt by gas injection process is the cheapest one among all others and the only one to have been as a continuous production. Foam panels can be produced at rates of up to 900 kg/hour. They have density 0.069-0.54 gm. /cm3, average size 3-25 mm and cell wall thickness 50-85 μm.
The main disadvantage of this process is the poor quality of the foams produced. The cell size is large and often irregular, and the foams tend to have a marked density gradient.

2.1.2 Foaming Melts with Blowing Agents

Addition of blowing agent into the melt is the other way of foaming melts. The blowing agent decomposes under the influence of heat and releases gas. The first stage of the foam production about 1.5 wt. % calcium metals is added to the aluminum melt at 680 °C. Then melt is stirred for several minutes during which the viscosity of the melt continuously forms the oxides like CaAl2O4, which thicken the liquid metal. Titanium hydride is added in an amount typically 1.6 wt. %, which acts as a blowing agent according to the reaction:

$$\mathbf{TiH_2\ (s) \rightarrow Ti\ (s) + H_2\ (g)}$$

The melt starts to expand slowly and gradually fills the foamy vessel. The whole foaming process can take 15 minutes for a typical batch of about 0.6 m3. After cooling the vessel below the melting point of the alloy, the liquid foam turns into solid aluminum foam and can be taken out of the mold for further processing.
BLOWING AGENTS FOR ALUMINIUM FOAMS
Foaming agent entrapped in the metal matrix after densification builds up an internal gas pressure upon heating of the compacts and leads to foam formation. Usually titanium hydride (TiH2) and zirconium Hydride (ZrH2) are used for aluminum foam. But titanium hydride is the best blowing agent for aluminum alloys because strong hydrogen release takes place between 400°C to 600°C which coincides with the melting point of aluminum (660°C). Titanium hydride has been characterized by the thermal analysis to characterize their decomposition temperature and to derive their suitability for foaming.

2.2 Foaming of Powder Compacts

The process starts with the mixing of metal powders - elementary metal powders, alloy powders or metal powder blends - with a powdered blowing agent, after which the mix is compacted. These techniques include compression, Extrusion used to produce a bar or plate and helps to break the oxide films at the surfaces of the metal powders. Foaming agent decomposes and the material expands by the released gas forces during the heating process gives a highly porous structure .A mixture of powders, metal powder and foaming agent was cold compacted and extruded to give solid metal material containing a dispersion of powdered foaming agent. When this solid was heated to the metal's melting temperature, the foaming agent decomposes to release gas into the molten metal, creating metal foam. During this process, cooling the foam is a problem. For this, after heating the precursor for foaming, the heat source could be turned off quickly. The foam has a closed-cell structure with pore diameters in the range of 1 mm to 5 mm and the process is called baking.

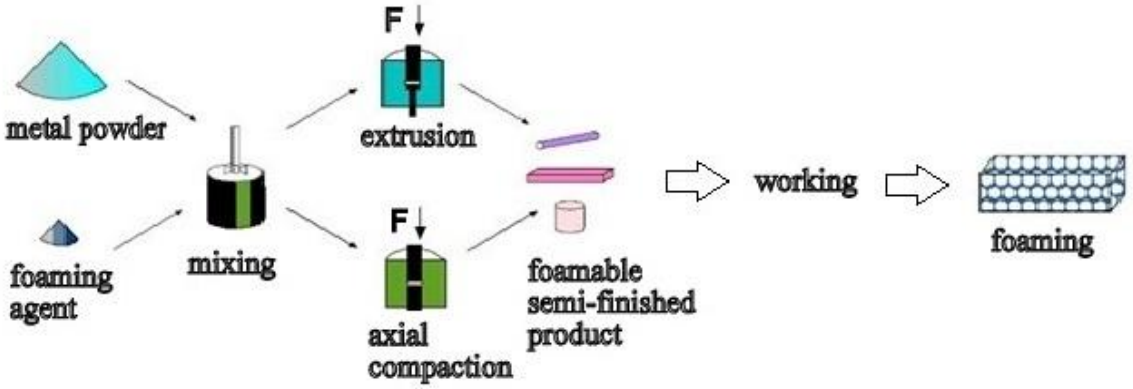

Fig.2 Foaming from powder compacts process.

III. PROPERTIES

3.1 Physical Properties and Values

Sr. No.	Physical Property	Value
1	Compression Strength	2.53 MPa
2	Tensile Strength*	1.24 MPa
3	Shear Strength	1.31 MPa
4	Modulus of Elasticity (Compression)*	103.08 MPa
5	Modulus of Elasticity (Tension)*	101.84 MPa
6	Shear Modulus	199.95 MPa
7	Specific Heat	0.895 $^{J}/_{g\text{-}C}$
8	Bulk Thermal Conductivity	5.8 $^{W}/_{m\text{-}C}$
9	Coefficient of Thermal Expansion (0-100°C)	23.58×10^{-6} $^{m}/_{m—C}$
10	Bulk Resistivity	7.2×10^{-5} ohm – cm
11	Melting Point	660°C

Table 1. Physical properties and their values.

These values were obtained from small samples. Larger samples having a minimum of 10-15 bubble diameters produce more general test results which are in better compliance with the equations.

3.2 Mechanical properties

The cellular structure of foams behaves differently in testing when compared to metal. Therefore conventional testing methods cannot be used, like tensile testing. The behavior was found for compressive stress-strain diagram with a division into three parts.

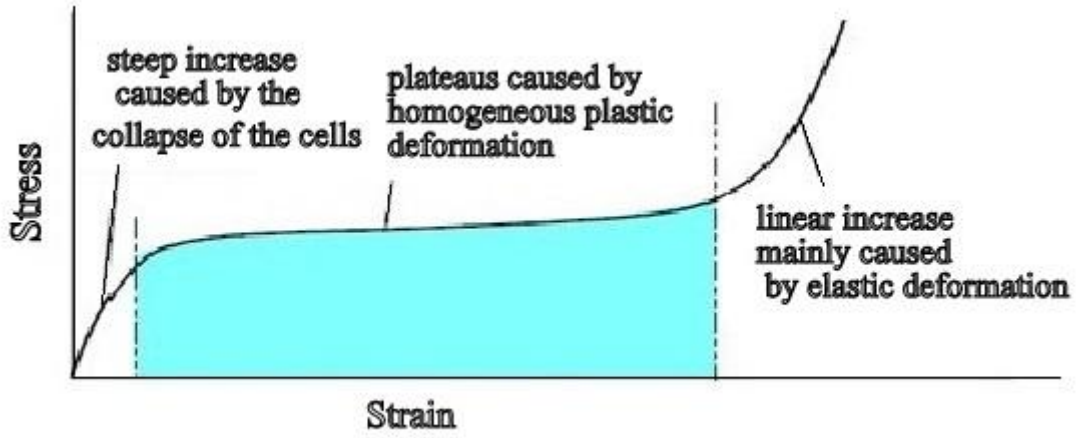

Graph 1 Stress-strain diagram for compressive test of aluminum foam.
It shows a linear increase of stress at the beginning of deformation. The first stage is caused by an elastic deformation. In foams plastic deformations can occur at low stresses.

A plateau region nearly constant stress in the middle. It is followed by a steep increase in flow stress at the end. The tensile strength of foams is nearly the same as the stress at which the plateau occurs. That's why this "plateau stress" is used as the main property value of foams.

3.2.1 Modulus of elasticity

The modulus of elasticity is, in combination with the geometry an important characteristic for the estimation of the stiffness of a finished metallic product. The specific modulus of aluminum foams is much lower than that of dense aluminum.

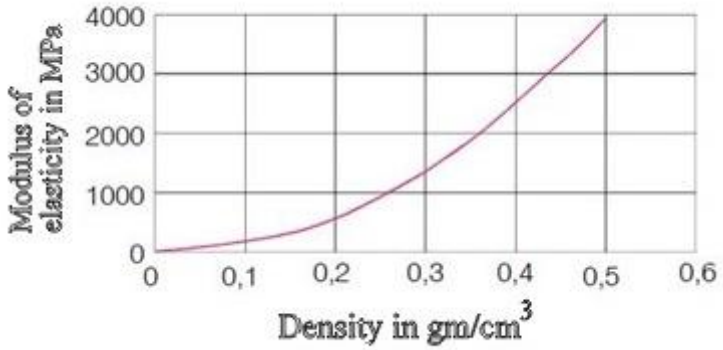

Graph 2 Modulus of elasticity of aluminum foams of several densities.

As shown in graph, the modulus of foams increases with increasing density. Therefore the modulus can be adapted to a special application by controlling the density of the foam.

3.3 Chemical properties

Aluminum foam is incombustible. Under the influence of heat foams do not release toxic gases. The corrosion behavior is comparable to that of dense aluminum alloys.

IV. ADVANTAGES

- Foam blocks can floats in Water.
- Foam blocks can saw drilled, cut and bend.
- By screwing & riveting foam blocks can join to dense material.
- Welding of foam blocks is possible, mainly laser welding.
- Foam blocks can paint with organic or inorganic paint.

V. DISADVANTAGES

- They are difficult to manufacture as precision manufacturing is required.
- High cost.
- Difficultly in manufacturing high temperature metal.
- Once damaged it cannot be repaired, the whole metal foam has to replace by new one.

VI. APPLICATIONS

- AUTOMOTIVE INDUSTRY:
  Firewalls, Energy Absorbing Bumpers, Door side impact bars, Floor panels, Helmets.
- MILITARY:
  Lightweight armor, mine blast containment.
- AEROSPACE INDUSTRY:
  Due to lightweight Al foam sheets could replace the expansive honeycomb structures.
- BUILDING & CONSTRUCTION:
  Good possibilities due to good fire penetration resistance & thermal insulations.
  Used as sound absorbing material in railway tunnels, under highway bridges or inside of building.
- HOUSEHOLD & FURNITURE INDUSTRY:
  Used for lamps, tables or household articles & accessories.

VII. CONCLUSION

Aluminum foam has high potential for various applications but there use is limited because of its cost and lack of uniformities in properties. But it is expected that the price of foams will decrease in the coming years as the volume of production increases. Recent technological advances in the field of metallic foams have led to the development of a wide range of processing techniques for the open as well as closed cell morphologies.

REFERENCES

[1]. Frantisek Simancik et.al,(March 6-9, 2000),"Alulight-Aluminum Foam for Lightweight Construction", *SAE TECHNICAL PAPER SERIES.*
[2]. Bernd Friedrich et.al,(18th March 2003)," Aluminum foam – Production, Properties and Recycling Possibilities", *ERZMETALL*, pages: 656-660.
[3]. V. Gergely*,et.al,(2003)," The FOAMCARP process: foaming of aluminum MMCs by the chalk-aluminum reaction in precursors", *Composites Science and Technology*, vol: 63, pages: 2301-2310.
[4]. M. Shiomia, et.al,(2010)," Fabrication of aluminum foams from powder by hot extrusion and foaming", vol: 210, pages: 1203-1208.
[5]. Dr. –Ing. Catrin Kammer et.al, (1999),"Aluminum foam", *TALAT Lecture 1410*.